

UNIVERSIDADE FEDERAL DE SÃO CARLOS  
CENTRO DE CIÊNCIAS EXATAS E DE TECNOLOGIA  
DEPARTAMENTO DE QUÍMICA  
PROGRAMA DE PÓS-GRADUAÇÃO EM QUÍMICA

**LASER-INDUCED BREAKDOWN SPECTROSCOPY (LIBS), WAVELENGTH  
DISPERSIVE X-RAY FLUORESCENCE (WDXRF) AND CHEMOMETRICS:  
POSSIBILITIES FOR ANALYTICAL APPLICATIONS IN FOOD ANALYSIS**

**Raimundo Rafael Gamela\***

Tese apresentada como parte dos requisitos  
para obtenção do título de DOUTOR EM  
CIÊNCIAS, área de concentração: QUÍMICA  
ANALÍTICA.

Orientador: Prof. Dr. Edenir Rodrigues Pereira Filho

\*Bolsista: CNPq/TWAS (process number: 158587/2017-0)

São Carlos-SP

2020



**UNIVERSIDADE FEDERAL DE SÃO CARLOS**

Centro de Ciências Exatas e de Tecnologia  
Programa de Pós-Graduação em Química

---

**Folha de Aprovação**

---

Defesa de Tese de Doutorado do candidato Raimundo Rafael Gamela, realizada em 14/07/2020.

**Comissão Julgadora:**

Prof. Dr. Edenir Rodrigues Pereira Filho (UFSCar)

Prof. Dr. Waldomiro Borges Neto (UFU)

Profa. Dra. Wanessa Melchert Mattos (ESALQ/USP)

Profa. Dra. Ana Rita de Araujo Nogueira (EMBRAPA)

Profa. Dra. Maria Márcia Pereira Sartori (UNESP)

O presente trabalho foi realizado com apoio da Coordenação de Aperfeiçoamento de Pessoal de Nível Superior - Brasil (CAPES) - Código de Financiamento 001.

O Relatório de Defesa assinado pelos membros da Comissão Julgadora encontra-se arquivado junto ao Programa de Pós-Graduação em Química.

**Dedico este trabalho aos meus pais Rafael Foquiço Raul Gamela e Maria Cerveja Pangaule Machau (*in memoria*). Dedico também a minha irmã Albertina Rafael Gamela (*in memoria*).**

## **AGRADECIMENTOS**

- ✓ Agradeço a Deus pelo dom da vida e por todas coisas maravilhosas que tem proporcionado na minha vida.
- ✓ A minha namorada Sandra Romão Chiponde pelo amor, carinho e paciência.
- ✓ Aos meus irmãos Roberto Paulo Machilico, Elsa Julião, Lúcia Rafael Gamela, Celina Rafael Gamela pelo amor, carinho, paciência e apoio durante a minha trajetória acadêmica.
- ✓ Ao Prof. Dr. Edenir Rodrigues Pereira Filho por ter aceite o desafio de me orientar, pelos ensinamentos, pela amizade durante esse período.
- ✓ Aos Prof. Drs. Joaquim Nóbrega e Ana Rita Nogueira, por todos ensinamentos ao longo desse percurso.
- ✓ Aos amigos do GAIA, por toda ajuda, ensinamentos, e risadas que tornaram os dias de tristezas em alegrias.
- ✓ Ao meus grandes amigos Msc. Wallace Martins, Dr. Vinicius Câmara Costa, Msc. Michelle Dos Santos Cordeiro e Msc. Beatriz Martins Fontoura pelos ensinamentos, amizade, conselhos, ajuda e pelas nossas brincadeiras e risadas como refúgio da nossa tristeza.
- ✓ Ao meu amigo Msc. Carlos José Domingos Alface, que sempre acreditou em mim, pelos conselhos e amizade incondicional ao longo desses anos.
- ✓ Ao Conselho Nacional de Desenvolvimento Científico e Tecnológico (CNPq) e a Academia Mundial de Ciências (TWAS) pela bolsa concedida (processo número: 158587/2017-0).
- ✓ Agradeço as editoras Elsevier, Spring Nature e Royal Society of Chemistry pela autorização para utilização dos artigos publicados no corpo da tese no formato original.

- ✓ O presente trabalho foi realizado com apoio da Coordenação de Aperfeiçoamento de Pessoal de Nível Superior - Brasil (CAPES) - Código de Financiamento 001

MUITO OBRIGADO

**This PhD thesis is based on the following published articles:**

**“Combining laser-induced breakdown spectroscopy (LIBS) and wavelength dispersive X-ray fluorescence (WDXRF) in a data fusion model to predict the concentration of K, Mg and P in bean seed samples”**

Raimundo R. Gamela, Vinícius C. Costa, Marco A. Sperança and Edenir R. Pereira-Filho. Food Research International, 132, 109037, 2020. Doi: <https://doi.org/10.1016/j.foodres.2020.109037>

**“Direct determination of Ca, K and Mg in cocoa beans by Laser-induced Breakdown Spectroscopy (LIBS): evaluation of three univariate calibration strategies for matrix-matching”**

Raimundo Rafael Gamela, Vinicius Câmara Costa, Diego Vitor Babos, Alisson Silva Araújo and Edenir Rodrigues Pereira-Filho. Food Analytical Methods, 13, 1017-1026, 2020. Doi: <https://doi.org/10.1007/s12161-020-01722-6>

**“Hyperspectral images: a qualitative approach to evaluate the chemical profile distribution of Ca, K, Mg, Na and P in edible seeds employing laser-induced breakdown spectroscopy”**

Raimundo R. Gamela, Marco A. Sperança, Daniel F. Andrade and Edenir R. Pereira-Filho. Analytical Methods, 11, 5543-5552, 2019. Doi: [10.1039/c9ay01916b](https://doi.org/10.1039/c9ay01916b)

**LIST OF ACRONYNS**

AAS – Atomic Absorption spectrometry

CCD – charge coupled device

CF – Calibration free

DoE – Design of experiments

F AAS – Flame atomic absorption spectrometry

OF– Optical fiber

ICP OES – Inductively coupled plasma optical emission spectrometry

ICP-MS – Inductively coupled plasma mass spectrometry

KNN – K -nearest neighbor

LDA – Linear discriminant analysis

LIBS – Laser-induced breakdown spectroscopy

MEC – Multienergy calibration

MLR – Multiple linear regression

NIR – Near infrared spectroscopy

OP GSA – One-point gravimetric standard addition

OP MLC – One-point and multiline calibration

PCR – Principal component regression

PLS – Partial least squares

PLSDA – Partial least squares discriminant analysis

RSD – Relative standard deviation (%)

SECV – Standard error of cross validation

SIMCA – Soft independent modeling of class analogy

SRM – Surface response methodology

SSC – Single sample calibration

TP CT – Two-point calibration transfer

WDXRF – Wavelength dispersive X-ray fluorescence

XRF – X-ray fluorescence



## LIST OF FIGURES

<b>Figure 1.</b> Basic schematic of LIBS equipment, composed by optical fiber (FO), charge coupled device (CCD) and detector .....	5
<b>Figure 2.</b> Number of publications according to the Web of Science Database in the last 10 years involving LIBS and food samples .....	7
<b>Figure 3.</b> Basic schematic of WDXRF, composed by x-ray tube and detection system .....	9
<b>Figure 4.</b> Number of publications according to the Web of Science Database in the last 10 years involving WDXRF and food samples.....	10
<b>Figure 5.</b> Schematic description of the data fusion strategy .....	15

## RESUMO

ESPECTROSCOPIA DE PLASMA INDUZIDO POR LASER (LIBS) E ESPECTROSCOPIA DE FLUORESCÊNCIA DE RAIOS-X COM COMPRIMENTO DE ONDA DISPERSIVO (WDXRF): POSSIBILIDADES E APLICAÇÕES ANALÍTICAS EM ANÁLISE DE ALIMENTOS. Esta tese de doutorado propõe a avaliação das possibilidades e aplicações das técnicas de espectroscopia de plasma induzido por laser (LIBS) e espectroscopia de fluorescência de raios-x com comprimento de onda dispersivo (WDXRF) para determinação de elementos químicos em amostras de sementes comestíveis como feijão, abóbora, ervilha, lentilha e amêndoa de cacau. Essas sementes são importantes na dieta da população brasileira, pois além de fibras dietéticas, aminoácidos, vitaminas, compostos fenólicos, contém elementos químicos importantes para o organismo humano. A utilização da LIBS e a WDXRF permitem análise direta de amostras sem ou com um mínimo preparo de amostra, alta frequência analítica, menor consumo de reagentes químicos, o que as torna atrativas quando comparada com as técnicas de análise convencional. No entanto, uma das desvantagens relacionadas com a técnica LIBS é a sua baixa sensibilidade, altos limites de detecção e ausência de materiais de referência para calibração. Além disso, a determinação elementar por análise direta de sólidos usando LIBS e WDXRF apresenta desafios devido a efeitos de matriz causados por interferências espectrais, características físicas das amostras e o fenômeno de auto-absorção que podem comprometer a exatidão e a precisão dos métodos. Dessa forma, diferentes estratégias de calibração foram avaliadas para análise direta de amostras sólidas por LIBS. Além disso, foi avaliada a possibilidade de uso de imagens hiperespectrais para caracterizar o perfil químico da distribuição dos elementos nas sementes. Em todos os casos, foram utilizadas ferramentas quimiométricas para tratamento de dados.

## ABSTRACT

LASER-INDUCED BREAKDOWN SPECTROSCOPY (LIBS) AND WAVELENGTH DISPERSIVE X-RAY FLUORESCENCE (WDXRF): POSSIBILITIES AND ANALYTICAL APPLICATIONS IN FOOD SAMPLES. This PhD thesis proposes evaluation of the possibilities and analytical applications of the laser-induced breakdown spectroscopy (LIBS) and wavelength dispersive x-ray fluorescence (WDXRF) techniques for the determination of chemical elements in edible seeds as bean seeds, pumpkin, pea, lentil, and cocoa bean. These seeds are important for diet of the Brazilian population because, besides dietetic fibers, amino acids, vitamins phenolic compounds, it contains chemical elements that play different rules in human organism. The use of the LIBS and WDXRF allow the direct solid samples without or with a minimum sample treatment, high analytical frequency, lower reagent consumption, which become attractive when compared with conventional techniques. However, the disadvantage of the LIBS is its lower sensitivity, high limit of detection and absence of certified reference material for calibration. Moreover, the elemental determination by direct solid analysis using LIBS and WDXRF present challenges due to matrix effects caused by spectral interferences, physic characteristic of the samples and self-absorption phenomena, which can compromise the accuracy of the methods. In this sense, different calibration strategies were evaluated for direct solid sample analysis by LIBS. Moreover, was evaluated the possibility of the use of hyperspectral images to characterize the chemical profile of the distribution of the elements on the seeds. In all cases, chemometrics tools were used for data treatment.

## SUMMARY

<b>CHAPTER 1 - INTRODUCTION .....</b>	<b>1</b>
<b>1.1. Introduction .....</b>	<b>2</b>
<b>1.2. Laser-induced breakdown spectroscopy (LIBS) .....</b>	<b>4</b>
<b>1.3. Wavelength dispersive X-ray fluorescence (WDXRF) .....</b>	<b>8</b>
<b>1.4. Chemometrics and data treatment .....</b>	<b>11</b>
<b>1.5. Calibration strategies for LIBS .....</b>	<b>12</b>
<b>1.6. Goals .....</b>	<b>16</b>
<b>1.7. References .....</b>	<b>18</b>
<b>CHAPTER 2 – PUBLISHED RESULTS .....</b>	<b>27</b>
<b>CHAPTER 3 - PUBLISHED RESULTS .....</b>	<b>38</b>
<b>CHAPTER 4 - PUBLISHED RESULTS .....</b>	<b>49</b>
<b>CONCLUSIONS .....</b>	<b>63</b>

# **CHAPTER 1 - INTRODUCTION**

## 1.1. Introduction

Brazil is one of the biggest producers of edible seeds worldwide due to the existence of fertile soil and favorable climate conditions that allows the normal growth of the seeds [1]. Edible seeds have received more attention and their consumption brings benefits to human health [1-3]. Among the several types of edible seeds, bean seeds and cocoa bean can be highlighted.

Common bean seed (*Phaseolus vulgaris* L.) is basic food and is the most consumed type of feeding in Brazil [4] and in the underdeveloped countries where the poverty and malnutrition are prevalent [5]. These seeds contain dietetic fibers, amino acids, vitamins, micro and macronutrients, which are important to supply the nutritional needs in the human metabolism [6-8].

Brazil is considered one of the largest producers and consumer of bean seeds worldwide, with a projection of production around 3 million tons in the 2020/2021 crop. The main producer states of bean seeds are Paraná, Minas Gerais, São Paulo, Goiás and Bahia, that correspond around of 65% of total national production [9]. In addition, the main produced species of bean seeds through genetics improving are *P. vulgaris* L. (black bean, white bean, and kidney bean), *V. unguiculata* L. Walp (cowpea), *C. cajan* L (pigeon pea), and *L. purpureus* L. sweet (Mangalô) [10].

On the other hand, cocoa bean (*Theobroma cacao*) is a culture commonly produced in Brazil, which make this country together with Côte d'Ivoire, Ghana, Indonesia, Nigeria, Cameroon, Ecuador and Malaysia the most producer worldwide, representing around 90% of the world production [11]. Therefore, in Brazil, the southern Bahia is responsible for 94% of total production of the country [12].

There are three varieties of cocoa bean, namely criollo, forastero and trinitário [13]. The forastero group is the most widespread variety, and most prevalent in Bahia plantations. From the genetic mutation of the forastero group, a new variety called catongo and almeida have emerged. While the trinitário emerged from crossing between criollo and forastero, and reproduced asexually (stake rooting, or grafting) consisting of clones [14]. Cocoa beans present high levels of bioactive natural compounds (methylxanthines and phenolic compounds) and antioxidants that are beneficial for human health [3]. Due its chemical composition, cocoa beans have been commonly used in the food processing industry to produce different cocoa-based products, such as handmade chocolate [15], chocolate bars [16], cocoa powder and powdered cocoa drink [17].

Therefore, the determination of inorganic constituents in this type of foodstuff proves to be important to ensure the better quality of food and simultaneously for the consumers. In addition, in specific case of cocoa bean, the reported studies in the literature are related to the bioactive and antioxidant compounds, and have been received more attention, and the information about the elemental composition is still scarce.

Commonly the determination of inorganic constituents in bean seeds and cocoa beans have been performed using inductively coupled plasma optical emission spectrometry (ICP OES) [7,8,10], inductively coupled plasma mass spectrometry (ICP-MS) [11,18], flame atomic absorption spectrometry (F AAS) and graphite furnace atomic absorption spectrometry (GF AAS) [19, 20]. However, the use of these techniques requires a sample preparation step before analysis using various reagents and handling of the samples for long period of time, that increases the risk of

contamination of the samples, affecting the accuracy of the results [19,20]. Therefore, the best way to minimize these drawbacks is, do not perform samples preparation.

Direct solid analysis is an alternative approach that is well-established in the last decades in different fields. In this sense, Laser-induced breakdown spectroscopy (LIBS) and Wavelength dispersive X-ray spectroscopy (WDXRF) are spectroanalytical techniques that allow the direct solid sample analysis of inorganic constituents in different matrices with minimal or no sample preparation. Moreover, these techniques present multielemental capability, high analytical frequency, and low reagents consumption [21-24]. Taking this information in consideration, the variety of the application of the LIBS and WDXRF, these techniques were used for the determination of inorganic constituents in bean seeds and cocoa beans samples. However, the quantitative analysis mainly by LIBS, can be affected by the several matrix effects due the complexity of the samples. Therefore, to minimize these drawbacks and to obtain accurate results, chemometric tools and different calibration strategies, such as univariate and multivariate calibration were used for the data treatment that will be discussed in the next section.

## **1.2. Laser-induced breakdown spectroscopy (LIBS)**

Laser-induced breakdown spectroscopy (LIBS) is a spectroanalytical technique that employs micro-sampling by laser ablation used to detect signals of atomic and molecular emission of the elements present in the micro-plasma during and/or immediately after ablation, and is performed for qualitative and quantitative measurements of elemental composition [23,25]. In this technique, an intense pulsed laser beam is focused on the material for analysis, and this rapid deposition of energy



on the object generates high temperature and density plasma, which results in the material breaking into atoms and emitting characteristic radiation of constituent elements of the sample [23,25,26]. The emitted radiation is analyzed using high resolution optical instruments and its intensities are measured usually with fast solid-state detectors. Together, these devices allow the generation and measurement of a wide-range emission spectrum of the phenomenon induced by the laser pulse. The LIBS consists of an optical set to direct and focus the laser radiation on the sample and to collect the radiation emitted by the plasma; a wavelength selector, such as an optical filter or a grid polychromator; a detector, such as a photomultiplier (to monitor discrete wavelengths) or a set of sensors in the solid state [23,25,26], as depicted in Figure 1.

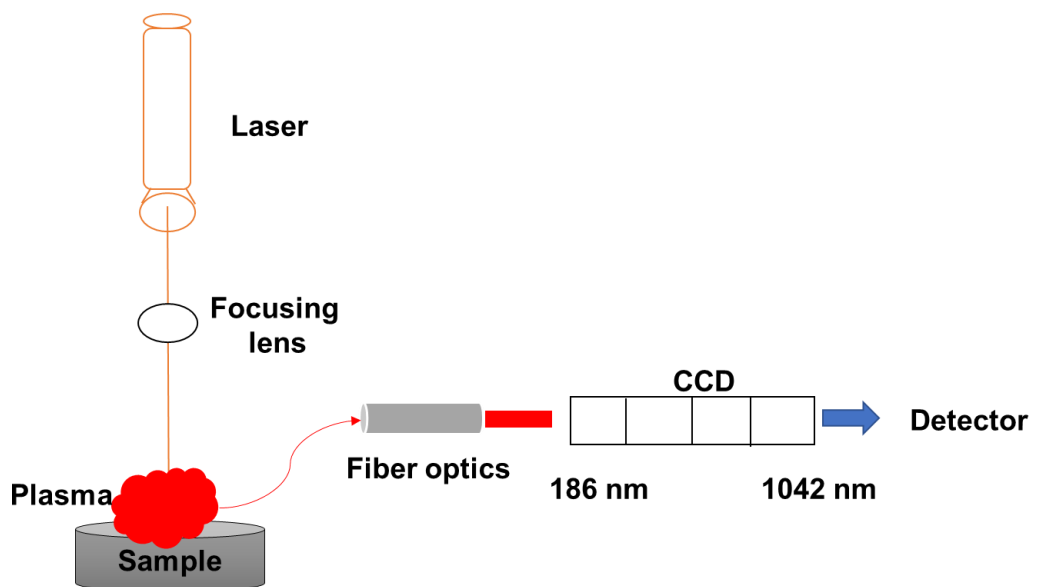


**Figure 1.** Basic schematic of LIBS instrument, composed by optical fiber (OF), charge coupled device (CCD) and detector.

In the last decade, LIBS has become one of the most effective approaches for monitoring samples to elucidate its elemental composition, since it allows the rapid and simultaneous detection of various elements in the  $\text{mg kg}^{-1}$  range and provides *in situ* information, analysis and measurement in real time in any environment and in any type of material (solid, liquid, gas, aerosols) [23,27]. The LIBS technique has been easily used in qualitative analysis, but requires considerable effort in quantitative analysis, given the difficulties of calibration. When compared to well-established spectroanalytical techniques, such as FAAS and ICP OES, the LIBS technique is very versatile and presents the following characteristics [23,25-27]:

- (I) allows direct (*in situ*) and fast analysis;
- (II) sampling mass from 0.1 e 100  $\mu\text{g}$ ;
- (III) minimize the sample preparation and it is possible the direct analysis of hard materials;
- (IV) applicable for gas, liquid and solid (conductors and non-conductors);
- (V) allows elemental analysis of surfaces and in different depths of the solid samples with spatial resolution of few  $\mu\text{m}$ ;
- (VI) it can be used in unhealthy environments and remote monitoring of dangerous samples.

An interesting feature of the LIBS is the large amount of information provided, with spectra containing many peaks related to the elements from the ultraviolet to infrared. This type of information is extremely suitable combined with chemometric tools, whether for data exploration, classification, or calibration. These

strategies will be used in the identification and differentiation of samples and for quantitative analysis.

Several studies were reported in the literature using LIBS for food analysis. Figure 2 shows the number of studies published in last 10 years according to the Web of Science Database, which reports around 122 studies on the search for “laser-induced breakdown spectroscopy and food”. There is an increasing number of studies with food samples employing LIBS due to development of technological advances, feasibility, and the application of chemometric tools for data treatment.

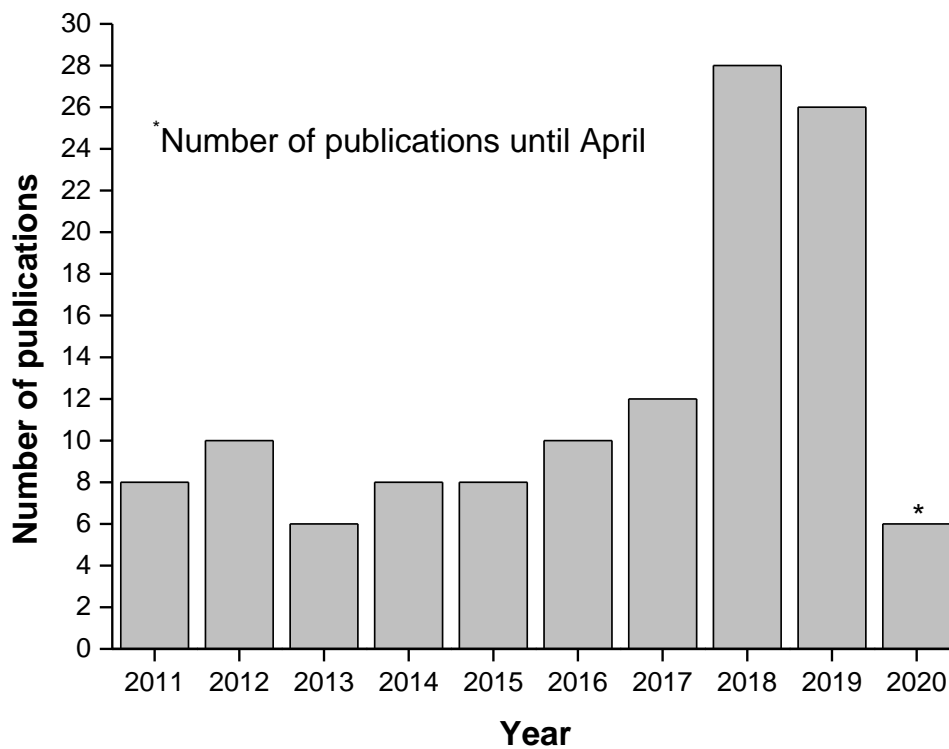


**Figure 2.** Number of publications according to the Web of Science Database in the last 10 years involving LIBS and food samples.

### 1.3. Wavelength dispersive X-ray fluorescence (WDXRF)

X-ray fluorescence spectrometry (XRF) is a non-destructive technique and can be considered as an alternative for the determination of chemical elements in different samples due its sensitivity, feasibility, simplicity, and the measurements are performed sequentially. Moreover, this technique is selective and allows the qualitative and quantitative determination (typically from Na to U) employing direct analysis of solid and liquid samples [28,29]. Wavelength dispersive X-ray fluorescence (WDXRF) is one of the variants of XRF. This technique contains a rhodium tube that emits x-ray with enough energy, which is focused at the sample surface to excite the electrons, and the x-ray characteristic intensities of each element can be used for the determination of the elemental composition in the samples [30-33].

Figure 3 shows the basic schematic of WDXRF technique composed of x-ray tube and detection system. The WDXRF spectrometer is essentially composed of a crystal and a single channel that are used for sequential measurements of various wavelength, or by a multi-channel detector that present a set of crystals (act as monochromator) and detectors for simultaneous measurements. In the conventional spectrometers a crystal with interplanar space known as crystal analyzer, is moved by a goniometer, acting as diffraction grade. One of the great advantages related to the use of WDXRF instruments is that, the analyzes are performed almost without spectral interferences due to the higher resolution provided by crystal/goniometer system [28,29]. It allows a wavelength selection with maximum efficiency in the interesting line or minimum efficiency in the interfering lines. Moreover, there are filters that permits the elimination of interferences between the source characteristic lines and the

emission signal of the interesting element, as well as the correct choice of the analyzer crystal that permits to separate and select a specific region of x-ray emission [28,29].

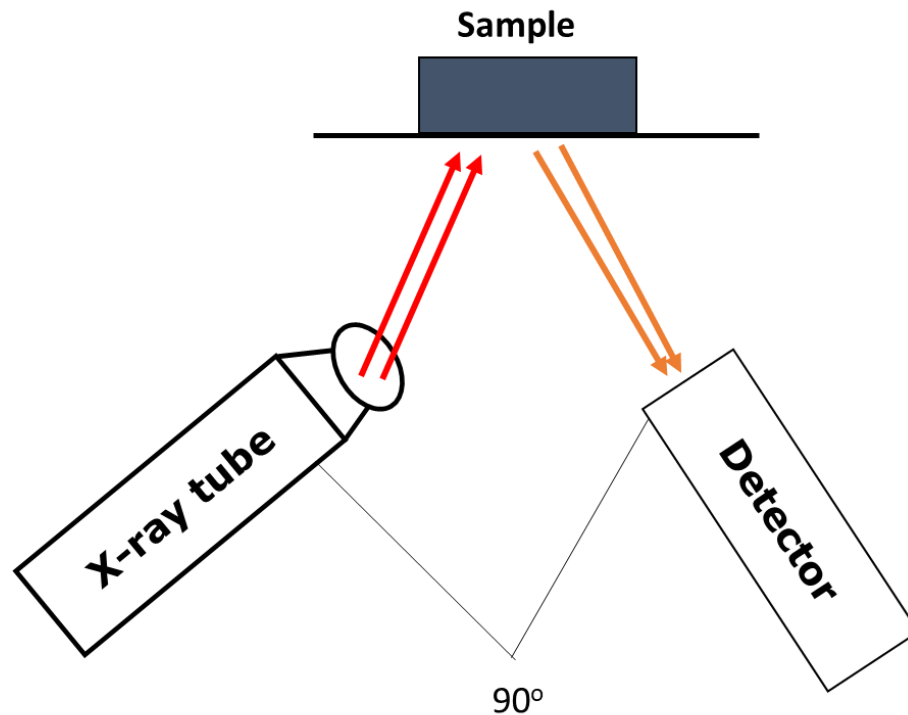


**Figure 3.** Basic schematic of WDXRF, composed of x-ray tube and detection system.

The WDXRF technique has good potential for solid sample analysis without any dissolution or chemical pre-treatment [30,31]. As non-destructive technique, it is possible to reuse the samples in the subsequent analyzes. Therefore, make WDXRF an important tool to reduce time of the analyzes when compared with other analytical techniques, such as ICP OES, ICP-MS and AAS, which involve high cost of operation. In the literature several studies are reported using WDXRF for determination of chemical composition in different samples. Figure 4 shows the

publications in the last 10 years employing WDXRF for determination of metal and non-metals in food samples. This information was obtained according to the Web of Science Database and, is possible to note that there are few studies published (around 11), and the topic search was “wavelength dispersive X-ray fluorescence and food”.

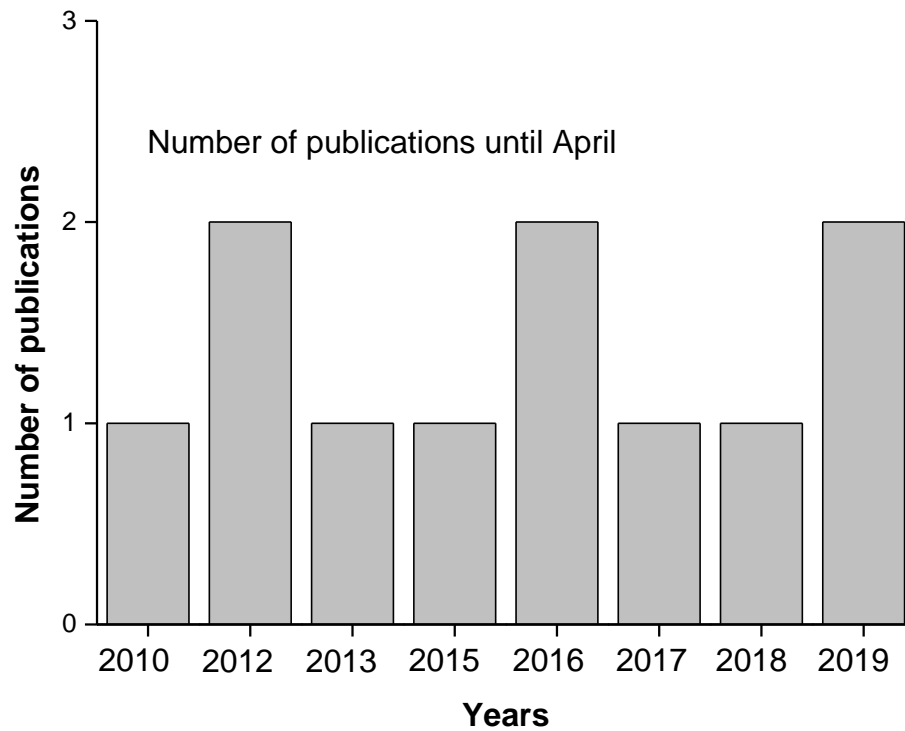


**Figure 4.** Number of publications according to the Web of Science Database in the last 10 years involving WDXRF and food samples.

Therefore, the literature presents few studies employing WDXRF for food analysis. However, due to the characteristic of this technique, it is commonly used for the analysis of geological materials.

#### 1.4. Chemometrics and data treatment

Chemometrics is a science and can be defined as a multidisciplinary approach used to extract chemical relevant information from data produced in chemical experiments [32]. Therefore, with the technological advances, such as computational and statistical algorithms, chemometrics tools have become increasingly important for modeling the dataset generated in analytical techniques. In the case of the LIBS, the data obtained by this technique are complex due to laser-sample, laser-plasma interactions, and chemical characteristic of the samples. In this sense, to minimize these variations and to avoid the incorrect results, data normalizations have been used for this purpose.

There are several types of normalizations that can be employed for preprocessing the data obtained by LIBS, such as normalization by average of all spectra, by Euclidean norm, by sum of all spectra, by highest signal, internal standardization, and others [33]. Moreover, the data can be mean-centering when entire spectra (full spectral profile) is used, and autoscaled when a specific region containing chemical information from an element is selected (variable selection). After that, chemometrics tools can be employed. However, for WDXRF these preprocesses are not necessary due to well defined peak signals of the elements are recorded and is less sensitive to the problems previously described for LIBS. Chemometrics is divided in three main areas: (i) design of experiments (DoE) and surface response methodology (SRM) [34-38], (ii) classification models (exploratory analysis that is unsupervised and supervised pattern recognition) [39] and (iii) multivariate calibration [40]. According to the characteristic of the techniques, some instrumental parameters mainly in LIBS, such as laser pulse fluence and delay time need to be optimized to

obtain optimal conditions of analysis using experimental design. Other chemometrics tools have been used to propose classification models using supervised pattern recognition with most notably, such as k -nearest neighbor (KNN), soft independent modeling of class analogy (SIMCA), linear discriminant analysis (LDA) and partial least squares discriminant analysis (PLS DA) [39,40,41].

Calibration in LIBS is still a challenge and requires considerable efforts for quantitative analysis due to several matrix effects. In this sense, multivariate calibration can be used for this purpose. Multiple linear regression (MLR) and partial least squares (PLS) are some of the main multivariate calibration tools used for elemental determination in different samples employing LIBS [42,43]. Therefore, the choose of a chemometric tool depends on the goal and the analytical application.

### **1.5. Calibration strategies for LIBS**

The use of LIBS for quantitative analysis present limitations due to several matrix effects, such as spectral interference; sample physical characteristics; sample chemical composition and self-absorption that affect the accuracy of the results [44]. Several approaches have been used to overcome these drawbacks, which improve analytical performance of the LIBS. Traditional univariate calibration, such as matrix-matching calibration [45], internal standardization [46,47] and standard addition [48] have been successfully used to minimize matrix effects during the elemental determination by LIBS. Other calibration strategies including multivariate calibration, such as PLS, principal component regression (PCR) and MLR, which are considered first-order multivariate calibrations that minimize the lack of selectivity. The



mathematical algorithms are used to obtain information to predict the concentration in the samples [40,49]. One of the main advantages is that, the models can be modeled in the presence of interference [40,49,50]. However, in some cases, these strategies present drawbacks and do not effectively correct or minimize matrix effects.

Nowadays considerable efforts have been made by different researchers in the study of new calibration strategies as alternative to traditional calibration as previously described. Calibration free (CF) [51], multienergy calibration (MEC) [52], one-point gravimetric standard addition (OP GSA) [53], one-point and multiline calibration (OP MLC) [54,55], single sample calibration (SSC) [55,56] and two-point calibration transfer (TP CT) [43] were proposed to overcome matrix effects and to improve the analytical performance of the LIBS.

All these strategies present several advantages, and more details will be given to OP MLC, SSC and TP CT used in this study. OP MLC is based on a single matrix matching, where one sample with known or certified value is used as standard [54,55]. In this strategy, the concentration of the analytes in unknown sample is calculated through the linear model, built using the emission intensities of unknown samples, which are plotted in *y*-axis and in the signal from the standard plotted in *x*-axis (with known or certified value) [54,55]. The concentration is calculated using the slope of the linear model, as depicted in equation 1.

$$C_{analyte} = slope \times C_{standard}$$

Equation 1

On the other hand, SSC a is simple calibration that uses the correlation between the spectral emission intensities and the concentration of the analytes, and do not require a calibration curve [55,56]. This strategy also uses one sample as standard with known concentration to determine the concentration values of the analytes in unknown samples. Other chemical elements present in the plasma from the sample can be used to estimate the concentration of the analytes in unknown samples, calculated by equation 2 [55,56].

$$C_{analyte} = \frac{\frac{C_{standard\ analyte} \times I_{analyte\ sample}}{I_{analyte\ standard}}}{\sum_{i=1}^N \frac{C_{standard\ element}^N \times I_{element\ sample}^N}{I_{element\ standard}^N}} \quad \text{Equation 2}$$

where  $C_{standard\ analyte}$  and  $I_{analyte\ standard}$  are the concentration and intensity of the emission line of the analyte in the sample, respectively, used for standard calibration.  $I_{analyte\ sample}$  is the emission intensity of the analyte in the unknown sample.  $I_{element\ sample}^N$  is the emission intensity of the element N in the sample of unknown concentration, and  $C_{standard\ element}^N$  and  $I_{element\ standard}^N$  are the concentration and the emission intensity of the element N, respectively, in the sample used as standard calibration [55,56].

For TP CT, a sample with intermediate concentration is choose as calibration standard. In this strategy, a spectral set (it can be the same used in other calibration strategies previously described) is divided in two parts (2 points), where the second set contains the double number spectra of the first one [43,55]. These spectral sets are separately summed (normalization mode number 5). In this sense, both spectra sets are used to build the linear model, where the x-axis contain the number of spectra (both separated sets) and the y-axis is the intensity emission of both points.

This process must be performed for the unknown sample and for the sample chosen as the standard. Therefore, the combination of the slopes from both linear models ( $\text{slope}_{\text{sample}}$  and  $\text{slope}_{\text{standard}}$ ) and the standard concentration ( $C_{\text{standard}}$ ) can be used to calculate the concentration value in the unknown sample as described by equation 3 [43,55].

$$C_{\text{sample}} = C_{\text{standard}} \times \frac{\text{Slope}_{\text{sample}}}{\text{Slope}_{\text{standard}}} \quad \text{Equation 3}$$

However, other calibration strategies have emerged to arise the alternatives to overcome the problems caused by the matrix effect in the elemental determination by LIBS. Recently, data fusion was proposed to minimize matrix effects in the direct solid analysis [57,58]. This strategy combines information (data) from different sources (eg. LIBS and WDXRF/NIR) to produce a single model, as shown in Figure 5.

The spectral data obtained by both techniques need to be separately processed before concatenated matrices, so that, the known of chemometric tools is required. The use of data fusion present some advantages, such as the complementarity from different techniques; improve the predictive capability of the models; identify the variation source of errors and more details of the analytical data; and reduce the errors of the models when compared with those obtained by the individual input sources [57,58].

In the literature, data fusion has been commonly used to improve the classification models in foods, instead identification of botanical origin of honey [59], and authentication and quality assessment of food and beverage [60]. However, few studies were reported using data fusion for calibration purpose, and therefore, this

strategy become important considering the complexity of new matrices, which will need efficient strategies to obtain accurate results.

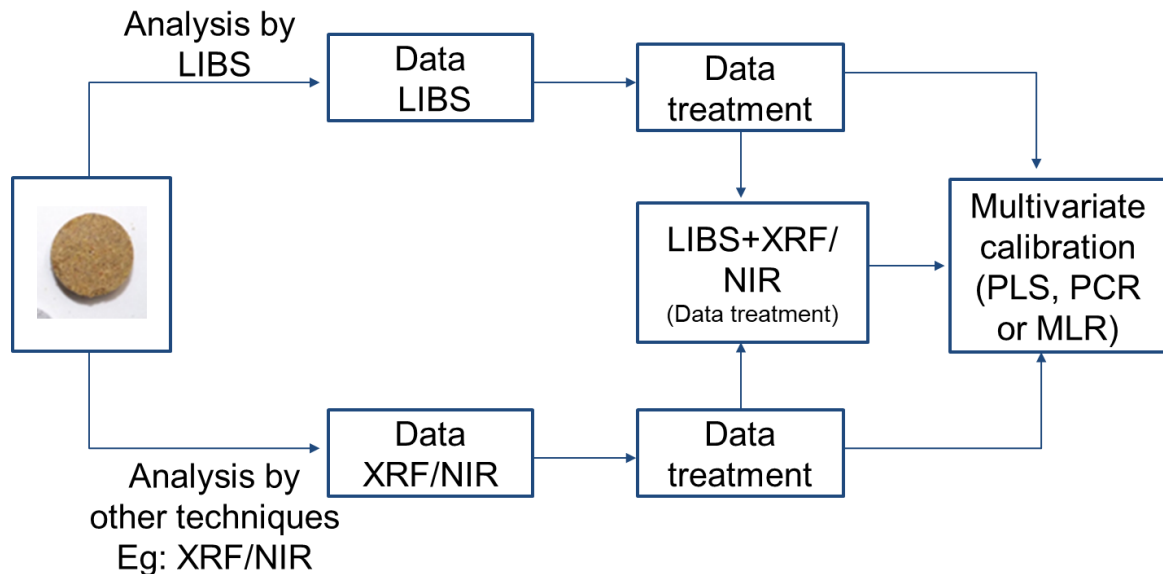


**Figure 5.** Schematic description of the data fusion strategy

## 1.6. Goals

The main goal of this thesis was to develop analytical strategies that allow the use of the LIBS and WDXRF techniques for qualitative and quantitative analysis of edible seeds.

The specific goals were:

1- Evaluate the possibility of direct solid analysis of K, Mg and P in been seed samples employing LIBS and WDXRF (data fusion);

2- Evaluate different calibration strategies for determination of Ca, K and Mg in cocoa bean using LIBS;

3- Evaluate the possibility of the use of hyperspectral images to characterize the chemical profile distribution in different seeds employing LIBS.

The next sections show three published articles about the studies developed in this thesis. The first article is about the use of laser-induced breakdown spectroscopy (LIBS), wavelength x-ray fluorescence (WDXRF), and data fusion to predict the concentration of K, Mg and P in bean seed samples. In this study, traditional univariate, multivariate calibration (MLR) and data fusion strategy were evaluated to build regression models to determine the concentration values of K, Mg and P in bean seeds. Therefore, data fusion strategy combined with MLR presented the best results, where the obtained SECV values were 0.12% for K, 0.019% for Mg and 0.10% for P. The good results obtained, make data fusion a reliable alternative with minimum sample preparation to minimize matrix effect in bean seeds.

The second article is related to evaluate three univariate calibration strategies for the determination of Ca, Mg and K in cocoa bean using LIBS. Calibration strategies as one-point multiline calibration (OP MLC), single sample calibration (SSC) and two-point calibration transfer (TP CT) were evaluated for matrix matching. All of them use one sample with known concentration as standard. Among these strategies, OP MLC and TP CT presented acceptable trueness values, which ranged from 80 to 120% for most analyzed samples. These strategies showed to efficient and reliable alternative to conventional univariate calibration. In all cases for the determination of inorganic constituents in food samples, ICP OES was used as reference technique.

In third article, LIBS was used to evaluate chemical distribution of major elements as Ca, K, Mg, Na and P in edible seeds through hyperspectral images. For that, chemometric tools were used for data treatment of the spectra collected on the surface and depth of the samples. Thus, using score maps and loadings was possible to observe that the distribution profile of the chemical elements from the surface to depth of the seeds is inhomogeneous. This behavior can be associated to the lower absorption capability of the nutrients, which is strictly related to the type of soil. Moreover, using correlation Pearson graph was possible to make an exploratory analysis to evaluate a possible correlation among elements, and associate it with the type of fertilizers used. Therefore, some elements, such as Mg and Na, P and Na, S and P, S and Zn, are extremely correlated. To confirm the presence of these elements in these seeds, ICP OES was used as reference.

### **1.7. References**

- [1] DA SILVA, B. P.; ANUNCIAÇÃO, P. C.; DA SILVA, J. C. M.; LUCIA, C. M. D.; MARTINO, H. S. D.; PINHEIRO-SANT'ANA, H. M. "Chemical composition of Brazilian chia seeds grown in different places". *Food Chem.* 221:1709-1716, 2017.
- [2] LÓPEZ-AMORÓS, M. L.; HERNÁNDEZ, T.; ESTRELLA, I. "Effect of germination on legume phenolic compounds and their antioxidant activity". *J. Food Compos. Anal.* 19:277-283, 2006.
- [3] ORACZ, J.; NEBESNY, E. "Antioxidant properties of cocoa beans (*Theobroma cacao* L.): Influence of cultivar and roasting conditions". *Int. J. Food Prop.* <http://dx.doi.org/10.1080/10942912.2015.1071840>. 2015.

- [4] REZENDE, A. A.; PACHECO, M. T. B.; da SILVA, V. S. N.; FERREIRA, T. A. P. C. "Nutritional and protein quality of dry Brazilian beans (*Phaseolus vulgaris* L.)". *Food Sci. Technol.* 38:421-427, 2018.
- [5] ONWULIRI, V. A.; OBU, J. A. "Lipids and other constituents of *Vigna unguiculata* and *Phaseolus vulgaris* grown in northern Nigeria". *Food Chem.* 78:1-7, 2002.
- [6] MEKASSA B.; CHANDRAVANSI B. S. "Levels of selected essential and non-essential metals in seeds of korarima (*Aframomum corrorima*) cultivated in Ethiopia". *Braz. J. Food Technol.* 18, 102-111, 2015.
- [7] DOS SANTOS, W. P. C.; GRAMACHO, D. R.; TEIXEIRA, A. P. COSTA, A. C. S.; KORN, M. G. A. "Use of Doehlert Design for Optimizing the Digestion of Beans for Multi-Element Determination by Inductively Coupled Plasma Optical Emission Spectrometry". *J. Braz. Chem. Soc.* 19:1-10, 2008.
- [8] SANTOS, W. P. C.; CASTRO, J. T.; BEZERRA, M. A., FERNANDES, A. P.; FERREIRA, S. L. C.; KORN, M. G. A. "Application of multivariate optimization in the development of an ultrasound-assisted extraction procedure for multielemental determination in bean seeds samples using ICP OES". *Microchem. J.* 91:153-158, 2009.
- [9] Ministério da Agricultura, Pecuária e Abastecimento (MAPA). "Projeções do agronegócios – Brasil 2017/2018 a 207/208. Brasília, 2018.
- [10] DOS SANTOS, W. P. C.; SANTOS, D. C. M. B.; FERNANDES, A. P.; CASTRO, J. T.; KORN, M. G. A. "Geographical characterization of beans based on trace elements after Microwave-assisted digestion using diluted nitric acid". *Food Anal. Methods* 6:1133-1143, 2013.

- [11] Rinat Levi Yanus, Hagit Sela, Eitan J.C .Borojovich, Yevgeni Zakon, Magal Saphier, Andrey Nikolski, Efi Gutflais, Avraham Lorber, Zeev Karpas. "Trace elements in cocoa solids and chocolate: An ICPMS study". *Talanta* 119:1-4, 2014.
- [12] International Cocoa Organization-ICCO (2018) Production - Latest figures from the Quarterly Bulletin of Cocoa Statistics. Available in: <[http://www.icco.org/about-us/international-cocoa-agreements/cat\\_view/30-related-documents/46-statistics-production.htm](http://www.icco.org/about-us/international-cocoa-agreements/cat_view/30-related-documents/46-statistics-production.htm)>.
- [13] BECKETT, S. T. "Industrial chocolate manufacture and use". 4 ed. London: Chapman and Hall, 20-23, 2009.
- [14] MANDARINO, E. P.; SENA GOMES, A. R. "Produtividade do cacauero (*Theobroma cacao* L.) cultivados em blocos monoclonais, no sul da Bahia, Brasil". Ilhéus, CEPLAC/CEPEC. Boletim Técnico n° 197. 32p, 2009.
- [15] COSTA, V. C.; PINHEIRO, F. C.; AMORIM, F. A. C.; SILVA, E. G. P.; PEREIRA-FILHO, E. R. "Multivariate optimization for the development of a sample preparation procedure and evaluation of calibration strategies for nutrient elements determination in handmade chocolate". *Microchem J.* 150:10416, 2019.
- [16] VILLA, J. E. L.; PEREIRA, C. D., CADORE, S. "A novel, rapid and simple acid extraction for multielemental determination in chocolate bars". *Microchem. J.* 121:199-204, 2015.
- [17] ANDREY, D.; DUFRIER, J. P.; PERRING, L. "Analytical capabilities of energy dispersive x-ray fluorescence for the direct quantification of iron in cocoa powder and powdered cocoa drink". *Spectrochem. Acta, Part B* 148:137-142, 2018.
- [18] DICO, G. M.; GALVANO, F.; DUGO, G.; D'ASCENZI, C.; MACALUSO, A.; VELLA, A.; GIANGROSSO, G.; CAMMILLERI, G.; FERRANTELLI, V. "Toxic metal levels in



cocoa powder and chocolate by ICP-MS method after microwave-assisted digestion”. *Food Chem.* 245:1163–1168, 2018.

[19] KORN, M. G. A.; MORTE, E. S. B.; DOS SANTOS, D. C. M. B. et al (2008) “Sample preparation for the determination of metals in food samples using spectroanalytical methods—a review”. *Appl Spectrosc. Rev.* 43:67–92, 2008.

[20] FERREIRA, S. L. C.; MIRÓ, M.; DA SILVA, E. G. P.; MATOS, G. D.; DOS REIS, P. S.; BRANDAO, G. C.; DOS SANTOS, W. N. L.; DUARTE, A. T.; VALE, M. G. R.; ARAUJO, R. G. O. “Slurry sampling—an analytical strategy for the determination of metals and metalloids by spectroanalytical techniques”. *Appl. Spectrosc. Rev.* 45:44–62, 2010.

[21] MARKIEWICZ-KESZYCKA, M.; CAMA-MONCUNILL, X.; CASADO-GAVALDA, M. P.; DIXIT, Y.; CAMA-MONCUNILL, R.; CULLEN, P. J.; SULLIVAN, C. “Laser-induced breakdown spectroscopy (LIBS) for food analysis: a review”. *Trends Food Sci. Technol.* 65:80–93, 2017.

[22] COSTA, V.C.; CASTRO, J. P.; ANDRADE, D. F.; BABOS, D. V.; GARCIA, J. A.; SPERANÇA, M. A.; CATELANI, T. A.; PEREIRA-FILHO, E. R. “Laser-induced breakdown spectroscopy (LIBS) applications in the chemical analysis of waste electrical and electronic equipment (WEEE)”. *Trends Anal. Chem.* 108:65–73, 2018.

[23] COSTA, V. C.; AUGUSTO, A. S.; CASTRO, J. P.; MACHADO, R. C.; ANDRADE, D. F.; BABOS, D. V.; SPERANÇA, M. A.; GAMELA, R. R.; PEREIRA-FILHO, E. R. “Laser-induced breakdown spectroscopy (LIBS): histórico, fundamentos, aplicações e potencialidades”. *Quim. Nova* 42:527–545, 2019.

[24] MACHADO, R. C.; ANDRADE, D. F.; BABOS, D. V.; CASTRO, J. P.; COSTA, V. C.; SPERANÇA, M. A.; GARCIA, J. A.; GAMELA, R. R.; PEREIRA-FILHO, E. R. “Solid

sampling: advantages and challenges for chemical element determination-a critical review". *J. Anal. At. Spectrom.* 35:54-77, 2020.

[25] PASQUINI, C.; CORTEZ, J.; SILVA, L. M. C.; GONZAGA, F. B. "Laser Induced Breakdown Spectroscopy". *J. Braz. Chem. Soc.* 18:463-512, 2007.

[26] CREMERS, D. A.; RADZIEMSKI, L. J. "Handbook of Laser-Induced Breakdown Spectroscopy". Ed. Chichester: John Wiley & Sons Ltd, 2006

[27] JANTZI, S. C.; MOTTO-ROS, V.; TRICHARD, F.; MARKUSHIN, Y.; MELIKECHI, N.; DE GIACOMO, A. "Sample treatment and preparation for laser -induced breakdown spectroscopy". *Spectrochem. Acta Part B*, 15:52-63, 2016.

[28] SKOOG, D. A.; HOLLER, F.J.; NIENMAN, T. A. "Princípios de Análise Instrumental". 5.ed. Porto Alegre: Bookman, 2002.

[29] WEST, M.; ELLIS, A. T.; POTTS, P. J.; STRELI, C.; VANHOOFE, C.; WOBRAUSCHEKC, P. "Atomic spectrometry update - a review of advances in X-ray fluorescence spectrometry". *J. Anal. At. Spectrom.* 29:1516–1563, 2014.

[30] COSTA, V. C.; AMORIM, F. A. C.; BABOS, D. V.; PEREIRA-FILHO, E. R. "Direct determination of Ca, K, Mg, Na, P, S, Fe and Zn in bivalve mollusks by wavelength dispersive X-ray fluorescence (WDXRF) and laser-induced breakdown spectroscopy (LIBS)". *Food Chem.* 273:91-98, 2019.

[31] PERRING, L.; ANDREY, D.; BASIC-DVORZAK, M.; BLANC, J. Rapid multimineral determination in infant cereal matrices using wavelength dispersive X-ray fluorescence. *Journal of Agricultural and Food Chemistry.* 53:4696-4700, 2005.

[32] WOLD, S. "Chemometrics; what do we mean with it, and what do we want from it?". *Chemometrics and Intelligent Laboratory Systems* 30:109-115, 1995.

- [33] CASTRO, J. P.; PEREIRA-FILHO, E. R. "Twelve different types of data normalization for the proposition of classification, univariate and multivariate regression models for the direct analyses of alloys by laser-induced breakdown spectroscopy (LIBS)". *J. Anal At. Spectrom.* 31:2005–2014, 2016.
- [34] PEREIRA-FILHO, E. R. "Planejamento Fatorial Em Química: Maximizando a Obtenção de Resultados". Edufscar, Editora, 2015.
- [35] NOVAES, C. G.; BEZERRA, M. A.; DA SILVA, E. G. P.; DOS SANTOS, A. M. P.; ROMÃO, I. L. S.; NETO, J. H. S. "A review of multivariate designs applied to the optimization of methods based on inductively coupled plasma optical emission spectrometry (ICP OES)". *Microchem. J.* 128:331-346, 2016.
- [36] PEREIRA, F. M. V.; PEREIRA-FILHO, E. R. "Aplicação de programa computacional livre em planejamento de experimentos: um tutorial". *Quim. Nova* 41:1061-1071, 2018.
- [37] FERREIRA, S. L. C.; SILVA, M. M. JR.; FELIX, C. S. A.; DA SILVA, D. L. F.; SANTO, S. A. S.; NETO, J. H. S.; DE SOUZA, C. T.; CRUZ, R. A. JR.; SOUZA, A. S. "Multivariate optimization techniques in food analysis – a review". *Food Chem.* 273:3–8, 2019.
- [38] BEZERRA, M. A.; SANTELLI, R. E.; OLIVEIRA, E. P.; VILLAR, L. S.; ESCALEIRA, L. A. "Response surface methodology (RSM) as a tool for optimization in analytical chemistry". *Talanta* 76:965-977, 2008.
- [39] COSTA, V. C.; AQUINO, F. W. B.; PARANHOS, C. M.; PEREIRA-FILHO, E. R. "Identification and classification of Polymer e-waste Using laser-induced breakdown spectroscopy (LIBS) and chemometric tools". 59:390-395, 2017.

- [40] OLIVIERI, A. C. "Practical guidelines for reporting results in single-and multi-component analytical calibration: A tutorial". *Anal Chem Acta* 868:10-22, 2015.
- [41] ARAÚJO, A.; MARINHO W.; GOMES, A. A. "A fast and inexpensive chemometric-assisted method to identify adulteration in acai (*Euterpe oleracea*) using digital images". *Food Anal. Methods* 11:1920-1926, 2018.
- [42] SPERANÇA, M. A.; ANDRADE, D. F.; CASTRO, J. P.; PEREIRA-FILHO, E. R. "Univariate and multivariate calibration strategies in combination with laser-induced breakdown spectroscopy (LIBS) to determine Ti on sunscreen: A different sample preparation procedure". *Opt. Laser Technol.* 109:648-653, 2019.
- [43] CASTRO, J. P.; BABOS, D. V.; PEREIRA-FILHO, E. R. "Calibration strategies for the direct determination of rare earth elements in hard disk magnets using laser-induced breakdown spectroscopy *Talanta* 208:120443, 2020,
- [44] TAKAHASHI T.; THORNTON B. "Quantitative methods for compensation of matrix effects and self-absorption in LIBS signals of solid". *Spectrochim Acta B* 138:31–42, 2017.
- [45] ANDRADE, D. F.; PEREIRA-FILHO, E. R. "Direct Determination of Contaminants and Major and Minor Nutrients in Solid Fertilizers Using Laser-Induced Breakdown Spectroscopy (LIBS)". *J. Agric. Food Chem.* 64:7890–7898, 2016.
- [46] GUPTA, G. P.; SURI, B. M.; VERMA, A.; SUNDARARAMAN, M.; UNNIKRISHNAN, V. K; ALTI, K.; KARTHA, V. B.; SANTHOSH, C. Quantitative elemental analysis of nickel alloys using calibration-based laser-induced breakdown spectroscopy. *J. Alloys Compd.* 509:3740–3745, 2011.
- [47] UNNIKRISHNAN, V. K.; NAYAK, R.; DEVANGAD, P.; TAMBOLI, M. M.; SANTHOSH, C.; KUMAR, G. A.; SARDAR, D. K. "Calibration based laser-induced

breakdown spectroscopy ( LIBS ) for quantitative analysis of doped rare earth elements in phosphors”. *Mat. Lett.* 107:322–324, 2013.

[48] BILGE, G., BOYACI, I. H.; ESELLER, K. E.; TAMER, U.; CAKIR, S. “Analysis of Bakery Products by Laser-Induced Breakdown Spectroscopy”. *Food Chem.* 181:186-190, 2015.

[49] ESCANDAR, G. M.; OLIVIERI, A. C.; FABER, N. M.; GOICOECHEA, H. C.; MUÑOZ, P. A.; POPPI, R. J. Second- and third-order multivariate calibration: data, algorithms and applications. *Trends Anal. Chem.* 26:752–765, 2007.

[50] Zhang, T., Tang, H.; Li, H. Chemometrics in laser-induced breakdown spectroscopy. *J. Chemom.* 32:e2983, 2018.

[51] TOGNONI, E.; CRISTOFORETTI, G.; LEGNAIOLI, S.; PALLESCHI, V. Calibration-free laser-induced breakdown spectroscopy: State of the art. *Spectrochim. Acta B* 65:1-14, 2010.

[52] BABOS, D. V., COSTA, V. C.; VIRGILIO, A.; DONATI, J. L.; PEREIRA-FILHO, E. R. “Multi-energy calibration (MEC) applied to laser-induced breakdown spectroscopy (LIBS)”. *J. Anal. At. Spectrom.* 33:1753-1762, 2018.

[53] BABOS, D. V.; BARROS, A. I.; NÓBREGA, J. A.; PEREIRA-FILHO, E. R. “Calibration strategies to overcome matrix effects in laser-induced breakdown spectroscopy: Direct calcium and phosphorus determination in solid mineral supplements”. *Spectrochim. Acta B* 155:90–98, 2019.

[54] HAO Z. Q.; LIU, L.; ZHOU, R.; MA, Y. W.; LI, X. Y.; GUO, L. B.; LU, Y. F.; ZENG, X. Y. “One-point and multi-line calibration method in laser-induced breakdown spectroscopy”. *Opt Express* 26:22926–22933, 2018.

- [55] GAMELA, R. R.; COSTA, V. C.; BABOS, D. V.; ARAÚJO, A. S.; PEREIRA-FILHO, E. R. "Direct determination of Ca, K, and Mg in cocoa beans by laser-induced breakdown spectroscopy (LIBS): Evaluation of three univariate calibration strategies for matrix matching". *Food Anal. Methods*. 13:1017-1026, 2020.
- [56] YUAN, R.; TANG, Y.; ZHU, Z.; HAO, Z.; LI, J.; YU, H.; YU, Y.; GUO, L.; ZENG, X.; LU, Y. "Accuracy improvement of quantitative analysis for major elements in laser-induced breakdown spectroscopy using single sample calibration". *Anal. Chim. Acta* 1064:11–16, 2019.
- [57] GAMELA, R. R.; COSTA, V. C.; SPERANÇA, M. A.; PEREIRA-FILHO, E. R. "Laser-induced breakdown spectroscopy (LIBS) and wavelength dispersive X-ray fluorescence (WDXRF) data fusion to predict the concentration of K, Mg and P in bean seed samples". *Food Res. Int.* 132:109037, 2020.
- [58] DE OLIVEIRA, D. M.; FONTES, L. M., PASQUINI, C. "Comparing laser induced breakdown spectroscopy, near infrared spectroscopy, and their integration for simultaneous multi-elemental determination of micro- and macronutrients in vegetable samples". *Anal. Chim. Acta* 1062:28-36, 2019.
- [59] BALLABIO, D.; ROBOTTI, E.; GRISONI, F.; QUASSO, F.; BOBBA, M.; VERCELLI, S.; GOSETTI, F.; CALABRESE, G.; SANGIORGI, E.; ORLANDI, M.; MARENGO, E. "Chemical profiling and multivariate data fusion methods for the identification of the botanical origin of honey". *Food Chem.* 266:79-89, 2018.
- [60] HOEHSE, M.; PAUL, A.; GORNUSHKIN, I.; PANNE, U. Multivariate classification of pigments and inks using combined Raman spectroscopy and LIBS. *Anal. Bioanal. Chem.* 402:1443-1450, 2012.

## **Chapter 2 – Published Results**



Contents lists available at ScienceDirect

## Food Research International

journal homepage: [www.elsevier.com/locate/foodres](http://www.elsevier.com/locate/foodres)

# Laser-induced breakdown spectroscopy (LIBS) and wavelength dispersive X-ray fluorescence (WDXRF) data fusion to predict the concentration of K, Mg and P in bean seed samples

Raimundo R. Gamela<sup>a</sup>, Vinícius C. Costa<sup>b</sup>, Marco A. Sperança<sup>a</sup>, Edenír R. Pereira-Filho<sup>a,\*</sup>

<sup>a</sup> Group of Applied Instrumental Analysis, Department of Chemistry, Federal University of São Carlos, P.O. Box 676, São Carlos, São Paulo State 13565-905, Brazil

<sup>b</sup> Laboratory of Toxicant and Drug Analyses (LATF), Federal University of Alfenas (Unifal), Alfenas, MG 37130-000, Brazil

## ARTICLE INFO

## Keywords:

Bean seeds  
Direct solid analysis  
Calibration strategies  
Multiple linear regression  
Univariate calibration  
Chemometrics

## ABSTRACT

The present study aims to develop a fast and simple method for the determination of potassium (K), magnesium (Mg) and phosphor (P) in bean seed samples employing a data fusion strategy in the low-level with laser-induced breakdown spectroscopy (LIBS) and wavelength dispersive X-ray fluorescence (WDXRF) techniques combined with direct solid sample analysis. Univariate and multivariate (multiple linear regression, MLR) calibration and leave-one-out cross validation strategies were evaluated to build the calibration models correlated with reference values obtained by inductively coupled plasma optical emission spectrometry (ICP OES) after microwave-assisted acid digestion. The proposed calibration models for WDXRF and LIBS were tested using 14 samples, where the best results were obtained using the data fusion of both techniques. The standard error of cross validation (SECV) obtained were: 0.12% for K, 0.019% for Mg and 0.10% for P, and the trueness ranged between 89 and 124% for K, 82 to 125% for Mg and 73 to 128% for P. These values showed a good accuracy, precise and robustness of the method and a greater reliability of the results. In addition, the predicted concentrations ranged from 0.97 to 1.55% for K, 0.14 to 0.28% for Mg, and 0.27 to 0.82% for P.

## 1. Introduction

In developing and underdeveloped countries, bean seeds have been used as an important source of nutrients to reduce the rate of malnutrition and, at the same time, guarantee an adequate food security for the population (Onwuliri & Obu, 2002). Moreover, bean seeds are rich in protein, carbohydrate, dietary fiber, and are good source of antioxidants, as well as vitamins and minerals (Rezende, Pacheco, da Silva, & Ferreira, 2018; Shimelis & Rakshit, 2005). Regarding mineral content, potassium (K), magnesium (Mg) and phosphor (P) are the most available elements in this type of food, which play an important role in the human body (Santos, Santos, Fernandes, Castro, & Korn, 2013).

The scientific literature reports several studies employing different analytical techniques for the determination of macro and micro-nutrients in food matrices. The most techniques used for these analyzes are: flame atomic absorption spectrometry (FAAS) (Amorim et al., 2017; Gamela, Barrera, Duarte, & Boschetti, 2019; Mir-Marqués, Cervera, & De La Guardia, 2016) and inductively coupled plasma optical emission spectrometry (ICP OES) (Mir-Marqués et al., 2016; Santos et al., 2008a, 2008b, 2009).

However, these techniques require a prior step of sample preparation, such as acid mineralization or dissolution, which represents one of the main challenges in the elemental analysis, because it is laborious, intensive, time consuming, and is major source of errors due to analyte loss and/or sample contamination (Ferreira et al., 2010).

Laser-induced breakdown spectroscopy (LIBS) become an excellent alternative to overcome the aforementioned drawbacks. LIBS has a laser that is focused in the sample surface. After that, several phenomena take place: sample vaporization, analytes ionization and later emission. The emission signals can be recorded, and an emission spectrum is generated, and, each analyte is related to several emission lines. Apart from direct solid sample analysis with minimal or no sample preparation, this technique brings important features, such as multielemental capability, high analytical frequency, and low reagents consumption (Hahn & Omenetto, 2012; Markiewicz-Keszycka et al., 2017; Costa et al., 2018a). Several studies are reported using LIBS for the determination of chemical composition in different types of matrices, for example, powdered milk and dietary supplements (Augusto, Barsanelli, Pereira, & Pereira-Filho, 2017), bivalve mollusks (Costa, Amorim, Babos, & Pereira-Filho, 2019), cassava flour (Costa et al., 2018b),

\* Corresponding author.

E-mail address: [erpf@ufscar.br](mailto:erpf@ufscar.br) (E.R. Pereira-Filho).

<https://doi.org/10.1016/j.foodres.2020.109037>

Received 8 October 2019; Received in revised form 23 January 2020; Accepted 25 January 2020

Available online 28 January 2020

0963-9969/ © 2020 Elsevier Ltd. All rights reserved.



medicinal herbs (Andrade, Pereira-Filho, & Konieczynski, 2017), solid fertilizers (Andrade & Pereira Filho, 2016), and soils (Junior et al., 2009).

Besides LIBS, wavelength dispersive X-ray fluorescence (WDXRF) is a non-destructive technique that contain rhodium as x-ray source. The x-ray with enough energy is generated and focused at the solid sample surface to excite the electron near the nuclei of the atom. In the specific case of Mg, for instance, the electron near the nucleus is ejected and an electron from K level emits energy and replace the electron ejected.

This technique is considered selective and the measurements are performed sequentially (West et al., 2014). The literature presents several applications of WDXRF for the determination of macro and micronutrients in different types of samples, such as bivalve mollusks (Costa et al., 2019), infant cereals (Perring, Andrey, Basic-Dvorzak, & Blanc, 2005), milk and dairy products (Pashkova, 2009), human hair (Santos, Sperança, & Pereira, 2018), and pharmaceutical products (Balaram, 2016).

Due to specific features of LIBS, some instrumental parameters as laser pulse fluence and delay time need to be optimized and, in this sense, chemometric tools become necessary. Factorial design, central composite, Box-Behnken and Doehlert designs have been frequently used for the optimization in analytical applications due its several advantages, such as reduced number of experiments, possibilities to evaluate interactions among variables, reliable results, optimization of the experiments in a short period of time, and the selection of optimal experimental conditions (Bezerra, Santelli, Oliveira, Villar, & Escaleira, 2008; Ferreira et al., 2018).

Univariate models have been commonly used for calibration using single analytical sources for elemental determination in different matrices. However, a new data fusion strategy has aroused interest in analytical chemistry field for different purposes (Liu & Brown, 2004; Whittle, Gillet, & Willett, 2006). This strategy combines multiple sources of data to produce a single model, and it provides complementarity and improvements of the capability of prediction of the models when compared with individual input sources (Liu & Brown, 2004; Whittle et al., 2006; Willett, 2013). Furthermore, data fusion allows to build regression models with better statistical parameters (predictions with lower error), identify the variation sources and more detailed information of analytical data (Spiteri et al., 2016). An interesting feature of data fusion is the fact that, the data can be independently generated from each analytical technique, and then, combined and used to calculate regression models and predict the concentrations in the samples (Ballabio et al., 2018; Borrás et al., 2015; Assis et al., 2019).

Different data fusion strategy employing several analytical techniques were already reported in the literature for different purposes as identification of botanical origin of honey (Ballabio et al., 2018; Hoehse, Paul, Gornushkin, & Panne, 2012), and authentication and quality assessment of food and beverage (Borrás et al., 2015).

For elemental determination, only one study was found employing data fusion using LIBS and near infrared spectroscopy (NIR) for the determination of micro and macronutrients in vegetable samples (De Oliveira, Fontes, & Pasquini, 2019). In the light of this, the goal of the present study was to evaluate the possibility of the use of data fusion, strategy combining information from both LIBS and WDXRF for the determination of K, Mg and P in bean seed samples. In addition, univariate and multiple linear regression (MLR) calibrations were evaluated to calculate regression models.

## 2. Material and methods

### 2.1. Instrumentation

The determination of K, Mg and P in bean seed samples was carried out using a LIBS instrument, J200 model from Applied Spectra (Freemont, USA) equipped with a Nd:YAG laser (1064 nm) used for

emission data acquisition step. The instrument contains a high efficiency particulate air cleaner (HEPA) to purge the ablated particles and the movement of the sample is automated with a XYZ stage. It also contains a  $1280 \times 1024$  complementary metal-oxide semiconductor (CMOS) color-camera imaging system. The optical fiber bundle is coupled to a 6-channel charged-coupled device (CCD) spectrometer to convert the plasma emission light into spectra, with a spectral range of emission signals between 186 and 1042 nm resulting in 12,288 variables. The gate width is the time that spectrometer collects the emission signals, which is 1.05 ms. For the identification of the emission lines of the elements was used an Aurora Software Package (also from Applied Spectra). All operational parameters were optimized using factorial design strategy and were:  $2699 \text{ Jcm}^{-2}$  laser pulse fluence and 1.9  $\mu\text{s}$  delay time. Detailed information about the optimization will be presented in the next sections.

A commercial wavelength dispersive X-ray fluorescence (WDXRF) instrument from Thermo Fischer Scientific (Madison, WI, USA) Perform-X ARL model was used for direct analysis of the samples. This instrument contains a rhodium X-ray source, which was used for all the acquisitions with a maximum of 4200 W power. These acquisitions were possible due to the detectors that register the count *per* second of the X-ray emission lines that correspond to each crystal used. These crystals reflect in different regions of wavelength, varying from 0.124 Å (0.0124 nm) (LiF220) to 162.662 Å (16.2662 nm) (AX16c). The instrument has 5 crystals that can be used in the wavelength dispersion; and the choice of specific crystal is based on the characteristic wavelength of the element of interest. Moreover, there are 4 different collimators (0.15 mm, 0.40 mm, 1.00 mm and 2.60 mm) and 2 detectors: a flow proportional counter (FPC) and a scintillation counter (SC). In the present study, only the electronic transition  $K\alpha$  was considered for all elements and for each one, depending on its wavelength, different crystals were employed.

Reference concentration values of K, Mg and P were obtained using an ICP OES, model iCAP 7000 (Thermo Fisher Scientific, USA). The plasma conditions and the emission lines used in ICP OES analysis are described in Table 1S as supplementary material.

### 2.2. Reagents

High purity deionized water (18 MΩ cm resistivity) produced from a Milli-Q® Plus (Millipore Corp, Bedford, MA, USA) was used to prepare all solutions throughout the study. All glassware and polypropylene vessels were previously decontaminated using detergent and by soaking in a nitric acid (HNO<sub>3</sub>) 10% (v v<sup>-1</sup>) (Synth, Diadema, Brazil) solution *per* 24 h and rinsed with ultrapure water before use. The external calibration curves for K, Mg and P were prepared using appropriate dilution of stock standard solutions of 1000 mg L<sup>-1</sup> (Specsol, São Paulo, Brazil) with HNO<sub>3</sub>, previously purified with a distillation system Distillacid™ BSB-939-IR (Berghof, Eningen, German). In addition, purified HNO<sub>3</sub> and hydrogen peroxide (H<sub>2</sub>O<sub>2</sub>) 30% (w w<sup>-1</sup>) (Synth) were used for samples mineralization.

### 2.3. Sampling and sample preparation

A total of 14 samples of dried bean seeds of different species, namely *P. vulgaris* (S1-S10), *V. unguiculate* (S11), *V. angularis* (S12), *V. radiata* (S13), and *C. cajan* (S14), were acquired at local markets (São Carlos, São Paulo, Brazil). Therefore, the selected samples for the present study represent the most popular species of bean seeds commercialized in Brazil. Also, the use of these different varieties allowed to evaluate the robustness of the proposed method.

Before analysis by LIBS and WDXRF, the samples were ground using a mill type Wyllie (model CE-430, CIENLAB, São Paulo, Brazil). This step aimed to reduce the particle size and to improve the homogeneity of the analytes in the samples. Furthermore, the samples were pressed using 60 t in<sup>-1</sup> to form pellets (~12 mm diameter) in order to facilitate

the analysis of the samples by both instruments (LIBS and WDXRF).

#### 2.4. Determination by ICP OES (reference values acquisition)

Sample masses of 0.350 g was directly weighted in the Teflon® flasks, and 4.0 mL of HNO<sub>3</sub> 65% v/v, 2.0 mL of H<sub>2</sub>O<sub>2</sub> 30% w/w and 2.0 mL of H<sub>2</sub>O were added. After that, a microwave radiation system (Speed four, Berghof, Eningen, BW, Germany) with DAP 60 Teflon® closed vessels were used for mineralization. The mineralization procedure was performed using the following heating program, performed in three steps (temperature in °C/ramp in min/hold in min): (i) 170/5/10; (ii) 200/1/15; (iii) 50/1/10. After the mineralization step, the content was transferred to volumetric flask and the final volume was completed to 40 mL. The acid mineralization was used for the determination of K, Mg and P to obtain reference concentrations for further calculation calibration models using LIBS and/ or WDXRF. All mineralization procedure was performed in triplicate (n = 3), and to verify the performance of the procedure, the certified reference material (CRM) Apple leaves (NIST-1515) was also mineralized.

#### 2.5. Optimization of instrumental conditions of LIBS

For LIBS elemental determination, several laser operating conditions (laser pulse fluence and laser energy) and emission measurement parameters (delay time and gate width) need to be optimized. Thus, prior to LIBS analysis of the samples, the instrumental parameters were evaluated using central composite design with 11 experiments (with 3 replicates in central point). The variables evaluated were: laser pulse fluence at five level (1448, 1811, 2699, 3511 and 3820) and delay time at five levels (0.5, 0.7, 1.5, 1.7 and 1.9), as shown in Table 1. The optimization was performed using a single sample, and approximately 600 spectra were collected at different regions of the pellet surface in raster mode. In addition, the laser settings used were a scan length of 8 mm, a laser repetition rate of 5.0 Hz, and ablation chamber speed of 1.0 mm s<sup>-1</sup>.

The central composite design monitored response was the area, height and signal-to-background ratio (SBR) obtained from the most intense atomic (I) and ionic (II) emission lines of K I 766.49, Mg II 279.55 and P I 213.62. In order to obtain a simultaneous optimization, desirability (*di*) function was calculated, employing equation (1), to find the best conditions for each response. The *di* function attributes values between 0 (undesirable response, lowest SBR, area and height) and 1 (desirable response, highest SBR, area and height). Thus, overall desirability (OD) is the geometric mean of all single responses, as can be seen in equation (2).

$$di = \left( \frac{y - L}{T - L} \right)^s \quad (1)$$

**Table 1**

Matrix of the central composition design with the variables used for the optimization of instrumental conditions employing LIBS, and the overall desirability values (OD) obtained.

Experiments	Laser pulse fluence (mJ cm <sup>-2</sup> )		Delay time (μs)		OD
	Real	Coded	Real	Coded	
1	1811	-0.996	0.7	-1.000	0.32
2	3514	1.004	0.7	-1.000	0.42
3	1811	-0.996	1.7	1.000	0.44
4	3514	1.004	1.7	1.000	0.57
5	2699	0.000	1.2	0.000	0.52
6	2699	0.000	1.2	0.000	0.46
7	2699	0.000	1.2	0.000	0.61
8	1448	-1.422	1.2	0.000	0.46
9	3820	1.363	1.2	0.000	0.47
10	2699	0.000	0.5	-1.414	0.37
11	2699	0.000	1.9	1.414	0.58

where *L* is the lowest acceptable value for the response, *T* is the target value, and *s* is the weight (when equal to 1 = linear desirability function). In the present study, *L* values were the lowest SBR, height and area in the set of experiments for each element and *T* values were the highest SBR, height and area for each element. The weight *s* was 1.

$$OD = \sqrt[m]{d_1 d_2 \dots d_m} \quad (2)$$

where *m* is the number of response variables evaluated simultaneously.

#### 2.6. Data treatment for LIBS

For the data treatment, Microsoft Excel was applied to calculate the univariate calibration models. MATLAB® 2018a (MathWorks, Natick, MA, USA) was used to apply homemade routines developed by our research group for the data processing (Castro & Pereira-Filho, 2016), and the Aurora software (Applied Spectra) was employed for the identification of the emission lines obtained by LIBS.

The spectra obtained by LIBS presents high complexity due to the sample microheterogeneity and signal fluctuation during data acquisition. In this case, in order to overcome the mentioned possible problems, normalization of the data is mandatory. In this sense, twelve (12) normalization modes were assessed: (1) signal average; (2) signal normalized by individual norm and then averaged; (3) normalized by area; (4) signal normalization by maximum and then, averaged; (5) signal sum; (6) signal sum after normalization by individual norm; (7) signal normalized by area; (8) signal normalization by maximum and then summed; (9) signal average after normalization by C I 193.09 nm, (10) signal sum after normalization by C I 193.09 nm; (11) signal average after normalization by C I 247.85 nm; (12) signal sum after normalization by C I 247.85 nm (Castro & Pereira-Filho, 2016).

#### 2.7. WDXRF analysis

For quantitative analysis of K, Mg and P using WDXRF, some operational parameters such as spot size, measurement time should be selected. Moreover, an FPC (flow proportional counter) detector and spot size of Ø10 mm, and a counting time of 20 s was used. The tube voltage and current were 30 KV and 40 mA for all determined elements. The measurements were carried out using the following wavelengths (Å) selected, which correspond the characteristics transitions for each element: K (Kα) 3.74, Mg (Kα) 9.89 and P (Kα) 6.1. All analyzes were performed in triplicate using pellets from different bean seed samples.

However, for WDXRF technique, the calculation of 12 normalization modes were not necessary, since the elements present well defined peak signals and is less sensitive to the aforementioned problems that could occur in LIBS analysis.

### 3. Results and discussion

#### 3.1. Reference method for LIBS and WDXRF

Bean seed samples were mineralized using microwave-assisted acid digestion and analyzed by ICP OES for the determination of K, Mg and P. The obtained concentration values were used as reference method for LIBS and WDXRF. Therefore, to evaluate the mineralization procedure CRM of Apple leaves (NIST-1515) was submitted to a microwave acid mineralization and the obtained concentration of all analytes was concordant with the certified values (Student *t* test at 95% of confidence level) showing that the procedure of sample preparation can be employed as reference method. The obtained concentration values of K, Mg and P in the samples and CRM are shown in Table 2S in the supplementary material.

### 3.2. Optimization of instrumental parameters for LIBS

During the analysis by LIBS, the interaction of the laser with sample is dependent on the matrix, analyte homogeneity, sample and surface. Furthermore, the properties of the laser induced by plasma, also can be affected by the laser operational conditions (Costa et al., 2018a; Hahn & Omenetto, 2012). In this sense, instrumental parameters were optimized using central composite design with 11 experiments. The optimized variables were laser pulse fluence and delay time, used in five levels coded between  $-1.422$  and  $1.422$ , as shown in Table 1.

Thus, the individual desirability ( $d_i$ ) was calculated using area and height signals, as well as the signal-to-background ratio (SBR) of K I 766.49, Mg II 279.55 and P I 213.62. In this case, each response was coded from 0 (undesirable response, lowest SBR, area and height) to 1 (desirable response, highest SBR, area and height). Therefore, the individual desirability was combined into a single response (overall desirability, OD), as depicted in Table 1.

After that, twelve normalization modes were performed, and each normalization mode was tested by analysis of variance (ANOVA). Thus, the normalization mode by sum (normalization 5) was chosen because it presented a better fit of the model. In this case, it was possible to verify that the regression model did not show lack of fit, i.e., comparing the Mean of Square of lack of fit (MSlof) and Mean of Square of pure error (MSpe), the  $F_{calculated}$  (0.41) is lower than  $F_{tabulated}$  (19.16). However, comparing the Mean of Square of Regression (MSR) and Mean of Square of Residue (MSRes), the  $F_{calculated}$  (2.9) should be higher than  $F_{tabulated}$  (5.05). Despite the regression was not significant, this detail does not affect the predictive capability of the model.

Fig. 1 shows the surface response of the optimized conditions and it is possible to observe that variable 1 (laser pulse fluence) was not significant including their interactions. Thus, this variable can be used in any condition tested in the experimental domain (from 1448 to 3820  $\text{mJ cm}^{-2}$ ). On the other hand, variable 2 (delay time) presented more influence, and high values of OD were obtained when high delay time is used (1.9  $\mu\text{s}$ ). Therefore, the central composite design generated the OD model described by Equation (3).

$$OD = 0.528 \pm 0.09 + 0.069 \pm 0.06v_2 \quad (3)$$

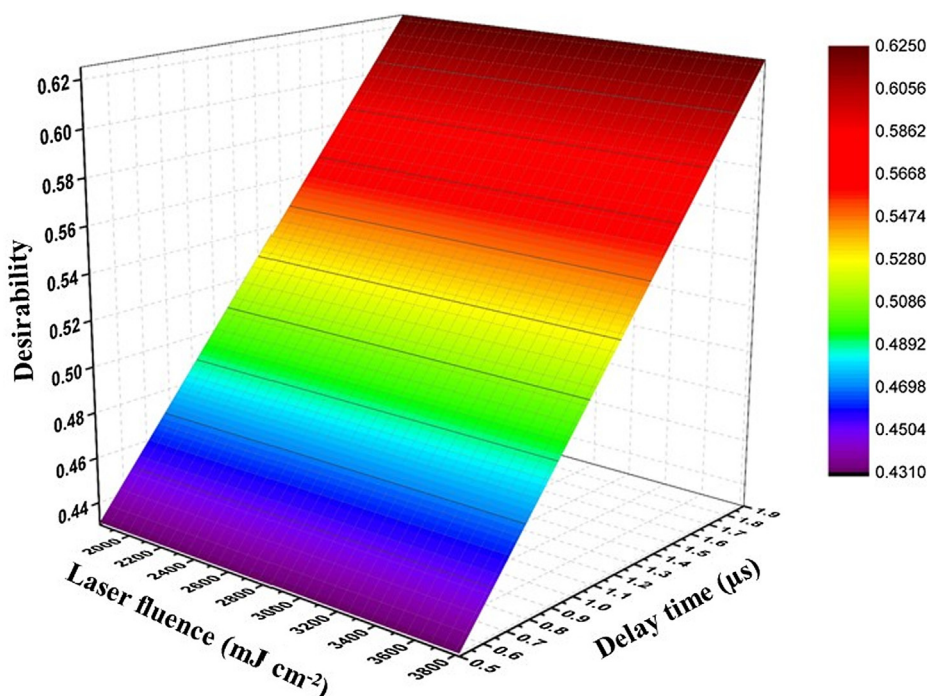


Fig. 1. Response surface of the optimized instrumental conditions for LIBS in function of the overall desirability obtained from central composite design for determination of K, Mg and P in bean seed samples.

Therefore, the best optimized conditions were found using experiment 11 (see Table 1), with values for delay time in 1.9  $\mu\text{s}$  and fluence in 2699  $\text{mJ cm}^{-2}$ , with 53 mJ for laser pulse energy and 50  $\mu\text{m}$  for spot size. These optimized conditions were used for further experiments.

### 3.3. Univariate calibration models for LIBS and WDXRF

After the acquisition of around 500 spectra for each sample by LIBS, 12 normalization modes were calculated, and a routine (libs\_par2) was used to calculate SBR, as well as both the signal area and height for the region of the emission line of interest specified by the user. The monitored emission lines of the elements were (nm): K I 766.49 and K I 769.89; Mg II 279.55, Mg II 279.79, Mg II 280.27, Mg I 383.83, and Mg I 518.36; P I 213.62 and P I 253.56. The calibration models were calculated employing univariate calibration and leave-one-out cross validation due to the limited number of samples.

Thus, for univariate calibration using LIBS, the best results were chosen considering the lowest standard error of cross validation (SECV), normalization modes, and their trueness values. In this case, for each analyte, the following normalization modes were chosen: K I 766.49 nm, signal normalized by individual norm and then averaged (Normalization 2), Mg I 518.36 nm signal sum after normalization by maximum (Normalization 8) and P I 213.62 nm, signal sum after normalization by maximum (Normalization 8) and considering the area of the region. For WDXRF, the univariate calibration and SECV were calculated, however, this normalization process was not needed due to the well-defined peak signals of the elements.

Fig. 2 shows the SECV obtained by LIBS and WDXRF using univariate calibration. The SECV obtained by LIBS (see light gray column) were 0.26% for K, 0.039% for Mg, and 0.14% for P, and the trueness values ranged from 66 to 150% for K, 41 to 161% for Mg, and 52 to 189% for P. In the other hand, for WDXRF (see gray column), the SECV were 0.58% for K, 0.021% for Mg and 0.13% for P, the trueness values ranged from 44 to 163% for K, 83 to 128% for Mg, and 51 to 182% for P. However, WDXRF technique presents the SECV values slightly lower than those obtained by LIBS (see Fig. 2)

In general, these univariate calibration models proposed by LIBS

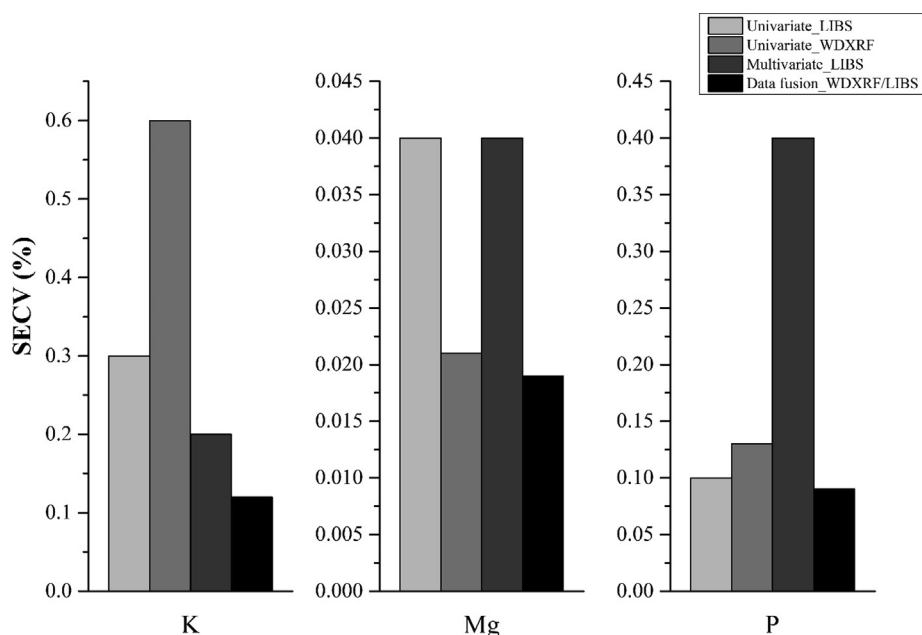


Fig. 2. Standard error of cross validation (%) for calibration strategies used for quantitative determination of K, Mg and P in bean seed samples.

and WDXRF failed to correctly predict the concentration values in the samples. This problem can be explained due to the complexity of sample, spectral interference, physical characteristics and homogeneity of the analytes, which compromise the determination of metals in these samples. This is mainly evident due to the high values of errors (SECV). Thus, other calibration strategy become necessary to improve the predictive capability of the models.

### 3.4. Multivariate calibration using LIBS data

Multiple linear regression (MLR) and the data from LIBS was used to calculate multivariate models. This tool is simple and have been widely used for calibration in chemometrics. MLR yields models that are simpler and easier to interpret; and more emission lines could be used in this multivariate tool (Fragkaki, Farmaki, Thomaidis, & Tsantili-Kakoulidou, 2012; Olivieri, 2015). However, one of the mathematical operation steps is a matrix inversion, and this is impossible if the number of emission lines (columns) is higher than the number of the samples (rows) or a high correlation exist among variables tool (Fragkaki et al., 2012; Olivieri, 2015).

In addition, a routine named "regression2" proposed by Pereira and Pereira-Filho (2018) was used to build the regression models and to calculate the predicted concentration values of the elements, where the X matrix e.g. for K was composed of 3 columns (b0, area or height from K I 766.49 nm, and area or height from K I 769.89) and the y vector represents the reference concentration values obtained by ICP OES. The same procedure was used to build the calibration models for Mg and P.

For multivariate calibration models calculated for K, Mg and P employing LIBS and MLR, the SEC obtained values were 0.17% for K, 0.044% for Mg and 0.38% for P (see dark gray column). The trueness values obtained ranged from 78 to 138% for K, 72 to 162% for Mg and 53 to 221% for P. However, these values were higher if compared with those obtained by univariate strategy with LIBS and WDXRF, except for K that presented lower value of SEC (see Fig. 2).

### 3.5. Multivariate calibration using WDXRF + LIBS data fusion

To improve the predictive capability of the models, data fusion strategy was tested. This strategy combines multiple sources of data yielding a new single model with fused data. Fig. 3 shows a pictorial

description that explains how this strategy can be employed for calibration and then predicts the concentration values of the elements in the samples.

Therefore, for the use of data fusion, it is mandatory that the data must be from different analytical techniques. Thus, in the present study, both emission and fluorescence intensities from LIBS and WDXRF techniques, respectively, were fused to build a new single calibration model. Data fusion models were built at low-level employing the strategy leave-one-out cross validation and the samples (14 samples) previously described. For the low-level data fusion model, the data, mainly those obtained by LIBS, were separately preprocessed (see Section 2.5 in data treatment for LIBS and WDXRF).

After that, the emission intensity values (normalization 1: average of all spectra) of the selected analytical lines from LIBS and the fluorescence intensities values from WDXRF were concatenated and auto-scaled. The new X matrix, for example for K, was composed of 4 columns (b0, K $\alpha$  from WDXRF, height from K I 766.49 nm, and height from K I 769.89). In the case of Mg, the X matrix to calculate the calibration model was composed of 14 rows (the samples) and 7 columns (b0, K $\alpha$ , and 5 emission from LIBS), see details at Fig. 3.

The SEC calculated employing data fusion strategy are shown in Fig. 2. The SEC values were 0.12% for K, 0.019% for Mg and 0.10% for P (see black column), and the trueness ranged between 73 and 124% for K, 81 to 127% for Mg and 74 to 127% for P. Therefore, an improvement was observed for all three determined elements, which shows that this strategy presented a good capability to predict the concentration values of K, Mg and P if compared with other calibration strategies as described above.

### 3.6. Analytical application

The proposed strategy of calibration employing data fusion (from WDXRF and LIBS) and MLR was applied for the determination of K, Mg and P in 14 bean seed samples, and the obtained results are presented in Table 2. The predicted concentration values obtained by data fusion model ranged from 0.97 to 1.55% for K, 0.14 to 0.28% for Mg, and 0.27 to 0.82% for P.

According to the results, K, Mg and P were found in high concentrations, and the bean seeds can be regarded as nutritional source for the human consumption. Moreover, these values were compared

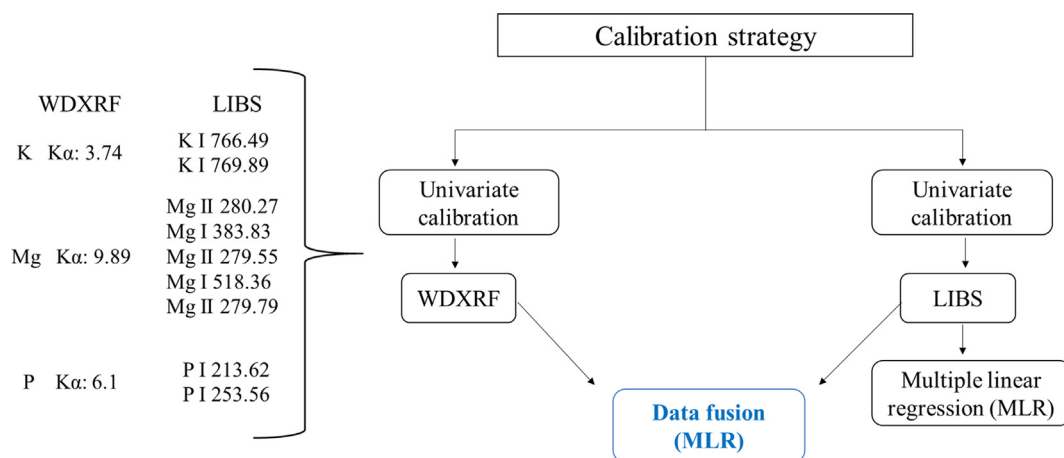


Fig. 3. Pictorial description of the data fusion strategy combining WDXRF and LIBS data.

with those obtained by the other analytical techniques reported in the literature for the determination of elemental composition in bean seeds. A study reported by Santos et al. (2008a) found the concentration values, which ranged between: 0.76 to 1.80% for K, 0.15 to 0.18% for Mg, and 0.31 to 0.48% for P. These values are similar to those obtained in present study, except for P that presented high concentration values. Santos et al. (2009), using ultrasound-assisted extraction, determined the minerals content in bean seeds samples. The authors found the concentration values, ranging from: 1.17 to 1.56% for K, and 0.10 to 0.16% for Mg. These values are slightly lower compared with those found in the present study. Shimelis and Rakshit (2005) determined P and other elements in bean seeds. The concentration values found of P ranged between 0.015 and 0.017%. These values correspond to 26–45 times lower than the concentrations of P found in the present study. Other study was performed by Onwuliri and Obu (2002) for the determination of the chemical constituent including K, Mg and P in bean seeds from Nigeria. These elements present the concentration values ranging between 1.08 and 2.90% for K, 0.16 to 0.35%, for Mg and 0.25 to 0.44% for P. Potassium presented higher concentration, whereas the Mg content is similar, and the concentration of P is slightly lower compared with our study.

Therefore, the difference in the concentration of the chemical composition in bean seed samples can be related to several factors, such as soil, weather conditions, and fertilizers used. So, it is important to determine the chemical composition in this type of edible seed to guarantee the safety of consumer.

#### 4. Conclusions

The use of LIBS and WDXRF showed to be fast and suitable for the determination of K, Mg and P in the bean seed samples. These analytical techniques are considered as non-destructive and allow the direct solid analysis with minimal or no sample preparation steps, which contribute to a sustainable environment and green chemistry. Moreover, the use of data fusion strategy employing LIBS and WDXRF combined with multivariate calibration (MLR) to build the regression models presented lower SECV and acceptable trueness (%) values when compared with those obtained by univariate calibration models for both techniques and multivariate calibration (MLR) for LIBS.

Thus, it is expected that data fusion strategy and the MLR can be used in different matrices using other analytical techniques for quantitative purposes (improvement of prediction capability of chemical elements).

#### CRedit authorship contribution statement

**Raimundo R. Gamela:** Formal analysis, Investigation. **Vinícius C. Costa:** Methodology. **Marco A. Sperança:** Methodology, Validation. **Edenir R. Pereira-Filho:** Conceptualization.

#### Declaration of Competing Interest

The authors declare that they have no known competing financial interests or personal relationships that could have appeared to

Table 2

Concentration values (%) of K, Mg and P in bean seed samples obtained by data fusion strategy (LIBS and WDXRF), reference method (ICP OES) and trueness (%).

Samples	K			Mg			P		
	ICP OES	Proposed method (data fusion)	Trueness (%)	ICP OES	Proposed method (data fusion)	Trueness (%)	ICP OES	Proposed method (data fusion)	Trueness (%)
S1 ( <i>P. vulgaris</i> )	0.99	1.23	124	0.14	0.14	100	0.40	0.35	88
S2 ( <i>P. vulgaris</i> )	1.00	1.08	108	0.16	0.16	100	0.69	0.59	86
S3 ( <i>P. vulgaris</i> )	1.12	1.26	113	0.19	0.19	100	0.34	0.34	100
S4 ( <i>P. vulgaris</i> )	1.05	1.11	106	0.17	0.21	124	0.54	0.48	89
S5 ( <i>P. vulgaris</i> )	1.54	1.55	101	0.19	0.16	84	0.72	0.57	79
S6 ( <i>P. vulgaris</i> )	1.13	1.31	116	0.18	0.19	106	0.38	0.47	124
S7 ( <i>P. vulgaris</i> )	1.59	1.51	95	0.17	0.16	94	0.80	0.82	103
S8 ( <i>P. vulgaris</i> )	1.01	1.12	111	0.15	0.17	113	0.62	0.58	94
S9 ( <i>P. vulgaris</i> )	1.07	1.01	94	0.17	0.14	82	0.29	0.37	128
S10 ( <i>P. vulgaris</i> )	1.27	1.21	95	0.21	0.19	90	0.67	0.55	82
S11 ( <i>V. unguiculata</i> )	1.20	1.17	98	0.22	0.23	105	0.54	0.64	119
S12 ( <i>V. angularis</i> )	1.52	1.35	89	0.26	0.28	108	0.79	0.65	82
S13 ( <i>V. radiata</i> )	1.31	1.25	95	0.23	0.19	83	0.44	0.32	73
S14 ( <i>C. cajan</i> )	0.93	0.97	104	0.12	0.15	125	0.27	0.27	100

influence the work reported in this paper.

## Acknowledgments

The authors are grateful for the financial support by the Conselho Nacional de Desenvolvimento Científico e Tecnológico (CNPq) (grants 160152/2015-1, 305637/2015-0, and 158587/2017-0), and Fundação de Amparo à Pesquisa do Estado de São Paulo (FAPESP, grant 2016/01513-0). This study was financed in part by the Coordenação de Aperfeiçoamento de Pessoal de Nível Superior - Brasil (CAPES) - Finance Code 001.

## Appendix A. Supplementary material

Supplementary data to this article can be found online at <https://doi.org/10.1016/j.foodres.2020.109037>.

## References

- Amorim, F. A. C., Costa, V. C., Da Silva, E. G. P., Lima, D. C., De Jesus, R. M., & Bezerra, M. A. (2017). Multivariate optimization of simple procedure for determination of Fe and Mg in cassava starch employing slurry sampling and FAAS. *Food Chemistry*, 227, 41–47. <https://doi.org/10.1016/j.foodchem.2016.12.029>.
- Andrade, D. F., & Pereira Filho, E. R. (2016). Direct determination of contaminants and major and minor nutrients in solid fertilizers using Laser-Induced Breakdown Spectroscopy (LIBS). *Journal of Agricultural and Food Chemistry*, 64(41), 7890–7898. <https://doi.org/10.1021/acs.jafc.6b04028>.
- Andrade, D. F., Pereira-Filho, E. R., & Konieczynski, P. (2017). Comparison of ICP OES and LIBS analysis of medicinal herbs rich in flavonoids from eastern Europe. *Journal of Brazilian Chemical Society*, 28(5), 838–847. <https://doi.org/10.21577/0103-5053.20160236>.
- Assis, C., Pereira, H., Amador, V., August, R., Oliveira, L., & Sena, M. (2019). Combining mid infrared spectroscopy and paper spray mass spectrometry in a data fusion model to predict the composition of coffee blends. *Food Chemistry*, 281, 71–77. <https://doi.org/10.1016/j.foodchem.2018.12.044>.
- Augusto, A. S., Barsanelli, P. L., Pereira, F. M. V., & Pereira-Filho, E. R. (2017). Calibration strategies for the direct determination of Ca, K, and Mg in commercial samples of powdered milk and solid dietary supplements using laser-induced breakdown spectroscopy (LIBS). *Food Research International*, 94, 72–78. <https://doi.org/10.1016/j.foodres.2017.01.027>.
- Balarâm, V. (2016). Recent advances in the determination of elemental impurities in pharmaceuticals – Status, challenges and moving frontiers. *Trends in Analytical Chemistry*, 80, 83–95. <https://doi.org/10.1016/j.trac.2016.02.001>.
- Ballabio, D., Robotti, E., Grisoni, F., Quasso, F., Bobba, M., Vercelli, S., ... Marengo, E. (2018). Chemical profiling and multivariate data fusion methods for the identification of the botanical origin of honey. *Food Chemistry*, 266, 79–89. <https://doi.org/10.1016/j.foodchem.2018.05.084>.
- Bezerra, M. A., Santelli, R. E., Oliveira, E. P., Villar, L. S., & Escalera, L. A. (2008). Response surface methodology (RSM) as a tool for optimization in analytical chemistry. *Talanta*, 76(5), 965–977. <https://doi.org/10.1016/j.talanta.2008.05.019>.
- Borras, E., Ferré, J., Boqué, R., Mestres, M., Aceña, L., & Busto, O. (2015). Data fusion methodologies for food and beverage authentication and quality assessment – A review. *Analytical Chimica Acta*, 891, 1–14. <https://doi.org/10.1016/j.aca.2015.04.042>.
- Castro, J. P., & Pereira-Filho, E. R. (2016). Twelve different types of data normalization for the proposition of classification, univariate and multivariate regression models for the direct analyses of alloys by laser-induced breakdown spectroscopy (LIBS). *Journal of Analytical Atomic Spectrometry*, 31(10), 2005–2014. <https://doi.org/10.1039/C6JA00224B>.
- Costa, V. C., Amorim, F. A. C., Babos, D. V., & Pereira-Filho, E. R. (2019). Direct determination of Ca, K, Mg, Na, P, S, Fe and Zn in bivalve mollusks by wavelength dispersive X-ray fluorescence (WDXRF) and laser-induced breakdown spectroscopy (LIBS). *Food Chemistry*, 273, 91–98. <https://doi.org/10.1016/j.foodchem.2018.02.016>.
- Costa, V. C., Castro, J. P., Andrade, D. F., de Babos, D. V., Garcia, J. A., Sperança, M. A., ... Pereira-Filho, E. R. (2018). Laser-induced breakdown spectroscopy (LIBS) applications in the chemical analysis of waste electrical and electronic equipment (WEEE). *Trends in Analytical Chemistry*, 108, 65–73. <https://doi.org/10.1016/j.trac.2018.08.003>.
- Costa, V. C., de Babos, D. V., de Aquino, F. W. B., Alex, V., Amorim, F. A. C., & Pereira-Filho, E. R. (2018). Direct determination of Ca, K and Mg in cassava flour samples by laser-induced breakdown spectroscopy (LIBS). *Food Analytical Methods*, 11(7), 1886–1896. <https://doi.org/10.1007/s12161-017-1086-9>.
- De Oliveira, M. D., Fontes, L. M., & Pasquini, C. (2019). Comparing laser induced breakdown spectroscopy, near infrared spectroscopy, and their integration for simultaneous multi-elemental determination of micro- and macronutrients in vegetable samples. *Analytica Chimica Acta*, 1062, 28–36. <https://doi.org/10.1016/j.aca.2019.02.043>.
- Ferreira, S. L. C., Lemos, V. A., de Carvalho, V. S., da Silva, E. G. P., Queiroz, A. F. S., Félix, C. S. A., ... Oliveira, R. V. (2018). Multivariate optimization techniques in analytical chemistry. *Microchemical Journal*, 140, 176–182. <https://doi.org/10.1016/j.microc.2018.04.002>.
- Ferreira, S. L. C., Miró, M., da Silva, E. G. P., Matos, G. D., Dos Reis, P. S., Brandão, G. C., ... Araujo, R. G. O. (2010). Slurry sampling—an analytical strategy for the determination of metals and metalloids by spectroanalytical techniques. *Applied Spectroscopy Reviews*, 45(1), 44–62. <https://doi.org/10.1080/05704920903435474>.
- Fragkaki, A. G., Farmaki, E., Thomaidis, N., Tsantili-Kakoulidou, A., Angelis, Y. S., Koupparis, M., & Georgakopoulos, C. (2012). Comparison of multiple linear regression, partial least squares and artificial neural networks for prediction of gas chromatographic relative retention times of trimethylsilylated anabolic androgenic steroids. *Journal of Chromatography A*, 1256, 232–239. <https://doi.org/10.1016/j.chroma.2012.07.064>.
- Gamela, R. R., Barrera, E. G., Duarte, A. T., Boschetti, W., Da Silva, M. M., Vale, M. G. R., & Dessuy, M. B. (2019). Fast sequential determination of Zn, Fe, Mg, Ca, Na, and K in infant formulas by high-resolution continuum source flame atomic absorption spectrometry using ultrasound-assisted extraction. *Food Analytical Methods*, 12(6), 1420–1428. <https://doi.org/10.1007/s12161-019-01478-8>.
- Hahn, D. W., & Omenetto, N. (2012). Laser-induced breakdown spectroscopy (LIBS), Part II: Review of instrumental and methodological approaches to material analysis and applications to different fields. *Applied Spectroscopy*, 66(4), 347–419. <https://doi.org/10.1366/11-06574>.
- Hoehse, M., Paul, A., Gornushkin, I., & Panne, U. (2012). Multivariate classification of pigments and inks using combined Raman spectroscopy and LIBS. *Analytical and Bioanalytical Chemistry*, 402, 1443–1450. <https://doi.org/10.1007/s00216-011-5287-6>.
- Junior, D. S., Nunes, L. C., Trevizan, L. C., Godoi, Q., Leme, F. O., Braga, J. W. B., & Krug, F. J. (2009). Evaluation of laser induced breakdown spectroscopy for cadmium determination in soils. *Spectrochimica Acta Part B: Atomic Spectroscopy*, 64(10), 1073–1078. <https://doi.org/10.1016/j.sab.2009.07.030>.
- Liu, Y., & Brown, S. D. (2004). Wavelet multiscale regression from the perspective of data fusion: New conceptual approaches. *Analytical and Bioanalytical Chemistry*, 380(3), 445–452. <https://doi.org/10.1007/s00216-004-2776-x>.
- Markiewicz-Keszcycka, M., Cama-Moncuñil, X., Casado-Gavaldá, M. P., Dixit, Y., Cama-Moncuñil, R., Cullen, P. J., & Sullivan, C. (2017). Laser-induced breakdown spectroscopy (LIBS) for food analysis: A review. *Trends in Food Science and Technology*, 65, 80–93. <https://doi.org/10.1016/j.tifs.2017.05.005>.
- Mir-Marqués, A., Cervera, M. L., & De La Guardia, M. (2016). Mineral analysis of human diets by spectrometry methods. *Trends in Analytical Chemistry*, 82, 457–467. <https://doi.org/10.1016/j.trac.2016.07.007>.
- Olivieri, A. C. (2015). Practical guidelines for reporting results in single- and multi-component analytical calibration: A tutorial. *Analytical Chimica Acta*, 868, 10–22. <https://doi.org/10.1016/j.aca.2015.01.017>.
- Onwuliri, F. A., & Obu, J. A. (2002). Lipids and other constituents of *Vigna unguiculata* and *Phaseolus vulgaris* grown in northern Nigeria. *Food Chemistry*, 78, 1–7. [https://doi.org/10.1016/S0308-8146\(00\)00293-4](https://doi.org/10.1016/S0308-8146(00)00293-4).
- Pashkova, G. V. (2009). X-ray fluorescence determination of element contents in milk and dairy products. *Food Analytical Methods*, 2, 303–310. <https://doi.org/10.1007/s12161-009-9080-5>.
- Pereira, F., & Pereira-Filho, E. R. (2018). Application of free computational program in experimental design: A tutorial. *Química Nova*, 41(9), 1061–1071. <https://doi.org/10.21577/0100-4042.20170254>.
- Perring, L., Andrey, D., Basic-Dvorzak, M., & Blanc, J. (2005). Rapid multimineral determination in infant cereal matrices using wavelength dispersive X-ray fluorescence. *Journal of Agricultural and Food Chemistry*, 53(12), 4696–4700. <https://doi.org/10.1021/jf047895+>.
- Rezende, A. A., Pacheco, M. T. B., da Silva, V. S. N., & Ferreira, T. A. P. C. (2018). Nutritional and protein quality of dry Brazilian beans (*Phaseolus vulgaris* L.). *Food Science and Technology*, 38, 421–427. <https://doi.org/10.1590/1678-457x.05917>.
- Santos, M. C., Sperança, M. A., & Pereira, F. M. V. (2018). Wavelength dispersive X-ray fluorescence (WDXRF) and chemometric investigation of human hair after cosmetic treatment. *X-Ray Spectrometry*, 47(3), 252–257. <https://doi.org/10.1002/xrs.2836>.
- Santos, W. P. C., Castro, J. T., Bezerra, M. A., Fernandes, A. P., Ferreira, S. L. C., & Korn, M. G. A. (2009). Application of multivariate optimization in the development of an ultrasound-assisted extraction procedure for multielemental determination in bean seeds samples using ICP OES. *Microchemical Journal*, 91(2), 153–158. <https://doi.org/10.1016/j.microc.2008.10.001>.
- Santos, W. P. C., Hatje, V., Lima, L. N., Trignano, S. V., Barros, F., Castro, J. T., & Korn, M. G. A. (2008a). Evaluation of sample preparation (grinding and sieving) of bivalves, coffee and cowpea beans for multi-element analysis. *Microchemical Journal*, 89(2), 123–130. <https://doi.org/10.1016/j.microc.2008.01.003>.
- Santos, W. P. C., Gramacho, D. R., Teixeira, A. P., Costa, A. C. S., & Korn, M. G. A. (2008b). Use of Doehlert design for optimizing the digestion of beans for multi-element determination by inductively coupled plasma optical emission spectrometry. *Journal of Brazilian Chemical Society*, 19(1), 1–10. <https://doi.org/10.1590/S0103-50532008000100002>.
- Santos, W. P. C., Santos, D. C. M. B., Fernandes, A. P., Castro, J. T., & Korn, M. G. A. (2013). Geographical characterization of beans based on trace elements after microwave-assisted digestion using diluted nitric acid. *Food Analytical Methods*, 6(4), 1133–1143. <https://doi.org/10.1007/s12161-012-9520-5>.
- Shimelis, E. A., & Rakshit, S. K. (2005). Proximate composition and physico-chemical properties of improved dry bean (*Phaseolus vulgaris* L.) varieties grown in Ethiopia. *LTW-Food Science and Technology*, 38(4), 331–338. <https://doi.org/10.1016/j.lwt.2004.07.002>.
- Spiteri, M., Dubin, E., Cotton, J., Poirel, M., Corman, B., Jamin, E., ... Rutledge, D. (2016). Data fusion between high resolution <sup>1</sup>H-NMR and mass spectrometry: A synergetic approach to honey botanical origin characterization. *Analytical and Bioanalytical*

- Chemistry*, 408(16), 4389–4401. <https://doi.org/10.1007/s00216-016-9538-4>.
- West, M., Ellis, A. T., Potts, P. J., Strelis, C., Vanhoofe, C., & Wobrauschek, P. (2014). Atomic spectrometry update - a review of advances in X-ray fluorescence spectrometry. *Journal of Analytical Atomic Spectrometry*, 29, 1516–1563. <https://doi.org/10.1039/C4JA90038C>.
- Whittle, M., Gillet, V. J., & Willett, P. (2006). Analysis of data fusion methods in virtual screening: Similarity and group fusion. *Journal of Chemical Information and Modeling*, 46(6), 2206–2219. <https://doi.org/10.1021/ci0496144>.
- Willett, P. (2013). Combination of similarity rankings using data fusion. *Journal of Chemical Information and Modeling*, 53(1), 1–10. <https://doi.org/10.1021/ci300547g>.

### Supplementary material

**Table 1S.** Plasma conditions and the emission lines used in ICP OES for the determination of K, Mg and P in bean seed samples

Instrumental parameters	Operational conditions
Radio frequency applied power (kW)	1.15
Integration time for low emission line (s)	15.0
Integration time for high emission line (s)	5
Sample introduction flow rate (mL min <sup>-1</sup> )	1.0
Pump stabilization time (s)	5
Argon auxiliary flow rate (L min <sup>-1</sup> )	0.5
Argon plasma flow rate (L min <sup>-1</sup> )	12
Argon nebulizer flow rate (L min <sup>-1</sup> )	0.7
Number of replicates (n)	3
Elements and wavelengths (nm); View modes: only radial <sup>a</sup> and axial <sup>b</sup>	<sup>a</sup> K I (766,490 nm), <sup>b</sup> Mg II (279,553 nm) and <sup>a</sup> P I (178, 20 nm)



**Table 2S.** Obtained concentration values of K, Mg and P in certified reference material of CRM Apple leaves (NIST-1515)

Samples	Concentration (in %)		
	K	Mg	P
Certified values	1.61±0.021	0.27±0.012	0.16±0.068
Digestion procedure	1.35±0.32	0.22± 0.014	0.16±0.086
(Trueness, %)	(84)	(82)	(97)

## **Chapter 3 – Published Results**



# Direct Determination of Ca, K, and Mg in Cocoa Beans by Laser-Induced Breakdown Spectroscopy (LIBS): Evaluation of Three Univariate Calibration Strategies for Matrix Matching

Raimundo Rafael Gamela<sup>1</sup> · Vinicius Câmara Costa<sup>1,2</sup> · Diego Vitor Babos<sup>1</sup> · Alisson Silva Araújo<sup>1</sup> · Edenir Rodrigues Pereira-Filho<sup>1</sup>

Received: 22 January 2020 / Accepted: 27 January 2020  
 © Springer Science+Business Media, LLC, part of Springer Nature 2020

## Abstract

This study is dedicated to the direct analysis of Ca, K, and Mg by employing laser-induced breakdown spectroscopy (LIBS). Three univariate calibration strategies, namely (i) one-point and multi-line calibration (OP MLC), (ii) single-sample calibration (SSC), and (iii) two-point calibration transfer (TP CT), were evaluated and compared. Only OP MLC and TP CT presented precise and accurate results, where the trueness values ranged from 80 to 120% for most of the analyzed samples. Moreover, the standard errors for all determined elements ranged from 0.01 to less than 0.20% of the concentration in the samples. These three calibration strategies showed that they are efficient and effective for matrix matching to correct matrix effects in complex samples using only one sample as the standard.

**Keywords** Cocoa beans · Direct solid analysis · Calibration strategies · Matrix effects · Macronutrients

## Introduction

Brazil is listed as the seventh largest producer of cocoa beans worldwide, with production of approximately 210 million tons per year, where the southern region of Bahia State corresponds to 94% of the total (International Cocoa Organization-ICCO 2018; World Cocoa Foundation-WCF 2018). Due to their composition, cocoa beans are considered raw materials to produce different products including chocolate, cocoa butter, jams, and others for modern human diets. In addition, cocoa beans are an important source of bioactive compounds, antioxidants, and mineral nutrients, representing a special matrix in the food processing industry (Andújar et al. 2012; Febrianto and Zhu 2019).

In this sense, for nutritional reasons, it is of strategic interest to determine the mineral content, as Ca, K, and Mg are considered essential for human health. Commonly, the determination of essential and toxic elements in cocoa beans and their

derivates has been performed employing different analytical techniques, such as inductively coupled plasma optical emission spectrometry (ICP OES) (Villa et al. 2014, 2015; Costa et al. 2019a) and inductively coupled plasma mass spectrometry (ICP-MS) (Yanus et al. 2014; Dico et al. 2018). However, aside from the advantages of ICP methods related to high sensitivity and multielemental capability, one of the main challenges is related to the sample preparation step, which contributes to the introduction of major sources of error in elemental determination.

Laser-induced breakdown spectroscopy (LIBS) is a qualitative and quantitative technique and has been used in recent decades as a reliable alternative for elemental determination in different matrices (Markiewicz-Keszycka et al. 2017; Costa et al. 2018, 2019b). In LIBS, the most attractive features are related to simultaneous, multielemental determination in a short period of time (< 1 s) and direct solid sample analysis with minimal or no preparation (Costa et al. 2019b; Machado et al. 2019). In this way, solid sample analysis contributes to lower waste generation and obviously contributes to a sustainable environment following green chemistry principles (Bendicho et al. 2012).

However, for quantitative analysis using LIBS, considerable efforts are required, mainly due to matrix effects as a result of the sample complexity, spectral interference, physical characteristics, self-absorption, and chemical composition,

✉ Edenir Rodrigues Pereira-Filho  
 erpf@ufscar.br

<sup>1</sup> Department of Chemistry, Group of Applied Instrumental Analysis, Federal University of São Carlos, São Carlos, SP 13560-270, Brazil

<sup>2</sup> Laboratory of Toxicant and Drug Analyses (LATF), Federal University of Alfenas (Unifal), Alfenas, MG 37130-000, Brazil

which compromise elemental determination (Cremers and Radziemski 2006; Noll 2012; Takahashi and Thornton 2017; Lepore et al. 2017).

The scientific literature presents several alternatives to overcome these limitations as a way to compensate the matrix effects, employing appropriate calibration strategies and simultaneously improving the analytical performance of LIBS. First-order multivariate calibration, such as partial least squares regression (PLS), principal component regression (PCR), and multiple linear regression (MLR), has been used mainly due to the possibility of calibrating models in the presence of interferences using entire spectral profiles or variable selection (Escandar et al. 2007; Olivieri 2015). In addition, multivariate calibration allows compensating for the lack of selectivity by employing a mathematical algorithm to extract information used to predict concentrations in the samples (Escandar et al. 2007; Olivieri 2015; Zhang et al. 2018).

However, the main problem associated with multivariate calibration, mainly PLS, is that when the entire spectrum is used to propose the calibration model, miscorrelations can occur among the emission lines during analyte determination (Safi et al. 2018; Sperança et al. 2019).

On the other hand, in MLR calibration, more emission lines can be used; however, one of the mathematical operation steps is a matrix inversion, and this is impossible if the number of emission lines (columns) is higher than the number of the samples (rows) or a high correlation exists among variables (Escandar et al. 2007; Olivieri 2015).

Moreover, other univariate calibration strategies, such as matrix-matching calibration (MMC) (Augusto et al. 2017), internal standardization (IS) (Gupta et al. 2011), standard addition (SA) (Wang et al. 2017), multi-energy calibration (MEC) (Babos et al. 2018; Castro et al. 2019; Andrade et al. 2019), and one-point gravimetric standard addition (OP GSA) (Babos et al. 2019), have been commonly used and reported as ways to compensate the matrix effects in LIBS. In MMC, the calibration standards are matched with the sample matrix, usually by employing a certified reference material (CRM) or a set of samples or matching the solid standards by the addition of concomitants that cause interference. In some cases, this strategy is not enough to avoid or correct strong matrix effects (Augusto et al. 2017; Babos et al. 2018).

For IS, it is necessary to choose an adequate internal standard, which represents a hard task, as the standard must be subjected to the same plasma treatment process as that of the analytes in the sample. In addition, this strategy is not able to overcome some severe matrix effects observed in LIBS (Gupta et al. 2011; Babos et al. 2018).

In the case of SA, this approach can be considered an effective alternative to minimize the main limitations in LIBS. This strategy is based on the addition of a constant amount of samples in the blank and in all calibration standards, allowing both standards and samples to be in the same conditions, minimizing

the matrix effects (Wang et al. 2017). Nevertheless, SA presents some limitations; for example, when there is a lower capability to identify the spectral interference, a large amount of sample is required, and when the calibration curve contains few calibration standards, it must be prepared for each sample (Wang et al. 2017; Babos et al. 2018).

MEC and OP GSA are recent univariate calibration strategies and are compatible with LIBS to efficiently minimize and correct the complex matrix effects in direct solid sample analysis. In addition, only 2 calibration standards are required per sample: S1 (blank plus standard) and S2 (sample plus standard). Moreover, multiple wavelengths of the elements are required, which make it easy to identify which emission line interferes and later eliminate the spectral interferences. In the case of OP GSA, the data treatment is the same as that used for MEC, but it is simpler and allows evaluation of the accuracy for each wavelength (Babos et al. 2019). However, when MEC and OP GSA are used, some challenges must be considered, such as the difficulties in choosing an appropriate blank, the concentration of standards that affect the accuracy, and the fact that both the blank and standard must be well homogenized to ensure good precision (Babos et al. 2018, 2019).

Recently, one-point and multi-line calibration (OP MLC) (Hao et al. 2018), single-sample calibration (SSC) and two-point calibration transfer (TP CT) (Castro et al. 2019) were proposed as alternatives to overcome matrix effects in direct solid analysis by LIBS. For OP MLC, the strategy is based on a single matrix-matching standard sample and multiple lines of analyzed elements (Hao et al. 2018). Therefore, the unknown concentration of the analyte can be determined by employing only one sample as a standard, i.e., the concentration of this sample can be certified or known (Hao et al. 2018).

On the other hand, when SSC is used, the concentration of the analyte is estimated using only one sample (CRM or sample with reference value) as the calibration standard and subsequently is based on the correlation of the different emission lines of the analyte and other elements present in this standard and sample (unknown) with the concentration of all the elements present in the calibration standard (Yuan et al. 2019). Additionally, it is necessary that the sample and standard have similar physicochemical properties, so that the matrix effects do not interfere with the concentration estimation, in addition to using only emission lines free of spectral interference (Yuan et al. 2019).

Another recent univariate calibration strategy is TP CT. This strategy is simple and considered effective for matrix matching because it uses a sample as a standard in the absence of CRM with a similar matrix. The approach is based on the amount of sample ablated by a laser pulse. Thus, by summing the emission intensity of different spectral sets, it is possible to propose linear calibration models and determine the concentration of the analyte in the sample (Castro et al. 2019).

Therefore, OP MLC, SSC, and TP CT univariate calibrations for quantitative analysis by LIBS are simple because they do not require the addition of standards for calibration or complicated calculations. The goal of this study was to evaluate the use of OP MLC, SSC, and TP CT as strategies for matrix matching in the determination of Ca, K, and Mg in cocoa beans using LIBS and direct solid sample analysis.

## Material and Methods

### Instrumentation

In the present study, a LIBS spectrometer model J200 from Applied Spectra (Freemont, USA) with a Nd:YAG laser (1064 nm) equipped with a 6-channel charge-coupled device (CCD) was used. The spectrometer covers a range from 186 to 1042 nm, resulting in 12,288 variables, and a gate width of 1.05 ms was used in the present study. In addition, a HEPA air cleaner was used to purge the ablated particles, and the movement of the sample was automated XYZ stage and a 1280 × 1024 (complementary metal-oxide semiconductor) CMOS color-camera imaging system. The instrumental conditions used in this study were as follows: delay time 1.9 μs and fluence 2699 mJ cm<sup>-2</sup>, using 53 mJ for the laser pulse energy and 50 μm for the spot size.

Moreover, an ICP OES system, model iCAP 7000 (Thermo Fisher Scientific, USA), was employed for determination of the analytes as a reference method for LIBS. The instrumental conditions and the emission lines used in the ICP OES determinations are described in Table 1.

### Standards, Reagents, and Samples

Analytical-grade reagents and deionized water (Milli-Q system, 18.2 MΩ cm, Millipore, Bedford, MA) were used to prepare all solutions and standards. The glass and quartz

materials were soaked in 10% v v<sup>-1</sup> HNO<sub>3</sub> solution for 24 h, washed with deionized water and dried before use. The multi-element solutions used for external calibration were prepared from 1000 mg L<sup>-1</sup> Ca, K and Mg standard solutions (Qhemis, São Paulo, SP, Brazil) using HNO<sub>3</sub> (Synth, Diadema, SP, Brazil) previously purified by a Distillacid™ BSB-939-IR subboiling distillation system (Berghof, Eningen, Germany).

A total of ten cocoa bean samples (*Theobroma cacao*) coded from S1 to S10 were obtained from Bahia State, which is considered the main producer in Brazil. The samples were acquired dried, and a simple maceration (using mortar and pestle) was necessary to reduce the particle size before digestion.

In addition, four certified reference materials (CRMs) of baking chocolate (NIST 2384), whole milk powder (NIST 8435), apples (NIST 1515), and spinach leaves (1570a), all from the National Institute of Standard and Technology (Gaithersburg, MD, USA), were used to evaluate the efficiency of the sample preparation method with diluted HNO<sub>3</sub>.

### Microwave-Assisted Digestion (Reference Method)

Approximately 200 mg of cocoa bean was accurately and directly weighed in perfluoroalkoxy alkane (PFA) vessels, and 5 mL of HNO<sub>3</sub> (3.75 mol L<sup>-1</sup>) and 1.75 mL of H<sub>2</sub>O<sub>2</sub> 30% v v<sup>-1</sup> were added. The samples were submitted to the following heating program (temperature in °C/ramp in min/hold in min): (i) 180/5/5; (ii) 210/5/10; and (iii) 230/5/10. Next, the contents were transferred to volumetric flasks, and the final volume was brought to 25 mL with ultrapure water before analysis by ICP OES.

### Acquisition and Data Treatment for LIBS Analysis

Analysis of all samples by LIBS was performed in triplicate using optimized instrumental conditions. For the evaluation and data processing, Microsoft Excel was used to calculate

**Table 1** Instrumental conditions and emission lines used by ICP OES analysis

Instrumental parameters	Operational conditions
Radio frequency applied power (kW)	1.15
Integration time for low emission line (s)	15.0
Integration time for high emission line (s)	5
Sample introduction flow rate (mL min <sup>-1</sup> )	1.0
Pump stabilization time (s)	5
Argon auxiliary flow rate (L min <sup>-1</sup> )	0.5
Argon plasma flow rate (L min <sup>-1</sup> )	12
Argon nebulizer flow rate (L min <sup>-1</sup> )	0.7
Number of replicates ( <i>n</i> )	3
Elements and wavelengths (nm); view modes: only radial	Ca II (396.847 nm), K I (766.490 nm), and Mg II (279.553 nm)

the univariate calibration models. MATLAB® 2018a (MathWorks, Natick, MA, USA) was used to apply homemade routines for the data processing, and Aurora software (Applied spectra) was used for identification of the obtained emission lines.

The spectra obtained by LIBS present high complexity due to the sample microheterogeneity and signal fluctuation during data acquisition. In this case, to overcome some drawbacks, normalization of the data was necessary. Accordingly, twelve (12) normalization modes were assessed: (1) average of all spectra; (2) signal normalization by the norm, then, average over all spectra; (3) signal normalization by the area, then, average over all spectra; (4) signal normalization by the highest signal, then, average over all spectra; (5) sum of all spectra; (6) signal normalization by the norm, then, sum over all spectra; (7) signal normalization by the area, then, sum over all spectra; (8) signal normalization by the highest signal, then, sum over all spectra; (9) signal normalization by C I 193.09-nm emission line, then, average over all spectra; (10) signal normalization by C I 193.09-nm emission line, then, sum over all spectra; (11) signal normalization by C I 247.85-nm emission line, then, average over all spectra; and (12) signal normalization by C I 247.85-nm emission line, then, sum over all spectra (Castro and Pereira-Filho 2016).

### Univariate Calibration Strategies

Three univariate calibration strategies, OP MLC, SSC, and TP CT, were evaluated and compared. All strategies used in the present study need to analyze samples as standards for matrix matching due to the lack of a certified reference material with sufficient similarity. In addition, these strategies can correct matrix effects in cocoa beans that present high quantities of fats and oils, which can be a challenge for traditional univariate calibrations.

For OP MLC, the general idea is as follows: the unknown concentration of the analyzed analytes can be determined by employing only one sample as a standard, i.e., the concentrations of this sample can be certified or known (Hao et al. 2018). In this sense, the emission intensities of multiple lines of an analyte obtained by standard and unknown sample analysis are used to build the linear model, as shown in Fig. 1. The emission intensities by standard (with known concentration,  $C_{\text{standard}}$ ) are plotted on the  $x$ -axis, the intensities of unknown samples are plotted on the  $y$ -axis, and the analyte concentration in unknown samples ( $C_{\text{analyte}}$ ) can be determined using the slope of the calculated linear model and Eq. 1 (Hao et al. 2018).

$$C_{\text{analyte}} = \text{slope} \times C_{\text{standard}} \quad (1)$$

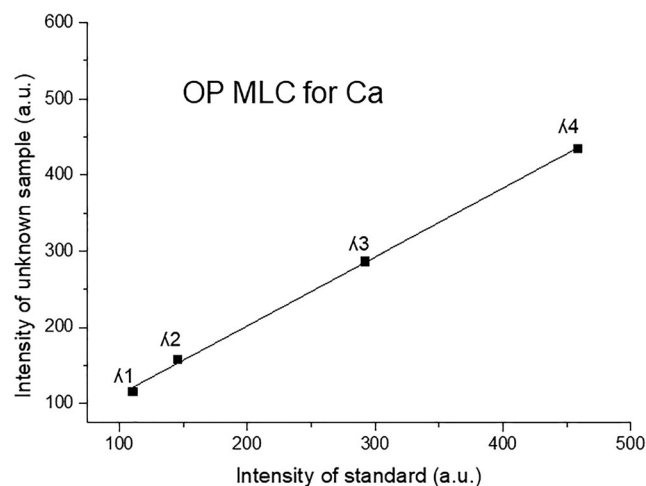


**Fig. 1** Linear model for univariate calibration: one-point and multi-line calibration

On the other hand, SSC does not require a calibration curve or linear models, just a correlation between spectral line intensity and concentration. Therefore, the concentration of the analytes is determined using only one sample (CRM or sample with reference value) as the calibration standard and subsequent correlation of the different emission lines of the analyte present in the standard and sample (unknown). Moreover, other spectral lines of the elements present in the plasma from the sample are employed in this correlation to estimate the analyte concentration, which enables good accuracy in the determinations. However, the number of spectral lines of analytes present in the sample should be  $\leq$  the number of spectral lines evaluated for the elements in the standard (Yuan et al. 2019). The concentration in the unknown sample is calculated by employing Eq. 2.

$$C_{\text{analyte}} = \frac{\frac{C_{\text{standard analyte}} \times I_{\text{analyte sample}}}{I_{\text{analyte standard}}}}{\sum_{i=1}^N \frac{C_{\text{standard element}}^N \times I_{\text{element sample}}^N}{I_{\text{element standard}}^N}} \quad (2)$$

where  $C_{\text{standard analyte}}$  and  $I_{\text{analyte standard}}$  are the concentration and intensity of the emission line of the analyte in the sample, respectively, used for standard calibration.  $I_{\text{analyte sample}}$  is the emission intensity of the analyte in the unknown sample.  $I_{\text{element sample}}^N$  is the emission intensity of the element  $N$  in the sample of unknown concentration, and  $C_{\text{standard element}}^N$  and  $I_{\text{element standard}}^N$  are the concentration and the emission intensity of the element  $N$ , respectively, in the sample used for standard calibration (Yuan et al. 2019).

For TP CT, with intermediate analyte concentration was used as standard (known concentration) due to the lack of a certified reference material. The spectral set (approximately 680) used for this strategy is the same as that used in other

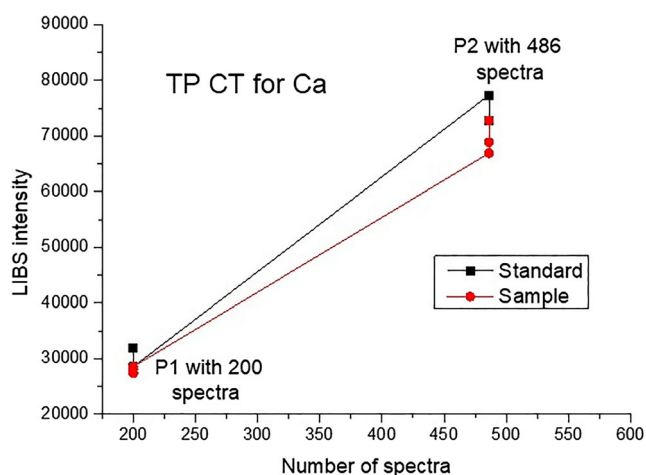


**Fig. 2** Linear model for univariate calibration two-point calibration transfer

previously described univariate calibration strategies. The spectral set was divided into two sets (2 points): the first with 200 spectra and the second with the remaining 480 spectra. The spectral sets were separately summed (normalization mode number 5). Thus, a linear model is calculated with only two points for each emission line evaluated, where the  $x$ -axis is the number of spectra (200 or 480) and the  $y$ -axis is the intensity emission of both points. This process was done for the unknown sample and for the sample chosen as the standard. The concentration in the unknown sample ( $C_{\text{sample}}$ ) is calculated by the combination of the slopes from both linear models ( $\text{slope}_{\text{sample}}$  and  $\text{slope}_{\text{standard}}$ ) and the standard concentration ( $C_{\text{standard}}$ ), as described by Eq. 3 (Castro et al. 2019).

$$C_{\text{sample}} = C_{\text{standard}} \times \frac{\text{Slope}_{\text{sample}}}{\text{Slope}_{\text{standard}}} \quad (3)$$

Moreover, to verify the linearity of the calibration curve calculated from two points, the  $F$  test, the ratio of  $F_{\text{experimental}}$  and  $F_{\text{calculated}}$ , was evaluated, as shown in Fig. 2.

For all strategies, the spectra were collected in triplicate, and to reduce the microheterogeneity effects and signal

fluctuation during data acquisition, 12 normalization modes were calculated, except for TP CT. In addition, a routine (`libs_par2`) was used to calculate the signal-background ratio (SBR), as well as both the signal area and height for the region of the emission line of interest specified by the user. The following element emission lines were used (nm): Ca II 393.37, Ca II 396.85, Ca I 422.67, and Ca II 431.87; K I 766.49 and 769.89; and Mg II 280.27, Mg II 279.55, Mg II 279.80, and Mg I 285.21.

Thus, for OP MLC and SSC, the best normalizations were chosen according to the lower relative standard deviation (RSD) and the acceptable trueness values calculated from the predicted concentration values by LIBS and the concentration values obtained from the reference method (ICP OES) after microwave-assisted digestion. In the case of TP CT, the same approach previously referenced was used, but only using normalization 5.

## Results and Discussions

### Reference Method by ICP OES

The ICP OES technique was used for determination of Ca, K, and Mg in cocoa bean samples after microwave-assisted acid digestion as reference method. In order to evaluate the performance of microwave-assisted digestion, four certified reference materials, namely baking chocolate (NIST 2384), whole milk powder (NIST 8435), apples (NIST 1515), and spinach leaves (1570a), were also digested using the same heating program described in the previous section (2.4. Determination by ICP OES). The obtained concentration values were statistically similar to that certified based on Student's  $t$  test at 95% confidence level. The results of the concentration values in CRM are shown in Table 2, and the trueness values for all analytes were in the range of 79 to 108%, demonstrating good accuracy.

Therefore, this sample preparation procedure was efficient and can be used as a reference method for cocoa bean analysis.

**Table 2** Concentration values of Ca, K, and Mg obtained in certified reference materials using diluted nitric acid (mean  $\pm$  standard deviation,  $n = 3$ )

Concentration in ( $\text{mg kg}^{-1}$ )

Elements	Baking chocolate		Apple leaves		Spinach leaves		Whole milk powder	
	Certified value	Proposed procedure	Certified value	Proposed procedure	Certified value	Proposed procedure	Certified value	Proposed procedure
Ca	840 $\pm$ 74	866 $\pm$ 0.2	15,250 $\pm$ 100	14,147 $\pm$ 126	15,270 $\pm$ 410	14,275 $\pm$ 52	9220 $\pm$ 490	9966 $\pm$ 445
K	8650 $\pm$ 400	7120 $\pm$ 17	16,080 $\pm$ 210	12,821 $\pm$ 198	29,030 $\pm$ 520	23,712 $\pm$ 433	13,630 $\pm$ 470	10,746 $\pm$ 139
Mg	2610 $\pm$ 120	2624 $\pm$ 101	2710 $\pm$ 120	2649 $\pm$ 33	*	*	814 $\pm$ 76	835 $\pm$ 3

(\*) value not informed

**Table 3** Concentration values (%) obtained for Ca, K, and Mg in cocoa bean samples after employing three univariate calibration strategies and LJBS

Samples	Ca (% w w <sup>-1</sup> )						K (% w w <sup>-1</sup> )						Mg (% w w <sup>-1</sup> )					
	ICP OES	OP MLC	SSC	TP CT	ICP OES	OP MLC	SSC	TP CT	ICP OES	OP MLC	SSC	TP CT	ICP OES	OP MLC	SSC	TP CT		
S1	0.084 ± 0.002	0.083 ± 0.014	0.070 ± 0.017	0.084 ± 0.012	0.971 ± 0.047	0.979 ± 0.039	0.654 ± 0.035	1.09 ± 0.38	0.242 ± 0.002	0.196 ± 0.045	0.278 ± 0.077	0.237 ± 0.019	0.242 ± 0.002	0.196 ± 0.045	0.278 ± 0.077	0.237 ± 0.019		
S2	0.052 ± 0.001	0.068 ± 0.015	0.053 ± 0.007	0.058 ± 0.004	0.734 ± 0.029	0.942 ± 0.228	0.771 ± 0.127	0.847 ± 0.114	0.229 ± 0.001	0.218 ± 0.044	0.249 ± 0.002	0.270 ± 0.066	0.229 ± 0.001	0.218 ± 0.044	0.249 ± 0.002	0.270 ± 0.066		
S3	0.089 ± 0.003	0.080 ± 0.004	0.076 ± 0.022	0.088 ± 0.018	1.09 ± 0.028	1.05 ± 0.13	0.990 ± 0.163	1.30 ± 0.24	0.241 ± 0.002	0.200 ± 0.029	0.152 ± 0.021	0.206 ± 0.022	0.241 ± 0.002	0.200 ± 0.029	0.152 ± 0.021	0.206 ± 0.022		
S4	0.113 ± 0.002	0.107 ± 0.007	0.084 ± 0.003	0.112 ± 0.012	0.973 ± 0.050	0.950 ± 0.108	0.971 ± 0.217	1.07 ± 0.11	0.252 ± 0.003	0.257 ± 0.076	–	0.276 ± 0.037	0.252 ± 0.003	0.257 ± 0.076	–	0.276 ± 0.037		
S5	0.196 ± 0.028	0.157 ± 0.003	0.115 ± 0.007	0.157 ± 0.051	0.937 ± 0.080	0.903 ± 0.199	1.11 ± 0.29	0.884 ± 0.049	0.218 ± 0.003	–	0.231 ± 0.057	0.203 ± 0.042	0.218 ± 0.003	–	0.231 ± 0.057	0.203 ± 0.042		
S6	0.070 ± 0.001	0.066 ± 0.009	0.061 ± 0.010	0.069 ± 0.001	0.740 ± 0.012	0.935 ± 0.023	0.705 ± 0.169	0.721 ± 0.036	0.197 ± 0.002	0.171 ± 0.022	0.215 ± 0.015	0.188 ± 0.021	0.197 ± 0.002	0.171 ± 0.022	0.215 ± 0.015	0.188 ± 0.021		
S7	0.092 ± 0.004	0.073 ± 0.019	0.078 ± 0.010	0.078 ± 0.006	1.03 ± 0.075	0.851 ± 0.047	0.766 ± 0.064	1.06 ± 0.29	0.249 ± 0.010	0.217 ± 0.007	0.286 ± 0.052	0.223 ± 0.032	0.249 ± 0.010	0.217 ± 0.007	0.286 ± 0.052	0.223 ± 0.032		
S8	0.056 ± 0.003	0.058 ± 0.005	–	0.065 ± 0.000	0.791 ± 0.069	0.989 ± 0.181	1.00 ± 0.15	0.885 ± 0.125	0.201 ± 0.010	0.202 ± 0.042	0.217 ± 0.058	0.216 ± 0.116	0.201 ± 0.010	0.202 ± 0.042	0.217 ± 0.058	0.216 ± 0.116		
S9	0.069 ± 0.005	–	0.061 ± 0.007	–	0.883 ± 0.011	–	0.734 ± 0.257	–	0.224 ± 0.010	0.257 ± 0.037	0.283 ± 0.111	–	0.224 ± 0.010	0.257 ± 0.037	0.283 ± 0.111	–		
S10	0.069 ± 0.003	0.058 ± 0.05	0.047 ± 0.001	0.071 ± 0.001	0.973 ± 0.057	0.870 ± 0.047	–	1.15 ± 0.13	0.245 ± 0.010	0.227 ± 0.043	0.229 ± 0.034	0.200 ± 0.055	0.245 ± 0.010	0.227 ± 0.043	0.229 ± 0.034	0.200 ± 0.055		

(–) sample used as calibration standard



## Evaluation of Univariate Calibration Strategies

The univariate calibration strategies evaluated in the present study were used as alternatives for traditional univariate (MMC, IS, and SA), nontraditional (MEC and OP GSA) and multivariate calibration (PLS, PCR, and MLR). The OP MLC, SSC, and TP CT strategies are simple to interpret and do not require standard addition including data treatment, which is very easy compared with the previously mentioned strategies. In this sense, OP MLC and SSC were evaluated and compared the 12 normalization modes and analytical signals (see details in “Acquisition and Data Treatment for LIBS”), and TP CT with only normalization mode 5, for Ca, K and Mg in all analyzed samples. Next, the best normalization mode for each element was chosen evaluating the RSD and trueness values of the elements.

The concentration values obtained using these three univariate calibration strategies are shown in Table 3. For the determination of Ca, samples #S8 and #S9 were used as standards, and the trueness values of this element ranged from 79 to 131% for OP MLC, 59 to 102% for SSC, and 80 to 116% for TP CT, as shown in Fig. 3. For K, samples #S9 and #S10 were used as standards. The trueness values ranged from 83 to 126% for OP MLC, 67 to 126% for SSC, and 94 to 123% for TP CT. For this element, the trueness values are depicted in Fig. 4. On the other hand, for the determination of Mg, samples #S4, #S5, and #S9 were used as standards; the trueness values ranged from 83 to 115% for OP MLC, 63 to 126% for SSC, and 82 to 118% for TP CT, and these results are shown in Fig. 5. In addition, the RSD (%) for Ca in all samples ranged from 2 to 26 for OP MLC, 3 to 29 for SSC and 2 to 33 for TP CT. For K, the RSD ranged from 3 to 24 for OPM LC, 5 to 35 for SSC, and 4 to 34 for TP CT. For Mg, the RSD (%) values ranged from 3 to 23 for OP MLC, 0.1 to 30

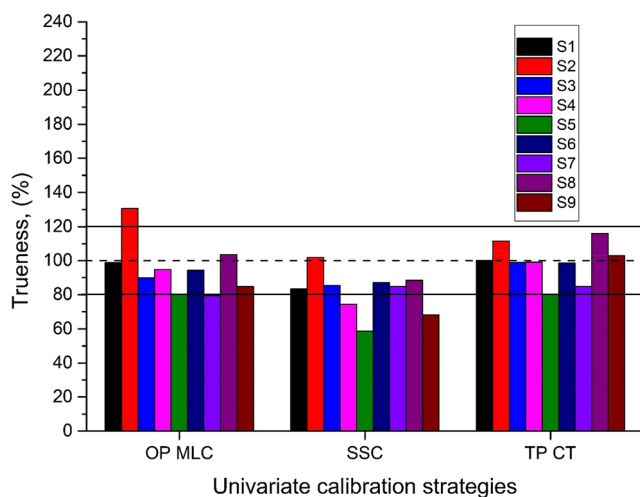


**Fig. 3** Trueness (%) values obtained for Ca employed three univariate calibrations

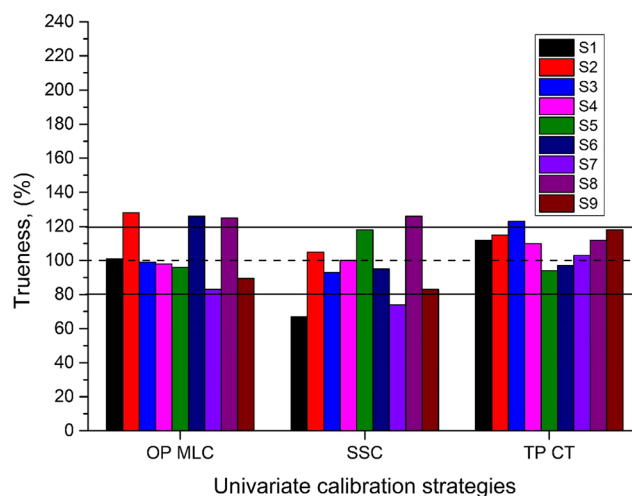


**Fig. 4** Trueness (%) values obtained for K employed three univariate calibrations

for SSC, and 5 to 28 for TP CT. These values showed good precision and are considerably acceptable for direct solid analysis by LIBS; more details of normalization modes, emission lines, signal type, and RSD range obtained in each calibration strategy are shown in Table 4.

The use of these univariate calibration strategies for matrix matching in cocoa bean samples presented good trueness values, except in some cases, where the trueness values were below 80%, mainly when SSC was used. This is probably related to the lower correlation of the elements to estimate the concentration.

However, among all calibration strategies discussed here, a particularity must be considered mainly when TP CT is used, i.e., the sample chosen as the standard and the analyzed samples must present similar physicochemical properties. Moreover, greater variability of the concentration

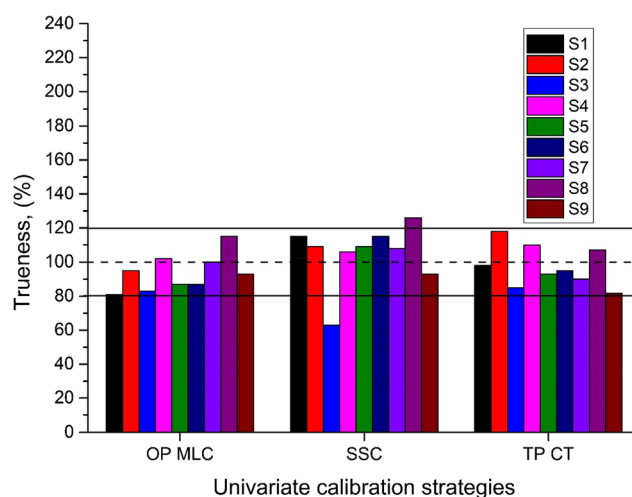


**Fig. 5** Trueness (%) values obtained for Mg employed three univariate calibrations

**Table 4** Parameters for univariate calibration

Element	OP MLC			SSC			TP CT			
	Best normalization	Signal type	RSD (% range)	Best normalization	Signal type	RSD (% range)	Best normalization	Signal type	Emission lines (nm)	RSD (% range)
Ca	1, 2, 5, and 6	Area/height	2–26	1, 3, 4, 7, and 9	Area/height	3–29	5	Area/height	Ca II 393.37, Ca II 396.85, Ca I 422.67, and Ca II 431.87	2–33
K	1 and 4	Area/height	3–24	1, 2, 3, and 11	Area/height	5–35		Area/height	K I 766.49 and K II 769.89	4–34
Mg	1, 2, 4, 6, and 11	Area/height	3–23	1, 2, 4, 7, and 11	Area/height	0.1–30		Height	Mg II 280.27, Mg II 279.55, Mg II 279.80, and Mg I 285.21	5–28

values between the standard and the samples cannot be observed. If this consideration is neglected, the accuracy can be compromised.

In addition, as TP CT uses two points, the F-test was used to evaluate the linearity of the curve, and the F-test ratio varied from 3 to 12,771 in all samples, showing good linearity of the models.

To evaluate the capability of all univariate calibration strategies for the determination of Ca, K, and Mg, the standard error (SE) was calculated using Eq. 4.

$$SE = \sqrt{\frac{\sum (y_i - \hat{y}_i)^2}{n-1}} \quad (4)$$

where  $y_i$  is the analyte reference concentration,  $\hat{y}_i$  is the concentration predicted by the calibration model, and  $n$  is the number of samples.

**Fig. 6** Standard errors (%) for each determined element using the proposed univariate calibration (OP MLC, SSC, and TP CT)

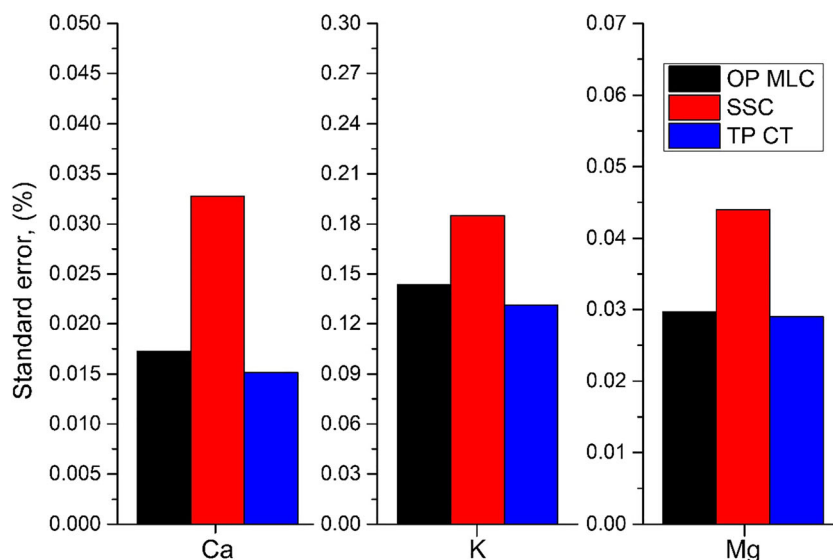


Figure 6 shows the SE results for the determined elements in all calibration strategies. According to the results, it is possible to note that in all strategies, low errors are observed compared with the lowest concentration in the samples: 0.052% (Ca), 0.734% (K), and 0.197% (Mg).

Therefore, each calibration strategy presents its own advantages and disadvantages and can be used according to its necessity, but it depends on several factors; for example, the intrinsic characteristics of the analyte, variability of the analyte concentration in the standard and sample, and the homogeneity of the sample can affect the accuracy and precision in the determination of the analytes. For example, in the determination of Ca, K, and Mg, SSC failed to minimize or correct the matrix effects in some samples.

In general, we can consider that these strategies are able to determine Ca, K and Mg in cocoa bean samples once good trueness and lower errors are obtained. In addition, it is important to mention that the determined concentration values of Ca, K, and Mg in cocoa beans showed that are

excellent sources of these important macronutrients for the human diet.

## Conclusions

The possibility of using the three univariate calibration strategies (OP MLC, SSC, and TP CT) for matrix matching to minimize matrix effects in the determination of metals in cocoa beans by employing LIBS was simple and fast because no standard addition is required, which simplifies the sample preparation process. Of the employed strategies, OP MLC and TP CT presented good results with robustness and precision when compared with those obtained by SSC. Therefore, in general, these strategies can be considered effective and suitable for elemental determination in complex matrices, which is a challenge in direct solid analysis by LIBS.

**Acknowledgments** The authors are grateful to the Conselho Nacional de Desenvolvimento Científico e Tecnológico (CNPq, Brazil, process number 158587/2017-0, 141311/2017-7, 305637/2015-0) and the Fundação de Amparo à Pesquisa do Estado de São Paulo (FAPESP, process number 2016/01513-0). The authors are also grateful to Prof. Dr. Fábio Alan Carqueija Amorim from State University of Santa Cruz (Ilhéus, Brazil) for cocoa bean samples supply.

**Funding Information** This study was financed in part by the Coordenação de Aperfeiçoamento de Pessoal de Nível Superior, Brasil (CAPES)—Finance Code 001).

**Compliance with Ethical Standards** Informed consent was obtained from all individual participants included in the study.

**Conflict of Interest** Raimundo Rafael Gamela declares that he has no conflict of interest. Vinicius Câmara Costa declares that he has no conflict of interest. Diego Vitor Babos declares that he has no conflict of interest. Alisson Silva Araújo declares that he has no conflict of interest. Edenir Rodrigues Pereira-Filho declares that he has no conflict of interest.

**Ethical Approval** This article does not contain any studies involving human participants or animals performed by any of the authors.

## References

- Andrade DF, Fortunato FM, Pereira-Filho ER (2019) Calibration strategies for determination of the In content in discarded liquid crystal displays (LCD) from mobile phones using laser-induced breakdown spectroscopy (LIBS). *Anal Chim Acta* 1061:42–49. <https://doi.org/10.1016/j.aca.2019.02.038>
- Andújar I, Recio MC, Giner RM, Ríos JL (2012) Cocoa polyphenols and their potential benefits for human health. *Oxidative Med Cell Longev*. <https://doi.org/10.1155/2012/906252>
- Augusto AS, Barsanelli PL, Pereira FMV, Pereira-Filho ER (2017) Calibration strategies for the direct determination of Ca, K, and Mg in commercial samples of powdered milk and solid dietary supplements using laser-induced breakdown spectroscopy (LIBS). *Food Res Int* 94:72–78. <https://doi.org/10.1016/j.foodres.2017.01.027>
- Babos DV, Virgílio A, Costa VC, Donati GL, Pereira-Filho ER (2018) Multi-energy calibration (MEC) applied to laser-induced breakdown spectroscopy (LIBS). *J Anal At Spectrom* 33:1753–1762. <https://doi.org/10.1039/C8JA00109J>
- Babos DV, Barros AI, Nóbrega JA, Pereira-Filho ER (2019) Calibration strategies to overcome matrix effects in laser-induced breakdown spectroscopy: direct calcium and phosphorus determination in solid mineral supplements. *Spectrochim Acta B At Spectrosc* 155:90–98. <https://doi.org/10.1016/j.sab.2019.03.010>
- Bendicho C, Lavilla I, Pena-Pereira F, Romero V (2012) Green chemistry in analytical atomic spectrometry: a review. *J Anal At Spectrom* 24: 1831–1857. <https://doi.org/10.1039/C2JA30214D>
- Castro JP, Pereira-Filho ER (2016) Twelve different types of data normalization for the proposition of classification, univariate and multivariate regression models for the direct analyses of alloys by laser-induced breakdown spectroscopy (LIBS). *J Anal At Spectrom* 31: 2005–2014. <https://doi.org/10.1039/C6JA00224B>
- Castro JP, Babos DV, Pereira-Filho ER (2019) Calibration strategies for the direct determination of rare earth elements in hard disk magnets using laser-induced breakdown spectroscopy. *Talanta*. <https://doi.org/10.1016/j.talanta.2019.120443>
- Costa VC, Castro JP, Andrade DF, Babos DV, Garcia JA, Sperança MA, Catelani TA, Pereira-Filho ER (2018) Laser-induced breakdown spectroscopy (LIBS) applications in the chemical analysis of waste electrical and electronic equipment (WEEE). *Trends Anal Chem* 108:65–73. <https://doi.org/10.1016/j.trac.2018.08.003>
- Costa VC, Pinheiro FC, Amorim FAC, Silva EGP, Pereira-Filho ER (2019a) Multivariate optimization for the development of a sample preparation procedure and evaluation of calibration strategies for nutrient elements determination in handmade chocolate. *Microchem J* 150:104166. <https://doi.org/10.1016/j.microc.2019.104166>
- Costa VC, Augusto AS, Castro JP, Machado RC, Andrade DF, Babos DV, Sperança MA, Gamela RR, Pereira-Filho ER (2019b) Laser induced-breakdown spectroscopy (LIBS): histórico, fundamentos, aplicações e potencialidades. *Quim Nova* 42:527–545. <https://doi.org/10.21577/0100-4042.20170325>
- Cremers DA, Radziemski LJ (2006) History and fundamentals of LIBS. In: Miziolek AW, Palleschi V, Schechter I (eds) *Laser-induced breakdown spectroscopy*. Cambridge University Press, New York
- Dico GM, Galvano F, Dugo G, D'ascenzi C, Macaluso A, Vella A, Giangrosso G, Cammilleri G, Ferrantelli V (2018) Toxic metal levels in cocoa powder and chocolate by ICP-MS method after microwave-assisted digestion. *Food Chem* 245:1163–1168. <https://doi.org/10.1016/j.foodchem.2017.11.052>
- Escandar GM, Olivieri AC, Faber NM, Goicoechea HC, de la Peña AM, Poppi RJ (2007) Second- and third-order multivariate calibration: data, algorithms and applications. *Trends Anal Chem* 26:752–765. <https://doi.org/10.1016/j.trac.2007.04.006>
- Febrianto NA, Zhu F (2019) Diversity in composition of bioactive compounds among 26 cocoa genotypes. *J Agric Food Chem* 67:9501–9509. <https://doi.org/10.1021/acs.jafc.9b03448>
- Gupta GP, Suri BM, Verma A, Sundararaman M, Unnikrishnan VK, Alti K, Kartha VB, Santhosh C (2011) Quantitative elemental analysis of nickel alloys using calibration-based laser-induced breakdown spectroscopy. *J Alloys Compd* 509:3740–3745. <https://doi.org/10.1016/j.jallcom.2010.12.189>
- Hao ZQ, Liu L, Zhou R, Ma YW, Li XY, Guo LB, Lu YF, Zeng XY (2018) One-point and multi-line calibration method in laser-induced breakdown spectroscopy. *Opt Express* 26:22926–22933. <https://doi.org/10.1364/OE.26.022926>
- International Cocoa Organization-ICCO (2018) Production - Latest figures from the Quarterly Bulletin of Cocoa Statistics. Available in: <[http://www.icco.org/about-us/international-cocoa-agreements/cat\\_view/30-related-documents/46-statistics-production.htm](http://www.icco.org/about-us/international-cocoa-agreements/cat_view/30-related-documents/46-statistics-production.htm)>. Accessed in: 21 of august 2019

- Lepore KH, Fassett CI, Breves EA, Byrne S, Giguere S, Boucher T, Rhodes JM, Vollinger M, Anderson CH, Murray RW, Dyar MD (2017) Matrix Effects in Quantitative Analysis of Laser-Induced Breakdown Spectroscopy ( LIBS ) of Rock Powders Doped with Cr , Mn , Ni , Zn, and Co. *Appl Spectrosc* 71:600–626. <https://doi.org/10.1177/0003702816685095>
- Machado RC, Andrade DF, Babos DV, Castro JP, Costa VC, Sperança MA, Garcia JA, Gamela RR, Pereira-Filho ER (2019) Solid sampling: advantages and challenges for chemical element determination—a critical review. *J Anal At Spectrom*. <https://doi.org/10.1039/C9JA00306A>
- Markiewicz-Keszyccka M, Cama-Moncunill X, Casado-Gavalda MP, Dixit Y, Cama-Moncunill R, Cullen PJ, Sullivan C (2017) Laser-induced breakdown spectroscopy (LIBS) for food analysis: a review. *Trends Food Sci Technol* 65:80–93. <https://doi.org/10.1016/j.tifs.2017.05.005>
- Noll R (2012) *Laser-induced breakdown spectroscopy: fundamentals and applications*, First edn. Springer-Verlag, Berlin Heidelberg
- Olivieri AC (2015) Practical guidelines for reporting results in single- and multi-component analytical calibration: a tutorial. *Anal Chim Acta* 868:10–22. <https://doi.org/10.1016/j.aca.2015.01.017>
- Safi A, Campanella B, Grifoni E, Legnaioli S, Lorenzetti G, Pagnotta S, Poggialini F, Ripoll-Seguer L, Hidalgo M, Palleschi V (2018) Multivariate calibration in laser-induced breakdown spectroscopy quantitative analysis: the dangers of a ‘black box’ approach and how to avoid them. *Spectrochim Acta B At Spectrosc* 144:46–54. <https://doi.org/10.1016/j.sab.2018.03.007>
- Sperança MA, Andrade DF, Castro JP, Pereira-Filho ER (2019) Univariate and multivariate calibration strategies in combination with laser-induced breakdown spectroscopy (LIBS) to determine Ti on sunscreen: a different sample preparation procedure. *Opt Laser Technol* 109:648–653. <https://doi.org/10.1016/j.optlastec.2018.08.056>
- Takahashi T, Thornton B (2017) Quantitative methods for compensation of matrix effects and self-absorption in LIBS signals of solid. *Spectrochim Acta B* 138:31–42. <https://doi.org/10.1016/j.sab.2017.09.010>
- Villa JEL, Peixoto RRA, Cadore S (2014) Cadmium and lead in chocolates commercialized in Brazil. *J Agric Food Chem*:628759–628763. <https://doi.org/10.1021/jf5026604>
- Villa JEL, Pereira CD, Cadore S (2015) A novel, rapid and simple acid extraction for multielemental determination in chocolate bars. *Microchem J*:121199–121204. <https://doi.org/10.1016/j.microc.2015.03.008>
- Wang J, Shi M, Zheng P, Xue S (2017) Quantitative analysis of lead in tea samples by laser-induced breakdown spectroscopy. *J Appl Spectrosc* 84:188–193. <https://doi.org/10.1007/s10812-017-0448-9>
- World Cocoa Foundation-WCF (2018) History of cocoa. Available in: <<http://worldcocoafoundation.org/about-cocoa/history-of-cocoa/>>. Accessed in: 18 of December 2019
- Yanus RL, Sela H, Borojovich EJC, Zakon Y, Saphier M, Nikolski A, Gutflais E, Lorber A, Karpas Z (2014) Trace elements in cocoa solids and chocolate: an ICPMS study. *Talanta* 119:1–4. <https://doi.org/10.1016/j.talanta.2013.10.048>
- Yuan R, Tang Y, Zhu Z, Hao Z, Li J, Yu H, Yu Y, Guo L, Zeng X, Lu Y (2019) Accuracy improvement of quantitative analysis for major elements in laser-induced breakdown spectroscopy using single-sample calibration. *Anal Chim Acta* 1064:11–16. <https://doi.org/10.1016/j.aca.2019.02.056>
- Zhang T, Tang H, Li H (2018) Chemometrics in laser-induced breakdown spectroscopy. *J Chemom* 32:2983. <https://doi.org/10.1002/cem.2983>



**Publisher's Note** Springer Nature remains neutral with regard to jurisdictional claims in published maps and institutional affiliations.

## **Chapter 4 – Published Results**



Cite this: DOI: 10.1039/c9ay01916b

# Hyperspectral images: a qualitative approach to evaluate the chemical profile distribution of Ca, K, Mg, Na and P in edible seeds employing laser-induced breakdown spectroscopy†

Raimundo R. Gamela, Marco A. Sperança, Daniel F. Andrade  and Edenír R. Pereira-Filho \*

In the present study, laser-induced breakdown spectroscopy (LIBS) combined with chemometric tools was used to investigate the metal composition in nine seed samples. The samples were directly analyzed, and a matrix with 9 rows and 9 columns (81 points) and 10 consecutive pulses were analyzed in each point. A total of 810 emission spectra were collected from 186 to 1042 nm from the surface and bulk of the sample. The dataset was normalized by Euclidian norm and principal component analysis (PCA) was used for the initial exploratory investigation. Calcium, Mg, Na, K and P were mainly identified in all samples; however, the distribution of metals in these samples is not completely homogeneous, *i.e.*, the composition of the elements change from one layer to another. This fact can be probably related to the absorption capability of nutrients resulting from different factors such as soil characteristics, physiology of the plant, water source composition and fertilizers which can influence the distribution of the elements in different seeds. To confirm the elements observed by LIBS, the samples were digested using microwave-assisted digestion, and Ca, K, Mg, Na and P were determined by inductively coupled plasma-optical emission spectrometry (ICP-OES). In addition, some minor nutrients such as S and Zn were also investigated and the relationships between elements were observed through the Pearson correlation graph, and some of them, such as Mg and Na, P and Na, S and P, S and Zn, are extremely correlated; it means that, for example, when the concentration of Mg increases, that of Na also increases.

Received 4th September 2019  
Accepted 23rd September 2019

DOI: 10.1039/c9ay01916b

rsc.li/methods

## 1. Introduction

Seeds and nuts have been mostly consumed due to the high concentration values of different nutrients, such as proteins, unsaturated fatty acids, vitamins and essential chemical elements, which play an important healthy role in the human body. In addition, some edible seeds are used in food industry processes to be converted into other products, such as oils for human consumption.<sup>1–3</sup>

Before human consumption, seeds are subject to several growth stages, which can be affected by different factors, such as morphological and physiological conditions. These factors can directly affect the nutritional efficiency caused due to the low absorption capability of the nutrients present in the soil.<sup>4</sup>

Therefore, our intention is to chemically characterize, *i.e.*, to evaluate the chemical profile distribution of Ca, K, Mg, Na and P in seed samples, and at the same time explain the variations in

the distribution process of these elements in different layers of seeds. However, this process would not be possible with simple digestion of the samples and analyte determination by analytical techniques, such as inductively coupled plasma optical emission spectrometry (ICP-OES) and flame atomic absorption spectrometry (FAAS).<sup>5–8</sup>

Taking these points into consideration, it is important to combine strategies for rapid and reliable analysis with little or no sample preparation. Laser-induced breakdown spectroscopy (LIBS) has been used for the analysis of different matrices due to its capability to combine direct solid sample chemical inspection and rapid simultaneous determination of several elements in few minutes and with high analytical frequency.<sup>9–12</sup> In addition, the combination of LIBS features and chemometric tools can generate hyperspectral images that can be mathematically decomposed using principal component analysis (PCA) (score maps and loadings). The use of hyperspectral images can help in the interpretation and observation of the chemical distribution of Ca, K, Mg, Na and P in seed samples simultaneously and identifying their relationship.<sup>13</sup>

This strategy has been used by several authors for qualitative determination and chemical distribution identification of solid

Group of Applied Instrumental Analysis, Department of Chemistry, Federal University of São Carlos, P.O. Box 676, São Carlos, São Paulo State, 13565-905, Brazil. E-mail: erpf@ufscar.br; Tel: +55 16 3351 8092

† Electronic supplementary information (ESI) available. See DOI: 10.1039/c9ay01916b

samples. Sperança *et al.*<sup>14</sup> used LIBS and hyperspectral images for direct evaluation of the chemical composition profile of coprolites. The authors correlated the chemical composition with the nature of the fossil and the environment and with the taphonomic process. McMillan *et al.*<sup>15</sup> (2014) used LIBS and hyperspectral images to map the Cu composition of ore samples. Carvalho *et al.*<sup>13</sup> (2015) investigated the metal composition of a printed circuit board (PCB) sample from a mobile phone, combining LIBS, hyperspectral images, and scanning electron microscopy with energy-dispersive X-ray spectroscopy (SEM-EDS).

Castro and Pereira-Filho<sup>16</sup> developed a study to assess technological elemental composition of magnets from computer hard disks. Besides the ICP-OES technique for quantitative analysis, the authors employed LIBS to obtain hyperspectral images to verify the chemical composition and certain special features. Other applications of hyperspectral images were employed by Carneiro and Poppi<sup>17,18</sup> for *in situ* analysis of a imiquimod pharmaceutical preparation presented as cream, and the homogeneity study of ointment dosage forms, respectively. These studies were performed by infrared imaging spectroscopy.

However, the literature reveals no studies using LIBS for hyperspectral images in seed samples. Thus, the present study reports the applicability of LIBS and chemometric tools to evaluate the chemical profile distribution of Ca, K, Mg, Na and P on the surface and in the bulk of the samples.

## 2. Materials and methods

### 2.1 Instrumentation

In this study, edible seed samples were directly analyzed employing a LIBS instrument: model J200 from Applied Spectra (Freemont, USA) with a Nd:YAG laser (1064 nm) used for emission spectra acquisition. To purge ablated particles, the equipment is fitted with a HEPA air cleaner, and the movement of the sample is performed by a automated XYZ stage and a 1280 × 1024 CMOS (complementary metal-oxide semiconductor) color-camera imaging system. For obtaining the emission spectra, the plasma emission light is conducted through an optical fiber bundle coupled to a 6-channel CCD (charge-coupled device) spectrometer with a spectral range from 186 to 1042 nm resulting in 12 288 variables, with a gate width of 1.05 ms. For the identification of the emission lines of the elements, the Aurora Software Package (Applied Spectra) was used. In addition, an ICP-OES, model iCAP 7000 (Thermo Fisher Scientific, USA) was employed for the determination of the elements identified by LIBS analysis. The plasma conditions and the emission lines used in ICP-OES determination are described in Table 1.

### 2.2 LIBS and ICP-OES analysis

Nine seed samples used in the present study were acquired from a local market in São Carlos city, São Paulo State, Brazil. The popular and scientific name of the samples is presented in Table 2.

Table 1 Operational conditions for determination by ICP-OES

Instrumental parameters	Operational conditions
Radio frequency applied power (kW)	1.15
Integration time for low emission line (s)	15
Integration time for high emission line (s)	5
Sample introduction flow rate (mL min <sup>-1</sup> )	1.0
Pump stabilization time (s)	5
Argon auxiliary flow rate (L min <sup>-1</sup> )	0.5
Argon plasma flow rate (L min <sup>-1</sup> )	12
Argon nebulizer flow rate (L min <sup>-1</sup> )	0.7
Replicates	3
Elements and wavelengths (nm); viewing mode: axial <sup>a</sup> and radial <sup>b</sup>	<sup>b</sup> Ca II (396.847), <sup>b</sup> K I (766.490), <sup>a</sup> Mg II (279.553), <sup>a</sup> Mn II (257.610), <sup>a</sup> Na I (588.593) <sup>b</sup> P I (178.284) <sup>b</sup> S I (180.731) and <sup>b</sup> Zn I (213.857)

Before analysis, experimental conditions for LIBS parameters were optimized using a central composite design. Thus, the optimized instrumental conditions were as follows: 53 mJ laser pulse energy, 50 μm spot size resulting in a fluency of 2699 mJ cm<sup>-2</sup> and 1.9 μs delay time. All edible seed samples were directly analyzed by LIBS without any sample preparation procedure. A pattern for analysis was applied from a matrix with 9 rows and 9 columns (9 × 9) for a total of 81 points according to the pictorial information described in Fig. 1. The distance between each point was 0.5 mm, an area of 16 mm<sup>2</sup> (4 × 4 mm) was covered, and 10 consecutive laser pulses per point were used to obtain elemental information along the surface and bulk of the sample; in each point, a total of 810 pulses were recorded for each sample.

To confirm the elements observed by LIBS, the samples were ground using a mill type Wyllie (model CE-430, CIENLAB, São Paulo, Brazil). After that, the samples were mineralized using a microwave system (Speedwave XPERT, Berghof, Eningen, BW, Germany). A sample mass of 0.350 g was directly weighed in

Table 2 The scientific and popular name of the seed samples studied

Description	Scientific name	Commercial name
S1	<i>Dipteryx alata</i>	Garbanzo seed
S2	<i>Lupinus albus</i> L.	Dried lupine
S3 <sup>a</sup>	<i>Lens culinaris</i>	Red lentil
S4 <sup>a</sup>	<i>Pisum sativum</i> L.	Pea seed
S5 <sup>a</sup>	<i>Cucurbita moschata</i>	Pumpkin seed
S6	<i>Salvia hispanica</i>	Chia seed
S7	<i>Linum usitatissimum</i> L.	Flaxseed
S8	<i>Myristica fragrans</i>	Nutmeg
S9	<i>Dipteryx alata</i>	Chestnut baru

<sup>a</sup> The samples used for hyperspectral images.

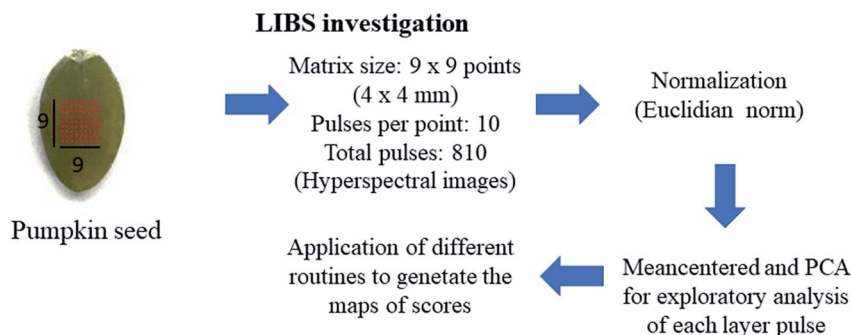


Fig. 1 Pictorial information of the data organization and treatment.

Teflon vessels (DAP 60) and 4.0 mL of  $\text{HNO}_3$  65% v/v, 2.0 mL of  $\text{H}_2\text{O}_2$  30% v/v and 2.0 mL of  $\text{H}_2\text{O}$  were added. The samples were subjected to the following heating program, performed in three steps (temperature in  $^\circ\text{C}$ /ramp in min/hold in min): (i) 170/5/10; (ii) 200/1/15; (iii) 50/1/10. After cooling, the samples were transferred to polyethylene flasks and a final volume of 40 mL was completed with ultrapure water (18 M $\Omega$  cm resistivity, Milli-Q® plus, Millipore Corp, Bedford, MA, USA).

Elemental standard solutions (Ca, Cu, K, Mg, Mn, Na P, S and Zn) containing 1000 mg  $\text{L}^{-1}$  (Merck, Darmstadt, Germany) were properly diluted to prepare the calibration solutions for determination by ICP-OES (reference method) using high purity water. The analyses were performed using the ICP-OES technique, and more details are provided in Table 1.

### 2.3 Data treatment

All data organization, treatment and calculations were performed in MATLAB 2018a (Mathworks, Natick, MA, USA) and Pirouette version 4.5 (Infometrix, Bothell, WA, USA). The dataset from each sample was organized in 81 lines (spectra) and 12 288 columns (emission lines from 186 to 1042 nm), and the data were normalized by norm to minimize problems related to sample surface microheterogeneity and signal fluctuation from the laser-matter interaction during the data acquisition.<sup>19</sup>

After that, principal component analysis (PCA) was performed, which consists of singular value decomposition (SVD) where  $\mathbf{X}$  matrix is decomposed into two new matrices,  $\mathbf{T}$  (scores) and  $\mathbf{P}$  (loadings),<sup>20</sup> *i.e.*, using  $\mathbf{T}$  and  $\mathbf{P}$  it is possible to identify patterns in the original matrix  $\mathbf{X}$  that normally contains the samples in the rows and variables in the columns. This tool is an unsupervised method that correlates different variables for the evaluation and characterization of the analytical data, identifying trends and sample clusters. In addition, PCA offers possibilities to evaluate the loading information of various elements in single images making data interpretation easy.<sup>20</sup> Therefore, using PCA is possible to correlate the distribution of the elements in different depth layers of the sample. In this study, the samples were the spectrum of each analyzed point, and the variables were the emission lines obtained by LIBS. Thus, PCA was performed using the normalized data (12 288 variables) for the initial exploratory analysis of each layer pulse,

in this case from 1 to 10. After that, the normalized dataset was mean centered (810  $\times$  12 288 variables). The third script designated as “libs”<sup>13</sup> was used to generate the score maps in a 4D tensor. In this sense, the scores  $\mathbf{T}$ , loadings  $\mathbf{P}$  and the explained variance for each PC were obtained. Hence, for this purpose, the number of laser pulses at each point, number of horizontal points (9), number of vertical points (9) and number of PC (5) are necessary as inputs in the “libs” script to create the hyperspectral image. The last script used, the so-called “libs\_plot” (Sperança *et al.*<sup>14</sup>), automatically plots the score maps for a specific pulse layer. Besides Matlab, all these scripts can be used in a free program named Octave. The same procedure was performed for other samples as describe previously.

## 3. Results and discussion

### 3.1 Optimization of instrumental parameters

To obtain reliable results employing LIBS, some measurement parameters such as delay time and fluence needed to be optimized to identify the best conditions for analysis. The additional laser settings used were fixed as follows: a scan length of 8 mm, a laser repetition rate of 5.0 Hz, and ablation chamber speed is fixed at 1.0 mm  $\text{s}^{-1}$ .

For this purpose, central composite design with 11 experiments (3 replicates in central point) was used to obtain both the highest area, height and signal-to-background ratio (SBR) for the most intense emission lines monitored (Ca, K, Mg, Na and P). The variables were evaluated in five levels coded between  $-1.422$  to  $1.422$ , and the experimental matrix of the central composite design is shown in Table 3. Due to instrumental limitations, the variable fluence was studied from 1448 ( $-1.422$ ) to 3820 mJ  $\text{cm}^{-2}$  (1.363) and around 600 spectra were collected through a matrix (raster) studied in different regions of the sample surface. The emission line intensities monitored were Ca II 393.36, K I 766.49, Mg II 279.55, Na I 589.59 and P I 213.0.

In this case, to achieve simultaneous optimization and to find the best conditions for each response, the desirability (di) function was calculated as a function of the SBR, area and height of all monitored elements, according to eqn (1). The di function allows us to attribute values between 0 (undesirable response, lowest SBR, area and height) and 1 (desirable response, highest SBR, area and height).



**Table 3** Matrix of the central composition design with the variables used for the optimization of instrumental conditions employing LIBS, and the overall desirability values (OD) obtained

Experiments	Fluence (mJ cm <sup>-2</sup> )		Delay time (μs)		OD
	Real	Coded	Real	Coded	
1	1811	-0.996	0.7	-1.000	0.32
2	3514	1.004	0.7	-1.000	0.42
3	1811	-0.996	1.7	1.000	0.44
4	3514	1.004	1.7	1.000	0.57
5	2699	0.000	1.2	0.000	0.52
6	2699	0.000	1.2	0.000	0.46
7	2699	0.000	1.2	0.000	0.61
8	1448	-1.422	1.2	0.000	0.46
9	3820	1.363	1.2	0.000	0.47
10	2699	0.000	0.5	-1.414	0.37
11	2699	0.000	1.9	1.414	0.58

$$d_i = \left( \frac{y - L}{T - L} \right)^s \quad (1)$$

where  $L$  is the lowest acceptable value for the response,  $T$  is the target value, and  $s$  is the weight (when equal to 1 = linear desirability function). In the present study,  $L$  values were the lowest for the SBR, height and area in the set of experiments for each element and  $T$  values were the highest for SBR, height and area for each element. The weight  $s$  was 1.

Thus, the overall desirability (OD) was combined into a single response, as can be seen in eqn (2).

$$OD = \sqrt[n]{d_1 d_2 \dots d_m} \quad (2)$$

where  $m$  is the number of response variables evaluated simultaneously.

Before the proposition of calibration models, to overcome some drawbacks of LIBS, normalization of the data is necessary. In this sense, 12 normalization modes<sup>19</sup> were assessed for the calibration strategy. After performing normalization, a chemometric routine (libs\_par2) was used to calculate the signal-to-background ratio (SBR) as well as both the signal area and height for a specified emission line. Thus, the normalization mode by sum (normalization 5) was considered suitable and presented a better fit of the model because the ratio between the *Mean of Square of lack of fit* (MSlof) and *Mean of Square of pure error* (MSep), the  $F$  calculated (0.41) is lower than  $F_{tabulated}$  (19.16). However, comparing the *Mean of Square of Regression* (MSR) and *Mean of Square of Residue* (MSRes), the  $F$  calculated (2.9) should be higher than  $F_{tabulated}$  (5.05). Despite the regression not being good enough, this observation does not affect the predictive capability of the model.

The surface response of the optimized conditions is shown in Fig. 2. Moreover, is possible to observe that variable 1 (laser pulse fluence) was not significant including their interactions, *i.e.*, any condition tested in the experimental domain can be used, while the variable 2 (delay time) is more significant, and high values of OD are obtained when long delay time was used. Therefore, the central composite design model generated the OD calculated from eqn (3).

In this sense, a delay time of 1.9 μs and a fluence of 2699 mJ cm<sup>-2</sup>, with 53 mJ laser pulse energy and 50 μm spot size were used for further experiments.

$$OD = 0.528 \pm 0.09 + 0.069 \pm 0.06v_2 \quad (3)$$

$v_2$ : delay time.

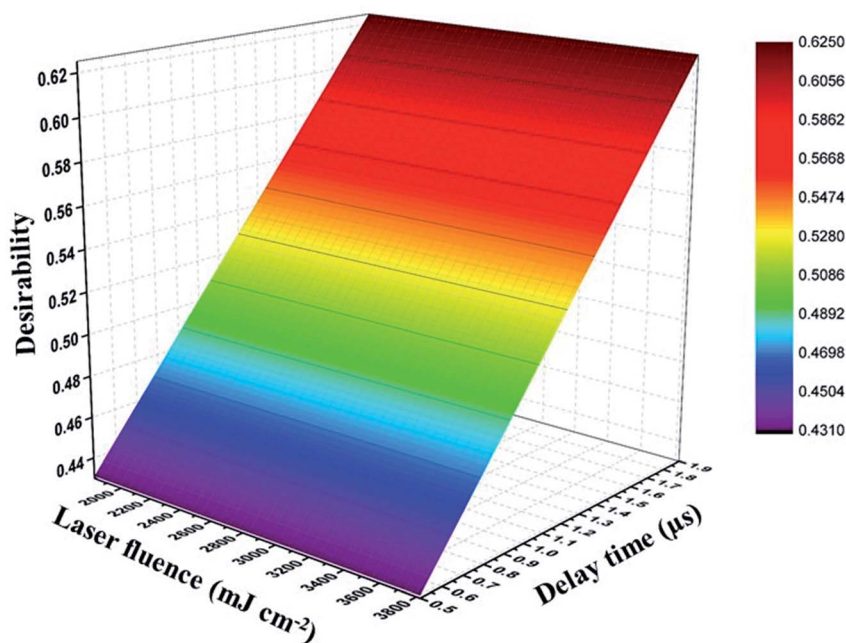


**Fig. 2** Response surface of the optimized instrumental conditions for LIBS as a function of the overall desirability (OD) obtained from the central composite design for the study of hyperspectral images in seed samples.

**Table 4** Concentration values of Ca, Cu, K, Mg, Mn, Na, P, S and Zn in seed samples obtained using the ICP-OES technique (mean  $\pm$  standard deviation,  $n = 3$ )

Samples	Concentration ( $\text{mg kg}^{-1}$ )								
	Ca	Cu	K	Mg	Mn	Na	P	S	Zn
S1#	1341 $\pm$ 125	10 $\pm$ 4	10 440 $\pm$ 425	1422 $\pm$ 170	40 $\pm$ 4	731 $\pm$ 21	6042 $\pm$ 314	2130 $\pm$ 234	35 $\pm$ 8
S2#	1544 $\pm$ 65	9 $\pm$ 1	6589 $\pm$ 42	1469 $\pm$ 58	217 $\pm$ 7	843 $\pm$ 18	4922 $\pm$ 126	2630 $\pm$ 138	45 $\pm$ 9
S3#	191 $\pm$ 3	7.0 $\pm$ 0.3	6696 $\pm$ 306	658 $\pm$ 8	8 $\pm$ 0.3	333 $\pm$ 14	4046 $\pm$ 147	1813 $\pm$ 18	45 $\pm$ 3
S4#	288 $\pm$ 20	6.0 $\pm$ 0.4	7898 $\pm$ 287	888 $\pm$ 35	8 $\pm$ 0.1	448 $\pm$ 26	4987 $\pm$ 53	2043 $\pm$ 44	25 $\pm$ 2
S5#	300 $\pm$ 24	12.0 $\pm$ 0.3	6227 $\pm$ 281	3928 $\pm$ 89	50 $\pm$ 0.3	1989 $\pm$ 111	25 986 $\pm$ 658	4321 $\pm$ 235	62 $\pm$ 4
S6#	4663 $\pm$ 132	6.0 $\pm$ 0.1	10 631 $\pm$ 341	2792 $\pm$ 103	46 $\pm$ 1	1419 $\pm$ 89	14 587 $\pm$ 621	4576 $\pm$ 241	56 $\pm$ 2
S7#	2435 $\pm$ 75	16 $\pm$ 1	7970 $\pm$ 321	3582 $\pm$ 110	47 $\pm$ 1	1815 $\pm$ 113	14 147 $\pm$ 513	3286 $\pm$ 175	68 $\pm$ 4
S8#	1628 $\pm$ 144	10.0 $\pm$ 0.3	3720 $\pm$ 230	1613 $\pm$ 72	15 $\pm$ 1.4	814 $\pm$ 2	3612 $\pm$ 153	1077 $\pm$ 102	13 $\pm$ 1
S9#	1403 $\pm$ 71	19.0 $\pm$ 0.4	13 957 $\pm$ 218	2694 $\pm$ 127	131 $\pm$ 2	1413 $\pm$ 89	16 093 $\pm$ 311	4379 $\pm$ 174	79 $\pm$ 1

### 3.2 ICP-OES analysis and the correlation of the elements

In this section, our intention was to use chemometric tools to evaluate the correlation of the samples. Elements such as Cu, Mn, S and Zn were not detected by LIBS; in this sense, they were determined by only ICP-OES and the quantitative data are shown in Table 4. The concentration level of the elements (in  $\text{mg kg}^{-1}$ ) ranged between 191–4663 for Ca, 6–19 for Cu, 20–98 for Fe, 3720–13 957 for K, 658–3928 for Mg, 8–217 for Mn, 333–1989 for Na, 3612–25 986 for P, 1077–4576 for S and 13–79 for Zn. It is worth noting that Ca, K, Mg, P and S presented the highest concentration values in all analyzed edible seed samples.

From the concentration of the elements, the data were organized as a matrix  $X$  ( $9 \times 9$ ) where the columns and rows are the elements with their concentration values, respectively. The data acquired by ICP-OES were subjected to an exploratory analysis using the Pearson correlation coefficient. This correlation ( $R$ ) shows the linear relationship between the element concentrations determined by ICP-OES. The higher absolute value near 1 indicates high dependence between two variables.

Each value obtained for these correlation coefficients is related to a specific color. Moreover, after this step, a Pearson correlation graph is generated to explain the possible correlation in the samples.

Fig. 3 shows the Pearson correlation graph used for the correlation of the elements in the samples and the red and blue colors represent high and low correlation of the elements. The correlation of an element with itself is always equal 1; in this way, the evaluation of correlation was performed for the different elements.

For example, P and Mg are highly positively correlated in these samples, *i.e.*, when the concentration value of P increases, the concentration value of Mg also increases. In addition, other elements such as Mg and Na, P and Na, S and P, S and Zn presented the same behavior of correlation and converge in the red color region of the Pearson correlation graph (see Fig. 3). However, Ca, Cu, K and Mn are inversely correlated when the concentration of other elements increases. For example, when the P concentration value increases, the concentration value of Ca, Cu and Mn decreases. This phenomenon can be explained

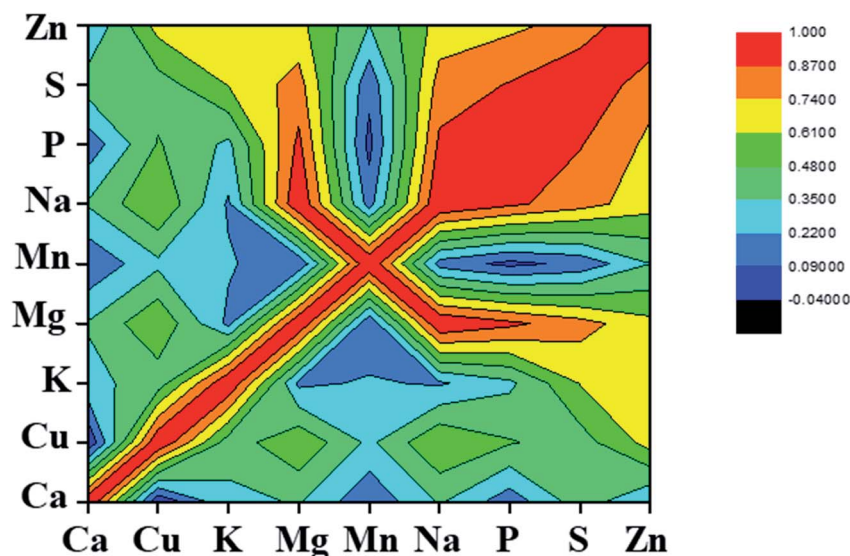


**Fig. 3** Pearson correlation graph used for the correlation of the elements in the sample.

to be due to the type of fertilizers used; it means that if P fertilizers, Zn fertilizers or a mixture of both was applied to the culture, it can influence nutrient concentrations, *i.e.*, no effect, increase or decrease individual nutrients. Experiments performed by Jiao *et al.*,<sup>21</sup> for example, show that P fertilizers can enhance the concentration of Mg; however, the addition of Zn can restrict the absorption of Ca and Cu, reducing the concentration of these elements. Therefore, this behavior explains the results as can be seen in Pearson correlation graphs (see Fig. 3).

### 3.3 Hyperspectral image interpretation

Complementary to ICP-OES and LIBS measurements, hyperspectral image analysis was performed under the optimized conditions to collect emission spectra of 3 samples, and another 6 samples, which present small dimensions making it difficult to study hyperspectral images (see Table 2). Fig. 4 shows a typical spectrum (a) before and (b) after normalization, which is composed of thousand emission lines (atomic lines, I and

ionic lines, II). The obtained loading values were used in combination with quantitative information acquired by ICP-OES (Table 4) to correlate the concentration values of the elements and their positions in the sample. Moreover, the score values were used to build score maps and analyzed together with the loading values to help better interpret the analyte profile distribution on the surface and in the bulk of the samples. The elements identified by LIBS and their emission lines are presented in Table 5.

All score maps were plotted using all variables (emission) of PC1 that presented high explained variance of the data. Fig. 5 shows the three score maps of pea seeds in layer pulses 1 (a), 5 (b) and 10 (c), and the loading plots using all variables (emission lines) studied for PC1 with 39%, 16% and 15% explained variance are shown in Fig. 1S in the ESI.† Fig. 1S(a)† presents the loading values of pulse 1, and Ca and K represent positive loading values related to the red color in the score map region, whereas in negative values of loadings, elements such as Mg and Na and some emission lines of Ca are related to the blue color region. On the other hand, Ca is less intense, with practically insignificant loadings in this layer.

In pulse 5, the loading values are represented in Fig. 1S(b).† Potassium, Mg and Na were found in positive loadings. In addition, fewer emission lines of Ca can be observed in this region. However, Na is the main element that presents high intensity and is distributed in the more intense red color region. For negative loading, only Mg is located in blue color in the score map region, while Ca presents less intensity and its loading values are near to zero.

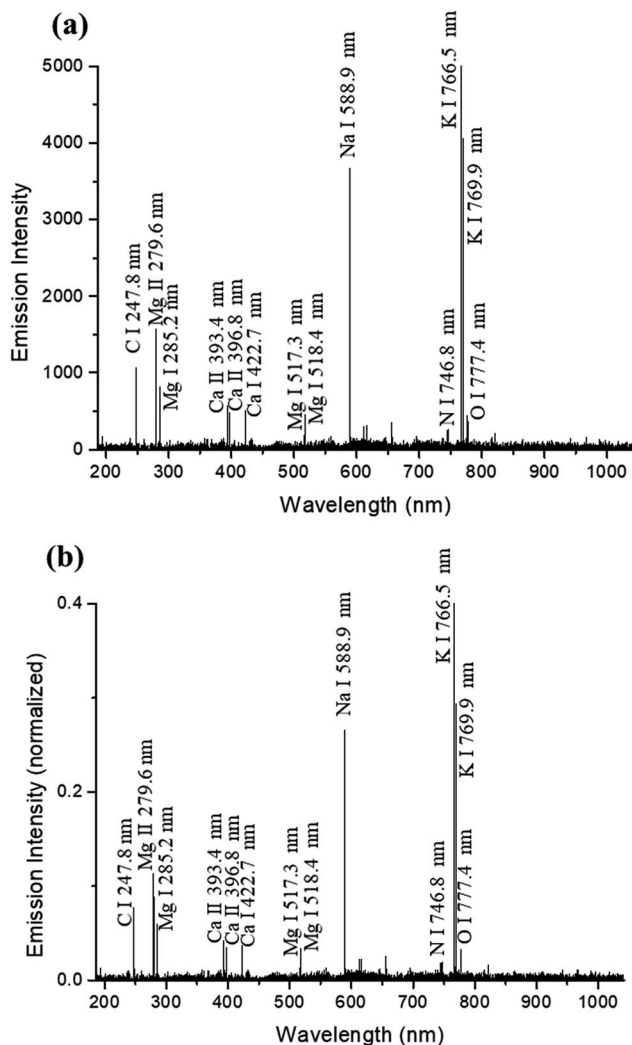


Fig. 4 Raw LIBS emission spectrum (a) and the emission spectrum normalized by the individual norm (b).

Table 5 Elements observed by LIBS with their emission lines and relative intensity<sup>a</sup>

Elements	Emission lines (nm)	Relative intensity <sup>b</sup>
Ca II	393.36	37 542
Ca II	396.84	34 742
Ca II	317.93	27 769
Ca II	373.68	27 247
Ca II	315.88	23 620
Ca I	422.67	8052
Ca I	558.87	3812
Ca I	643.90	3167
Ca I	649.38	1616
K I	766.49	3054
K I	769.89	1991
Mg II	280.27	352 473
Mg II	279.55	335 173
Mg I	518.36	321 771
Mg I	517.26	302 600
Mg I	285.21	232 716
Na I	588.99	10 000
Na I	589.59	10 000
P I	213.61	271

<sup>a</sup> I, Atomic emission line; II, ionic emission line. <sup>b</sup> Extracted from TruLIBS™ database software (Applied Spectra). TruLIBS™ emission lines were generated using a laser ablation source together with a highly sensitive UV spectrometer specially optimized to collect LIBS spectra. The resulting intensities and emission wavelengths are very accurate for LIBS.<sup>14</sup>

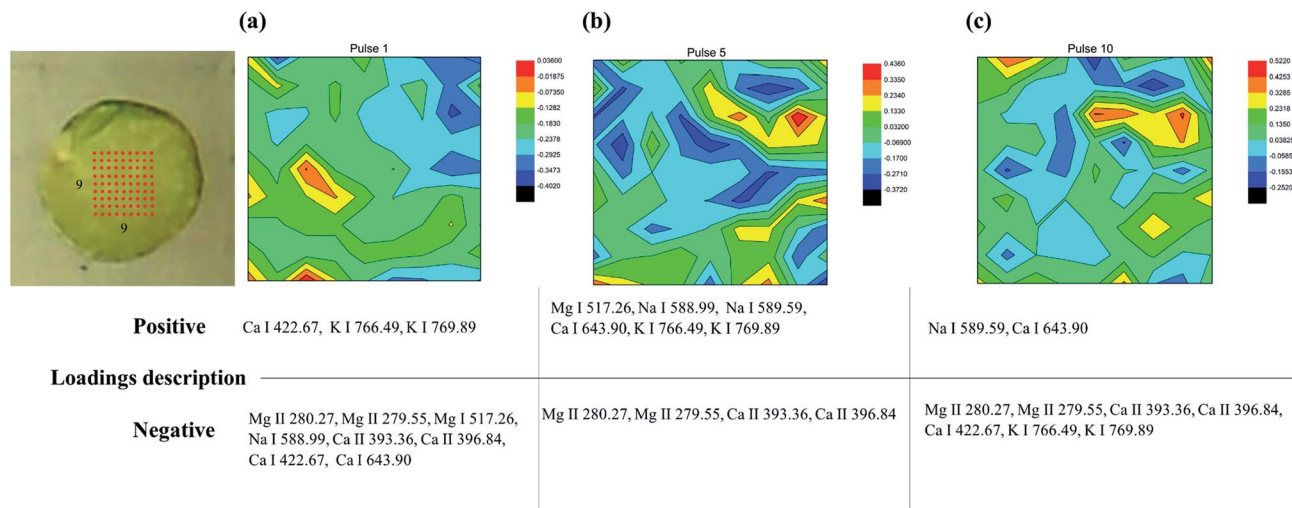


Fig. 5 Score maps for the pea seed for pulses 1 (a), 5 (b) and 10 (c).

The loading plots presented in Fig. 1S(c)† correspond to pulse 10. In this layer, Na has a positive loading, which is observed by the red color due its high intensity. Calcium, K and Mg have negative loadings, and K and Mg are found to be distributed in blue color, while Ca presents loadings near to zero.

Fig. 6 shows the comparison of the loadings of pulse 1, 5 and 10. As can be observed in Fig. 6(a and b) there is no correlation between pulse 1 and pulse 5 and pulse 1 and pulse 10, respectively. However, upon comparing pulse 5 and pulse 10 (Fig. 6(c)) it was possible to note that the loadings of these two layers are highly correlated ( $R^2 = 0.827$ ). In this sense, we can assume that

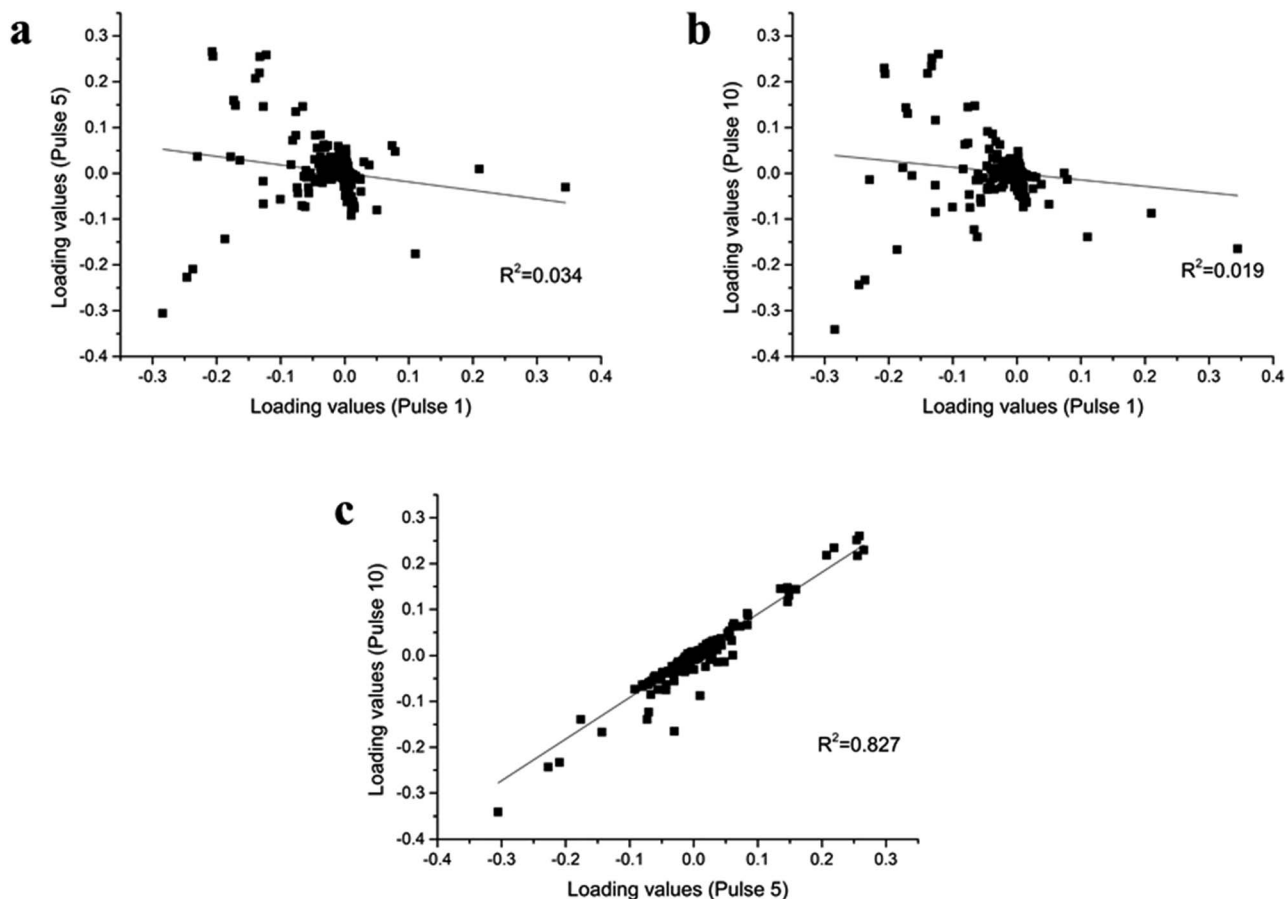


Fig. 6 Comparison among the loading values of pulses 1 (a), 5 (b) and 10 (c) in pea seed.

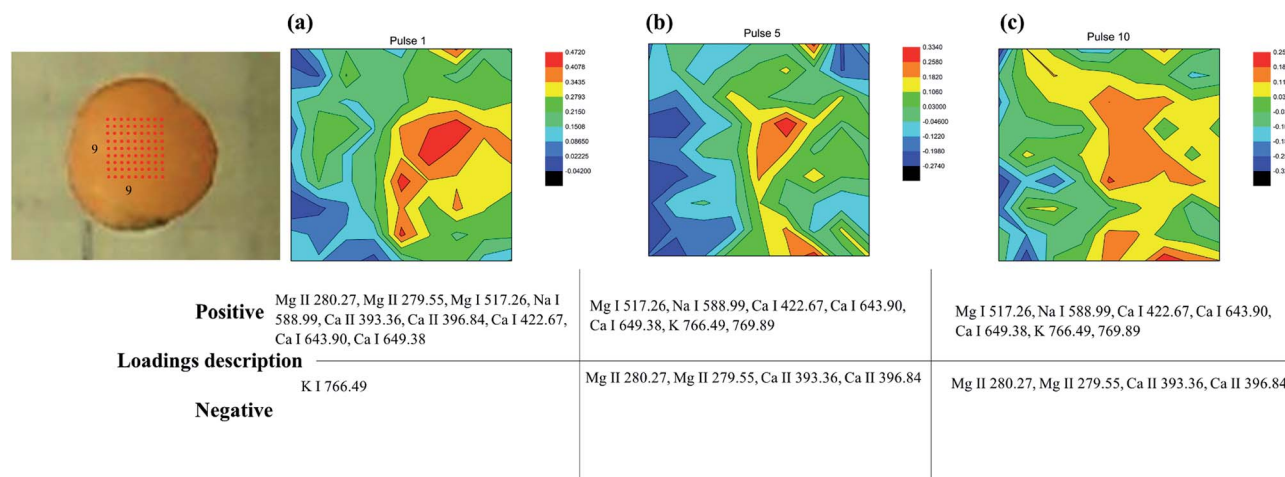


Fig. 7 Score maps for lentil seeds for pulses 1 (a), 5 (b) and 10 (c).

the sample composition of pulse 5 is approximately the same as the composition in pulse 10.

Fig. 7 shows the score maps of PC1 for the variables studied in the lentil seed sample with 40%, 9% and 8% explained variance for pulse 1, 5 and 10, respectively. Fig. 2S† represents the loading values of pulse 1, 5 and 10. Fig. 2S(a)† presents the loading values of pulse 1, where Ca, Mg and Na are in the positive score map (see red color), and the loading value of P is near to zero. On the other hand, only K presents negative loading values and is located in the negative score map (see blue color). Fig. 2S(b)† shows the loadings and the score map for pulse 5, where Na and K (positive loading) were the predominant constituents, as observed in red color regions (positive score). The other element is Mg which presents negative loading and is related to negative score values (see blue color regions). Calcium was present in low prevalence in red and blue color regions (positive and negative loadings).

Fig. 2S(c)† shows the last pulse (pulse 10) and it is possible to observe that both layers with 5 and 10 pulses present a similar composition, and it can be confirmed through the correlation graph of the pulses, as shown in Fig. 8 ( $R^2 = 0.646$ ). An important piece of information that needs to be mentioned is related to P. This element was only observed in the first layer (pulse 1, positive loading); however, in subsequent layers no signal was observed.

Fig. 9 shows the score maps obtained for pumpkin seeds for PC1 with 66%, 18% and 22% explained variance for pulse 1, 5 and 10, respectively. The loading values of pulse 1, 5 and 10 are shown in Fig. 3S.† In Fig. 3S(a)† it can be observed that Ca, Mg and Na are located in positive loading, and these are related to the red color in score maps, while K is present in the negative score map region (blue color). It is important to point out that Na and Mg are inversely correlated between pulse 1 and 5, *i.e.*, while the signal of Na increases, the signal of Mg decreases from pulse 1 to pulse 5. In Fig. 3S(b),† only Na is in the positive score map (see red color), while other elements, such as Ca, Mg and K, present negative loading, where Mg and K are more related to the blue color in score maps.

For the last pulse (pulse 10) presented in Fig. 3S(c),† it is possible to observe K in positive loading values (see red score maps). Other elements, such as Ca, Mg and Na, were identified in negative loading, and these elements are related to the blue color in the score maps. In addition, P was present in the first layer of the sample, *i.e.*, it was not observed in other deep layers.

In general, the score map color changed from one pulse to another, meaning that the distribution of the elements in these samples is not fully homogeneous. In addition, we can assume that most of the elements are more distributed on the seed surface, and as the depth increases, the composition and distribution of these elements reduce.

Therefore, studies involving the chemical profile of seeds are important, as they can provide qualitative information and show how these elements are distributed in the bulk and surface of the seeds. It is important to highlight that the chemical elements are dependent on soil characteristics, morphological and physiological factors, composition and fertilizers used for planting [4].

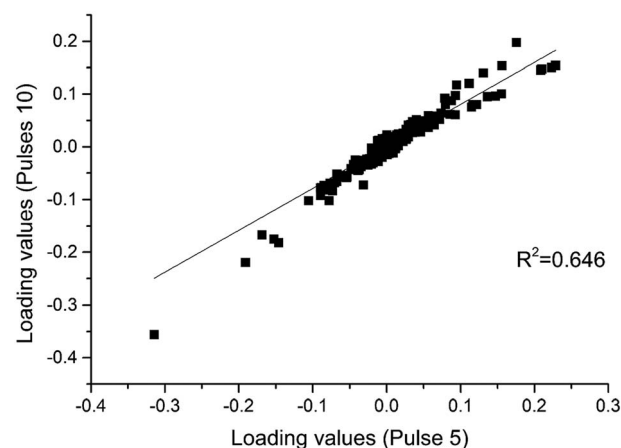


Fig. 8 Comparison among the loading values of pulses 5 and 10 in lentil seeds.

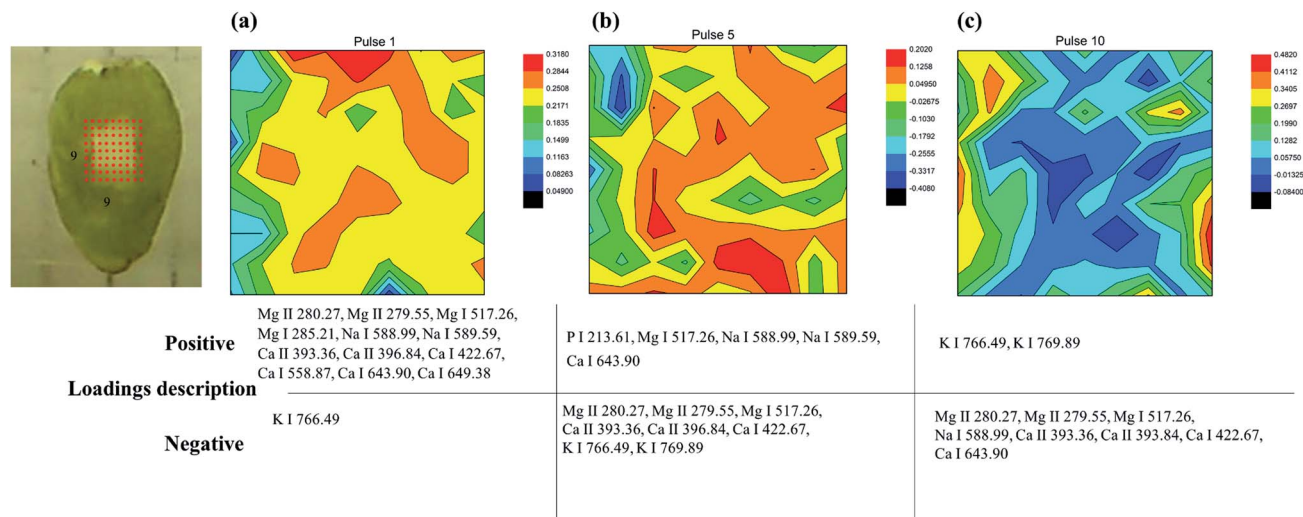


Fig. 9 Score maps for pumpkin seeds for pulses 1 (a), 5 (b) and 10 (c).

However, these factors can or cannot affect the nutritional absorption capability of the seeds, *i.e.*, depending on each species, the plants absorb and accumulate some chemical elements effectively and others ineffectively. Therefore, the lower absorption capability of the nutrients can probably influence the chemical distribution of the seeds. The evidence can be observed through hyperspectral images (score maps), which show inhomogeneous distribution of the evaluated elements.

According to qualitative information, it was possible to evaluate the chemical distribution of Ca, K, Mg, Na and P. Moreover, other chemical elements such as Cu, Mn, S and Zn are present; however they were not evaluated using LIBS because this technique did not present sufficient sensitivity for this purpose. The presence of these elements was confirmed using the ICP-OES technique. From this information, edible seeds are an important source of Ca, K, Mg, Na and P; besides they contribute to the normal development of plants, and these elements play important roles in the appropriate functioning of humans and at the same time guarantee a healthy diet.

## 4. Conclusions

Chemometric tools were used to evaluate the correlation of samples using concentration values of elements obtained using the ICP-OES technique. Many samples were highly correlated due to the presence of Na, Mg, P, S and Zn. Moreover, we concluded that high concentration values of some elements can restrict the absorption of other elements, and it can effectively influence the quality of seeds for human diet.

Moreover, the combination of LIBS with chemometric tools allowed us to obtain qualitative information about the sample composition which was correlated with that obtained by ICP-OES.

The use of hyperspectral images through loadings and score maps provided the elemental distribution on the surface and in the bulk of the samples. It was possible due to the collected

spectra, where 10 pulses were recorded for each point marked on the surface of the sample. Thus, from the generated scores maps the change of color (red or blue) from one layer to the other was observed, showing the variation of the elements in these layers.

It is expected that hyperspectral images employing LIBS can be used for other types of samples to evaluate the chemical distribution of elements.

## Conflicts of interest

There are no conflicts to declare.

## Acknowledgements

The authors acknowledge the financial support of the Conselho Nacional de Desenvolvimento Científico e Tecnológico (CNPq) (grants 160152/2015-1 and 158587/2017-0) and Fundação de Amparo à Pesquisa do Estado de São Paulo (FAPESP, grants 2016/01513-0 and 2016/17304-0). This study was financed in part by the Coordenação de Aperfeiçoamento de Pessoal de Nível Superior – Brasil (CAPES) – Finance Code 001.

## References

- 1 P. A. da Costa, C. A. Ballus, J. Teixeira-Filho and H. T. Godoy, *Food Res. Int.*, 2010, **43**, 1603–1606.
- 2 B. P. Da Silva, P. C. Anunciação, J. C. S. Matyelka, C. M. D. Lucia, H. S. D. Martino and H. M. Pinheiro-Sant'Ana, *Food Chem.*, 2017, **221**, 1709–1716.
- 3 B. R. Cardoso, G. B. S. Duarte, B. Z. Reis and S. M. F. Cozzolino, *Food Res. Int.*, 2017, **100**, 9–18.
- 4 J. Naozuka, E. C. Vieira, A. N. Nascimento and P. V. Oliveira, *Food Chem.*, 2011, **124**, 1667–1672.
- 5 F. C. Bressy, G. B. Brito, I. S. Barbosa, L. S. G. Teixeira and M. G. A. Korn, *Microchem. J.*, 2013, **109**, 145–149.

- 6 V. C. Costa, W. N. Guedes, A. S. Santos and M. M. Nascimento, *Food Anal. Methods*, 2015, **11**, 2004–2012.
- 7 F. A. Amorim, V. C. Costa, W. N. Guedes, I. P. De Sá, M. C. Dos Santos, E. G. P. Da Silva and D. C. Lima, *Food Anal. Methods*, 2015, **9**, 1719–1725.
- 8 A. Mir-marqués, M. L. Cervera and G. M. De La guardia, *Food Chem.*, 2016, **82**, 457–467.
- 9 S. Moncayo, S. Manzoor, J. D. Rosales, J. Anzano and J. O. Caceres, *Food Chem.*, 2017, **232**, 322–328.
- 10 Y. Dixit, M. P. Casado-Gavalda, R. Cama-Moncunill, X. Cama-Moncunill, M. Markiewicz-Keszycka, P. J. Cullen and C. Sullivan, *Anal. Methods*, 2017, **9**, 3314–3322.
- 11 M. Markiewicz-Keszycka, X. Cama-Moncunill, M. P. Casado-Gavalda, Y. Dixit, R. Cama-Moncunill, P. J. Cullen and C. Sullivan, *Trends Food Sci. Technol.*, 2017, **65**, 80–93.
- 12 V. C. Costa, J. P. Castro, D. F. Andrade, D. V. Babos, J. A. Garcia, M. A. Sperança, T. A. Catelani and E. R. Pereira-Filho, *Trends Anal. Chem.*, 2018, **108**, 65–73.
- 13 R. R. V. Carvalho, J. A. O. Coelho, J. M. Santos, W. B. Aquino, R. L. Carneiro and E. R. Pereira-Filho, *Talanta*, 2015, **134**, 278–283.
- 14 M. A. Sperança, W. F. Batista de Aquino, M. A. Fernandes, A. Lopez-Castilho, R. L. Carneiro and E. R. Pereira-Filho, *Geostand. Geoanal. Res.*, 2016, **41**, 273–282.
- 15 N. J. McMillan, S. Rees, K. Kochelek and C. McManus, *Geostand. Geoanal. Res.*, 2014, **38**, 329–343.
- 16 J. P. Castro and E. R. Pereira-Filho, *Talanta*, 2018, **189**, 205–210.
- 17 R. L. Carneiro and R. J. Poppi, *J. Pharm. Biomed. Anal.*, 2012, **58**, 42–48.
- 18 R. L. Carneiro and R. J. Poppi, *Spectrochim. Acta, Part A*, 2014, **118**, 215–220.
- 19 J. P. Castro and E. R. Pereira-Filho, *J. Anal. At. Spectrom.*, 2016, **31**, 2005–2014.
- 20 S. Wold, *Chemom. Intell. Lab. Syst.*, 1987, **2**, 37–52.
- 21 Y. Jiao, C. A. Grant and L. D. Bailey, *Can. J. Plant Sci.*, 2007, **87**, 461–470.

## Supplementary material

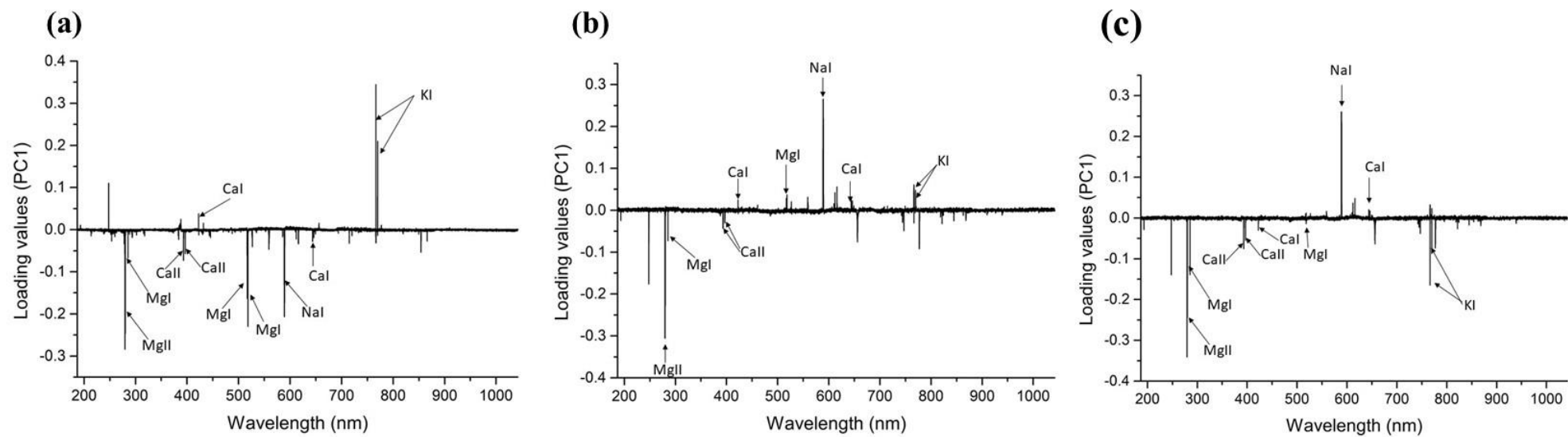


**Figure 1S.** Loading values for the pea seed for pulses: 1 (a), 5 (b) and 10 (c)



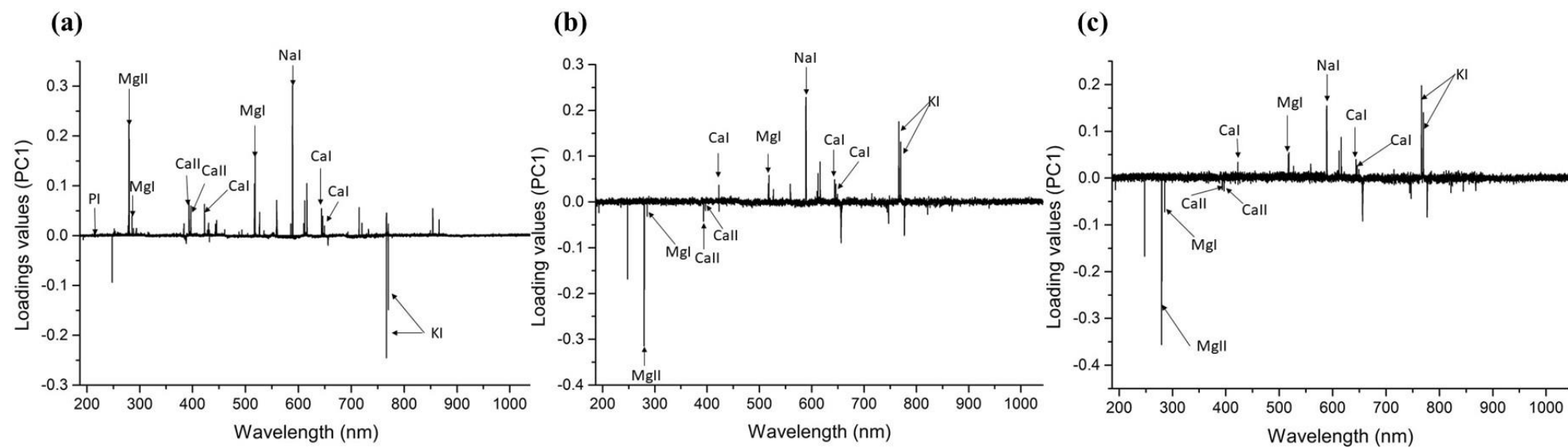


**Figure 2S.** Loading values for the lentil seed for pulses: 1 (a), 5 (b) and 10 (c)

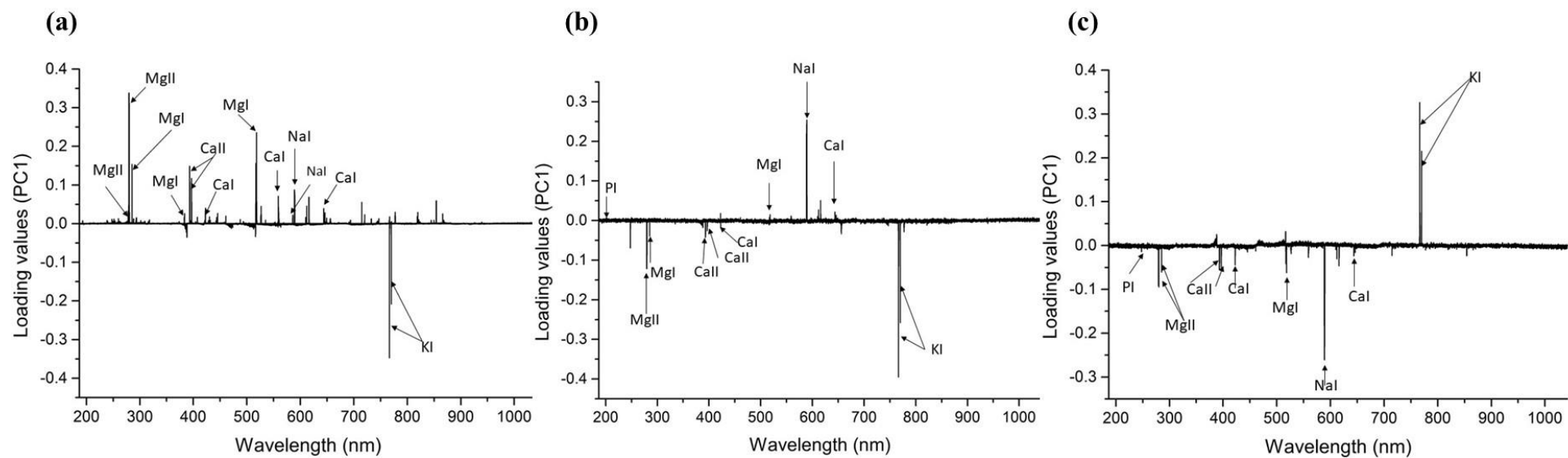


**Figure 3S.** Loading values for the pumpkin seed for pulses: 1 (a), 5 (b) and 10 (c)

## Conclusions

In this thesis it was possible to demonstrate possibilities and analytical applications of the use of LIBS and WDXRF for elemental determination in edible seeds. These techniques presented several advantages, however, the direct solid analysis with less handling of the samples and higher analytical frequency (time for data acquisition), mainly in the case of the LIBS, represent the most important feature of the proposed methods. In addition, the combination of these techniques with chemometrics tools enabled the spectral data treatment, which has become increasingly important nowadays.

New calibration strategy using data fusion from LIBS and WDXRF was developed to circumvent matrix effects in the determination of K, Mg and P in bean seeds employing LIBS. This strategy was suitable, as it presented lower standard error of cross validation (SECV) when compared with those obtained by univariate calibration in individual form (LIBS or WDXRF) and multivariate calibration (MLR). Moreover, other new univariate calibration strategies, such as OP MLC, SSC and TP CT were used for the determination of Ca, K and Mg in cocoa beans. These strategies, besides its simplicity, present advantages, i.e., they required only one sample as standard with known concentration for calibration. Moreover, acceptable trueness values and lower relative standard deviation (RSD) were obtained, showing a better capability to minimize the matrix effects in LIBS.

Other possibility and analytical application for LIBS was related to hyperspectral images. Through chemometric tools and LIBS was possible to evaluate qualitatively the chemical profile distribution of the elements in the surface and depth of the seeds. Therefore, in all cases, ICP OES was used as a complementary and reference technique.